

January 2014

Deuterium Tracer Study Of The Mechanism Of Iron Catalyzed Fischer-Tropsch Synthesis

Yunxin Liao
Eastern Kentucky University

Follow this and additional works at: <https://encompass.eku.edu/etd>

 Part of the [Organic Chemistry Commons](#)

Recommended Citation

Liao, Yunxin, "Deuterium Tracer Study Of The Mechanism Of Iron Catalyzed Fischer-Tropsch Synthesis" (2014). *Online Theses and Dissertations*. 288.
<https://encompass.eku.edu/etd/288>

This Open Access Thesis is brought to you for free and open access by the Student Scholarship at Encompass. It has been accepted for inclusion in Online Theses and Dissertations by an authorized administrator of Encompass. For more information, please contact Linda.Sizemore@eku.edu.

DEUTERIUM TRACER STUDY OF THE MECHANISM OF IRON
CATALYZED FISCHER-TROPSCH SYNTHESIS

By

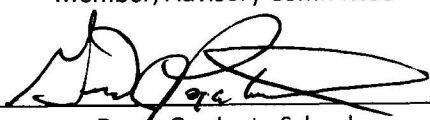
YUNXIN LIAO

Thesis Approved:


Chair, Advisory Committee


Member, Advisory Committee


Member, Advisory Committee


Dean, Graduate School

STATEMENT OF PERMISSION TO USE

In presenting this thesis in partial fulfillment of the requirements for a Master's degree at Eastern Kentucky University, I agree that the Library shall make it available to borrowers under rules of the Library. Brief quotations from this thesis are allowable without special permission, provided that accurate acknowledgment of the source is made. Permission for extensive quotation from or reproduction of this thesis may be granted by my major professor, or in [his/her] absence, by the Head of Interlibrary Services when, in the opinion of either, the proposed use of the material is for scholarly purposes. Any copying or use of the material in this thesis for financial gain shall not be allowed without my written permission.

Signature Yunxin Liao

Date 11/17/2014

DEUTERIUM TRACER STUDY OF THE MECHANISM OF IRON
CATALYZED FISCHER-TROPSCH SYNTHESIS

By

YUNXIN LIAO

Bachelor of Science

Changsha University of Science and Technology

Changsha, China

2011

Submitted to the Faculty of the Graduate School of

Eastern Kentucky University

In partial fulfillment of the requirements

For the degree of

MASTER OF SCIENCE

December, 2014

Copyright © Yunxin Liao, 2014
All Rights Reserved

DEDICATION

This thesis is dedicated to my parents Mr. Xiaodong Liao and Mrs. Zhiqing Song, who have given me invaluable educational opportunities.

ACKNOWLEDGMENTS

I would like to express my deepest appreciation to my advisor, Dr. Buchang Shi, who has given me this great opportunity to do this research and has continually given me help and valuable guidance. Without his encouragements and patience for these years, this thesis would never have been possible to be finished. I would like to thank my committee members, Dr. Darrin Smith and Dr. Donghui Quan, who have given me valuable advice and academic guidance. They taught me how to be a better student and researcher. I would also like to thank Mrs. Wu Lin and Miss. Jennifer Naumovitz for their help and encouragements.

I would like to thank the Chemistry Department of EKV for providing all the useful analytical instruments. I wish to thank Dr. Burtron H. Davis, Mr. Will Shafer and Mr. Dennis E. Sparks in the Center for Applied Energy Research for the instrumental help of Micro GC and GC-MS.

I am very thankful for my parants, Dongxiao Liao and Zhiqing Song, who have always given me supports and inspired me over year.

In addition, I acknowledge the URC of Easter Kentucky University and NFS-EPSCoR through contract number EPS-0814194 for financial supports.

ABSTRACT

The Fischer-Tropsch Synthesis (FTS) was invented in 1920s, shortly after its invention, it became an important way to produce synthetic fuels. The FTS is also an important way to understand the origin of life. Even though the FTS has been used to produce liquid fuels commercially for a relatively long time, the mechanism of FTS is still unclear, a mechanism can explain all the experimental observations has not been discovered yet.

By conducting H_2/D_2 switching experiments we found that there was an inverse isotope effect in the Fe catalyzed FTS. The rate of hydrocarbon production was increased when syngas H_2/CO was switched to D_2/CO . The inverse isotope effect was calculated to be 0.83 to 0.97 for Fe/Si/K runs and 0.71 for Fe/Si catalyzed FTS. These results can be explained by the modified alkylidene mechanism which was proposed based on Co catalyzed FTS studies.

The product analysis of H_2/D_2 switching experiments of iron catalyzed FTS showed that the ratios of $[1\text{-alkenes}]_H/[1\text{-alkenes}]_D$ are less than 1 while the ratios of $[2\text{-alkenes}]_H/[1\text{-alkenes}]_D$ are greater than 1, which is indicating that the 2-alkenes were produced through a different pathway from 1-alkenes. The formation pathway of 2-alkenes has been proposed based on the modified alkylidene mechanism.

We also conducted the H_2/D_2 competitive experiments by using an equal molar ratio of H_2 and D_2 as the syngas. The results showed that the H/D ratios in alkanes from C8 to C19 were less than 1. It clearly indicates that there is deuterium enrichment during iron catalyzed FT reactions. Unlike Co catalyzed FTS, in which the H/D ratio decreased with increasing carbon numbers, the H/D ratio in iron catalyzed FTS decreased from from C8

to C11 and became almost a constant from C11 to C19 during Fe/Si/K runs, while in Fe/Si run the H/D ratio decreased from C8 to C14 and start increasing from C15 to C16. These results can be explained by the modified alkylidene mechanism while other factors need to be taken into consideration.

TABLE OF CONTENTS

CHAPTER	PAGE
I. INTRODUCTION	1
II. REACTION METHODS	9
2.1 REAGENTS AND PREPARATION OF IRON CATALYSTS.....	9
2.2 SET UP OF THE FIXED BED REACTOR	11
2.3 FTS EXPERIMENTAL PROCEDURES.....	12
2.3.1 Activation of Iron Catalyst	12
2.3.2 H ₂ /D ₂ Switching Experiment Procedure.....	13
2.3.3 H ₂ /D ₂ Competition Experiment Procedure	14
2.4 PRODUCT ANALYSIS.....	14
2.5 IDENTIFICATION OF BRANCHED HYDROCARBONS IN FTS	16
2.5.1 Hydrogenation of Heavy Chain FTS Product.....	16
2.5.2 Identification of Branched Hydrocarbons.....	16
III. INVERSE ISOTOPE EFFECT IN IRON CATALYZED FISCHER-TROPSCH SYNTHESIS	18
3.1 INTRODUCTION	18
3.2 RESULTS OF H ₂ /D ₂ SWITCHING EXPERIMENT	19
3.2.1 CO Conversions	19
3.2.2 CO to Hydrocarbon Products Conversions in Different FTS Runs.....	21
3.2.3 The Inverse Isotope Effect during Methane Formation	22
3.2.4 CO to Gas Phase Product Conversion and Methane – CO ₂ Selectivity	23
3.3 DETERMINATION OF CHAIN GROWTH PROBABILITY (α) VALUE	26
3.4 DISCUSSION	30
3.4.1 The Modified Alkylidene Mechanism	30

3.4.2 Explanation of Inverse Isotope Effect Alkyl Mechanisms and Alkenyl Mechanism	34
3.4.3 Explanation of Inverse Isotope Effect by the Modified Alkyliene Mechanism	35
3.4.4 The Calculation of Inverse Isotope Effect in Iron Catalyzed FTS.....	37
3.5 CONCLUSION	40
IV. DEUTERIUM ENRICHMENT IN IRON CATALYZED FISCHER-TROPSCH SYNTHESIS	41
4.1 INTRODUCTION	41
4.2 THE ANALYSIS OF ISOTOPIC ISOMERS BY GC-MS.....	42
4.3 THE RESULTS OF IRON CATALYZED H ₂ /D ₂ COMPETITION EXPERIMENTS	46
4.3.1 The Results of Fe/Si/K Catalyzed H ₂ /D ₂ Competition Experiments.....	46
4.3.2 The Results of Fe/Si Catalyzed H ₂ /D ₂ Competition Experiments	49
4.4 DISCUSSION	51
4.4.1 The Difference of Iron and Cobalt Catalyzed H ₂ /D ₂ Competition Experiment Results	51
4.4.2 Calculation of Theoretical H/D Ratio	53
4.5 CONCLUSION	56
V. EXPLANATION OF FORMATION OF 2-OLEFINS AS SECONDARY PRODUCT DURING IRON CATALYZED FTS	57
5.1 INTRODUCTION	57
5.2 THE NORMAL ISOTOPE EFFECT IN IRON CATALYZED FTS.....	58
5.2.1 The Product Profiles of Iron Catalyzed FTS.....	58
5.2.2 The [1-Olefi] _H /[1-Olefi] _D and [2-Olefin] _H /[2-Olefin] _D Ratios in Fe Catalyzed FTS.....	60
5.3 THE PROPOSED 2-OLEFIN FORMATION PATHWAY	63
5.3.1 The Hypothetical Formation Pathway of 2-Alkenes	63

5.3.2 The Explanation for 2-Alkenes Formation by Modified Alkylidene Mechanism	65
5.3.3 The Explanation of $[\text{paraffin}]_{\text{H}}/[\text{paraffin}]_{\text{D}}$ Ratio in Iron Catalyzed FTS....	68
5.4 CONCLUSION	69
VI. SUMMARY AND FUTURE WORK.....	70
6.1 SUMMARY	70
6.2 FUTURE WORK	71
APPENDICES:	82
A. TABLE.....	82
B. FIGURES.....	84
C. FIGURES.....	90

LIST OF TABLES

TABLE	PAGE
3.1 CO conversions during H ₂ /D ₂ switching experiments	20
3.2 CO to hydrocarbon products conversions.....	21
3.3 Methane formations during iron catalyzed FTS.....	23
3.4 Product distribution during iron catalyzed FTS.....	23
3.5 Alkene and alkane selectivity of C ₂ and C ₃ products	25
3.6 The α values of each FTS run	29
3.7 Results of the inverse isotope effects (α_H/α_D) during iron catalyzed FTS.....	39
4.1 GC-MS analysis of isotopomers of n-nonane produced from Fe/Si/K catalyzed H ₂ /D ₂ competition experiment	45
4.2 Ratio of H/D during Fe/Si/K catalyzed runs.....	47
4.3 H/D ratio during Fe/Si catalyzed H ₂ /D ₂ competition experiment	50
5.1 Detailed product profile of each Fe/Si/K catalyst	59
5.2 The 1-olefin and 2-olefin fractions during H ₂ /D ₂ switching experiment.....	60
5.3 The ratio of [paraffin] _H /[paraffin] _D during the iron catalyzed FTS.....	68
A-1 Measured Real Flow Rate of Different Runs.....	83

LIST OF FIGURES

FIGURE	PAGE
1.1 Flow sheet of the Biomass to liquid via Fischer-Tropsch Synthesis process	2
1.2 Carbon-carbon bond formation in Alkyl mechanism	4
1.3 Carbon-carbon band formation in Alkenyl mechanism	4
1.4 Chain propagation step in modified alkylidene mechanism	5
1.5 GC spectra of FTS product from C7 to C9: Co/Al/Pt(A); Ru/SiO ₂ (B); Fe/Si/K(C); Fe/Si(D)	7
2.1 Set up of the Fixed Bed Reactor	12
2.2 A GC spectrum of C8 product. (A): before hydrogenation; (B): after hydrogenation .	17
3.1 CO conversion in Fe/Si/K catalyzed H ₂ /D ₂ switching experiment of the 3 rd run	20
3.2 Methane – CO ₂ selectivity for different runs: (A). Run 1; (B). Run 2; (C). Run 3; (D) Run 4.	24
3.3 GC spectrum of C8 product.....	27
3.4 Production distribution of Fe/Si/K product.....	29
3.5 The formation of C1 species and methane	31
3.6 The formation of C-C bond and C2 species in FTS	31
3.7 The chain propagation steps in FTS.....	32
3.8 Formation of branched hydrocarbons in FTS.....	33
3.9 The modified alkylidene mechanism of FTS	34
3.10 The carbon-carbon bond formation in Alkyl mechanism	34
3.11 The C-C bond formation in Alkenyl mechanism.....	35
3.12 The formation of methane and deuterated methane	36

3.13 Carbon-carbon bond formations in FTS.....	36
4.1 Mixture of isotopomers of n-dodecanes and trans-2-dodecenes	44
4.2 Isotopic isomer distributions in n-Octane (A) and n-Nonadecane (B) during Fe/Si/K catalyzed H ₂ /D ₂ competition experiment	46
4.3 The H/D ratios during Fe/Si/K catalyzed H ₂ /D ₂ competition experiments.....	48
4.4 Isotopic isomer distributions in n-Octane (A) and n-Hexadecane (B) during Fe/Si catalyzed H ₂ /D ₂ competition experiment	49
4.5 H/D ratio in Fe/Si catalyzed H ₂ /D ₂ competition experiment.....	50
4.6 The experimental and theoretical H/D ratios in Fe/Si/K catalyzed H ₂ /D ₂ competition experiments	55
4.7 The experimental and theoretical H/D ratios in Fe/Si catalyzed H ₂ /D ₂ competition experiments	55
5.1 The ratio of 1-alkene (H/D) and ratio of 2-alkene (H/D) in the first run	61
5.2 The ratio of 1-alkene (H/D) and ratio of 2-alkene (H/D) in the second run.....	62
5.3 The ratio of 1-alkene (H/D) and ratio of 2-alkene (H/D) in the third run.....	62
5.4 The hypothetical formation pathway of 1-alkenes and 2-alkenes in FTS	64
5.5 A brief production pathway of iron catalyzed FTS	65
5.6 The proposed mechanism for the formation of 2-alkenes	66
5.7 The metal-hydrogen atom addition-elimination mechanism	67
B-1 Isotopic isomer distributions in n-Nonane	85
B-2 Isotopic isomer distributions in n-Decane.....	85
B-3 Isotopic isomer distributions in n-Undecane.....	86
B-4 Isotopic isomer distributions in n-Dodecane.....	86
B-5 Isotopic isomer distributions in n-Tridecane	87

B-6 Isotopic isomer distributions in n-Tetradecane	87
B-7 Isotopic isomer distributions in n-Pentadecane	88
B-8 Isotopic isomer distributions in n-Hexadecane	88
B-9 Isotopic isomer distributions in n-Heptadecane	89
B-10 Isotopic isomer distributions in n-Octadecane.....	89
C-1 Isotopic isomer distributions in n-Nonane	91
C-2 Isotopic isomer distributions in n-Decane	91
C-3 Isotopic isomer distributions in n- Undecane.....	92
C-4 Isotopic isomer distributions in n- Dodecane.....	92
C-5 Isotopic isomer distributions in n- Tridecane	93
C-6 Isotopic isomer distributions in n- Tetradecane	93
C-7 Isotopic isomer distributions in n- Pentadecane	94

LIST OF SYMBOLS AND ABBREVIATIONS

FTS	Fischer-Tropsch Synthesis
ASF	Anderson_Schulz_Flory
BDE	Bond-dissociation energy
WGS.....	water-gas-shift
α	chain growth probability
k.....	rate constant
P	pressure
T	temperature

CHAPTER 1

INTRODUCTION

The Fischer-Tropsch Synthesis (FTS) was discovered by Franz Fischer and Hans Tropsch in 1920s [1]. The FTS is a collection of catalytic reactions that converts a mixture of carbon monoxide (CO) and hydrogen (H₂), which is also known as syngas, into liquid hydrocarbons and other products. As a key component of gas to liquids technology, FTS produces a synthetic lubrication oil and synthetic fuel, typically from coal, natural gas or biomass; it became a commercial scale industrial technique shortly after its invention even though many refinements and adjustments have been made since. Coal, biomass or other solid organic feedstock can be converted to syngas through gasification, which in turn can be converted to gasoline, diesel, wax and other chemicals through FTS. FTS is a very attractive technique especially for some petroleum-poor but coal-rich countries. For example, large scale FT plants were built in Germany during World War II in order to produce fuels. It has been reported that Fischer-Tropsch production accounted for an estimated 9% of German war production of fuels and 25% of the automobile fuel [2]. Another example is South Africa, which is a country with large coal reserves but little oil. The largest scale of Fischer-Tropsch technology is in a series of plants operated by Sasol in South Africa. Sasol uses coal and natural gas as feedstock and produces a variety of synthetic petroleum products, including most of the country's diesel fuels [3]. Because the limit of the fossil energy source, FTS is becoming more and more important since it is

an alternative way to convert coal or biomass into synthetic fuels. Figure 1.1 shows the general three main steps in the Biomass to Liquid via Fischer-Tropsch (BTL-FT) synthesis [4]. As shown in Figure 1.1, biomass is firstly converted to biomass-derived syngas (bio-syngas) through gasification. Then, a cleaning step is applied to remove the impurities, resulting in clean bio-syngas which can be used in FTS. Finally, the cleaned bio-syngas is introduced to the FTS reactor to produce desire products, such as gasoline, diesel and other biofuels.

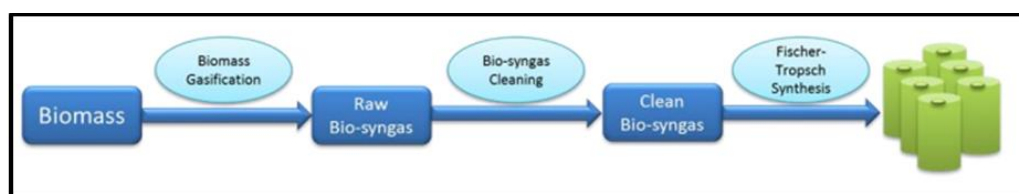


Figure 1.1 Flow sheet of the Biomass to liquid via Fischer-Tropsch Synthesis process.
Source: Hu, Jin, Fei Yu, and Yongwu Lu. "Application of Fischer–Tropsch Synthesis in Biomass to Liquid Conversion." *Catalysts* 2.2 (2012): 303-326.

The FTS has also been invoked to explain the formation of abiogenic hydrocarbons. It has been referred to explain the formation of abiogenic hydrocarbons in the Earth's crust [5, 6], meteorites [7, 8], and the formation of organic matters in the nebula [9, 10]. A recent study on abiogenic hydrocarbon production at the Lost City indicated that the hydrocarbons from C1 to C4 found at the Lost City were produced by FT-type reactions [11], which could be a common pathway for producing precursors of life-essential building blocks in the ocean-floor environment [12]. Therefore, the FTS is not only important in producing replacement fuels, but also important in understanding the origins of life.

The FTS can be generally expressed by eq. 1.1, where n is the carbon number.



Even though significant progresses have been made in understanding the FTS and the FTS has been widely commercially used during the past decades, the mechanism of FTS is still a topic of debating. One of the most important developments on the understanding of FTS was found that the FTS hydrocarbon product distribution follows the Anderson-Schulz-Flory (ASF) model [13]. The ASF equation is shown in eq. 1.2 [14].

$$m_n = (1 - \alpha) \alpha^{n-1} \quad (1.2)$$

In eq. 1.2, m_n is the mole fraction of compounds, n is carbon number, α is the chain growth probability. The FTS is also considered as a polymerization reaction [15], it involves chain initiation (r_i), chain propagation (r_p) and the chain termination (r_t). The chain growth probability α can be defined as eq. 1.3.

$$\alpha = \frac{r_p}{r_p + r_t} \quad (1.3)$$

Isotope labeling is one of the most useful experimental techniques that may be used in testing mechanisms of reactions. Based on the results of isotope tracer studies, the alkyl mechanism was proposed by Brady and Pettit in 1980s [16]. Figure 1.2 shows the carbon-carbon bond formation in the alkyl mechanism. As indicated in Figure 1.2, the monomer of this mechanism is $\text{M}=\text{CH}_2$, which is produced in situ by reaction of CO and H_2 on the surface of metal catalyst. The hydrogenation of monomer $\text{M}=\text{CH}_2$ gives the

intermediate $M-CH_3$ which can be formed to methane through hydrogenation or react with the monomer to generate $M-CH_2CH_3$. The growing chain $M-CH_2CH_3$ can be terminated to C2 hydrocarbons (ethene or ethane) or grow to longer chain by coupling with the monomer. This mechanism can explain some of the experimental observations such as the existence of the inverse isotope effect.

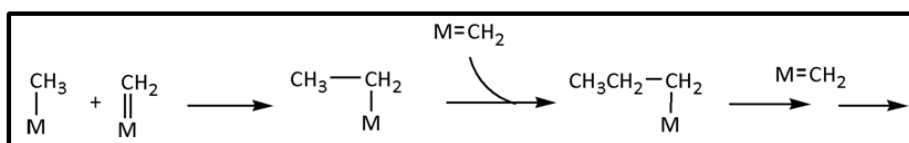


Figure 1.2 Carbon-carbon bond formation in Alkyl mechanism

In 1990s, the alkenyl mechanism [17] was proposed by Maitlis et al, which is shown in Figure 1.3. Similar to the alkyl mechanism, the monomer in alkenyl mechanism is also $M=CH_2$ and the growing chain is $M-CH=CHR$. As it can be seen in Figure 1.3, the coupling of monomer $M=CH_2$ with growing chain $M-CH_2=CH_2$ generates the intermediate $M-CH_2CH=CH_2$ which can undergo isomerization to form the growing chain $M-CH=CH-CH_3$, this growing chain can either react with monomer to form longer chain or can be terminated to produce 2-alkenes. Thus, the alkenyl mechanism can explain not only the formation of normal alkanes and 1-alkenes but also the formation of 2-alkenes.

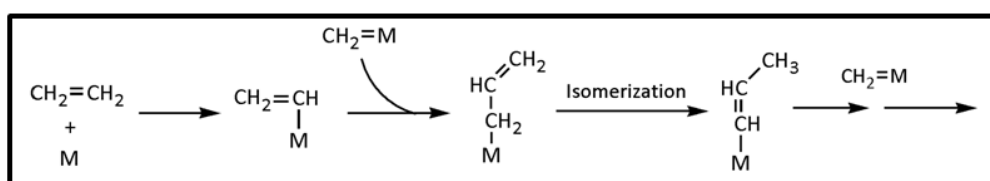


Figure 1.3 Carbon-carbon bond formation in Alkenyl mechanism

There are many other types of mechanisms, such as the hydroxymethylene mechanism [18], the CO insertion mechanism [19] and modified carbide mechanism [20-22] were proposed over decades.

In 2011, Shi et al proposed a modified alkylidene mechanism [23] which is shown in Figure 1.4. Figure 1.4 shows the carbon-carbon bond formation in the modified alkylidene mechanism, the monomer of this mechanism is $M\equiv CH$, the growing chain is the alkylidene group $M=CH-R$. The coupling of monomer and growing chain give an intermediate $RCH(M)-CH=M$ which can undergo hydrogenation to form longer growing chain. The growing chain can either react with monomer to form longer chain or can be terminated to form n-alkanes or 1-alkenes. The modified alkylidene mechanism can explain the formation of n-alkanes, 1-alkenes and branched products, and both inverse isotope effect and deuterium enrichments.

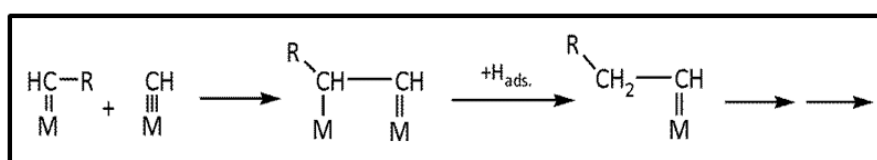


Figure 1.4 Chain propagation step in modified alkylidene mechanism

Through many years' of outstanding studies, there are substantial agreements have been made: (1) The FTS is a polymerization reaction and product distribution follows the ASF equation [24]; (2) there is inverse isotope effect and deuterium enrichment during cobalt catalyzed FTS [23]; (3) linear 1-alkenes and n-alkanes are the primary products of FTS [25, 26]; (4) the branched hydrocarbons are produced through the re-adsorption and

re-growth of the 1-alkenes [27] and so on. However, the formation of the 2-alkenes during FTS is still a topic of debating. The majority agrees that the internal alkenes are the secondary products of the FTS, but some research groups concluded that like 1-alkenes and n-alkanes, the 2-alkenes are the primary products through surface reaction of alkyl group on the metal surface [28].

The modified alkylidene mechanism was proposed based on the isotope tracer results based on cobalt catalyzed FTS. Since iron catalyzed FTS is a practically and theoretically important process, it is important to know whether the iron catalyzed FTS is through alkylidene pathway or through other mechanism. In this research, iron catalyst has been chosen. The advantages of using iron catalysts are [29]: (1) they are inexpensive; (2) specific activity for Fischer-Tropsch Synthesis (FTS) is high and (3) some iron catalysts have high water-gas-shift (WGS) activity.

It has been reported that several transition metal catalyst can be used as FTS catalyst, such as cobalt, iron, ruthenium and nickel [30-32]. From previous and current study, product produced from Co, Ru, Fe/Si/K and Fe/Si catalyzed FT reaction is found to be different from each other. Figure 1.5 shows four GC spectra of Co, Ru, Fe/Si/K and Fe/Si catalyzed FTS product from C7 to C9, respectively. As it shows in Figure 1.5, it can be found that the product produced from Co, Ru, Fe/Si/K and Fe/Si catalyzed FTS is different. For Co catalyzed FTS (shows in Figure 1.5A), the main product is n-paraffin, the amount of olefin and branched hydrocarbons is relatively low. The Ru catalyzed product is displayed in Figure 1.5B, the main product is 1-olefin, n-paraffin, trans-2-olefin and cis-2-olefin, the amount of branched hydrocarbons is not significant. Figure 1.5C shows

the product from Fe/Si/K, we can find that besides 1-olefin, n-paraffin, trans-2-olefin and cis-2-olefin, there is a significant amount of branched hydrocarbons. Finally, Figure 1.5D shows the product from Fe/Si, we can find that the biggest peak is n-paraffin, unlike Co catalyzed FT reactions, the amount of trans-2-olefins and cis-2-olefins is relatively high and the amount of branched hydrocarbons is more than which produced from Co catalyzed FTS.

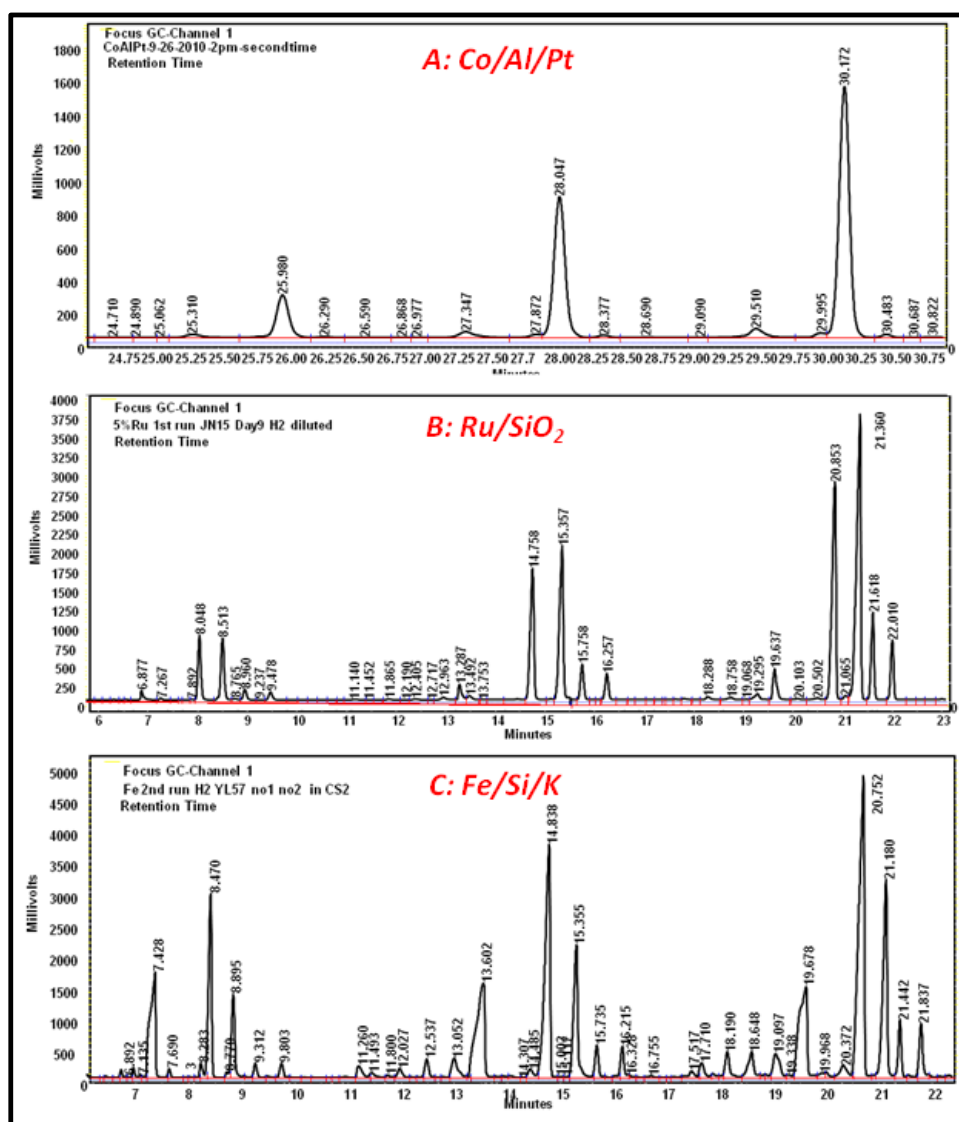


Figure 1.5 GC spectra of FTS product from C7 to C9: Co/Al/Pt(A); Ru/SiO₂(B); Fe/Si/K(C); Fe/Si(D)

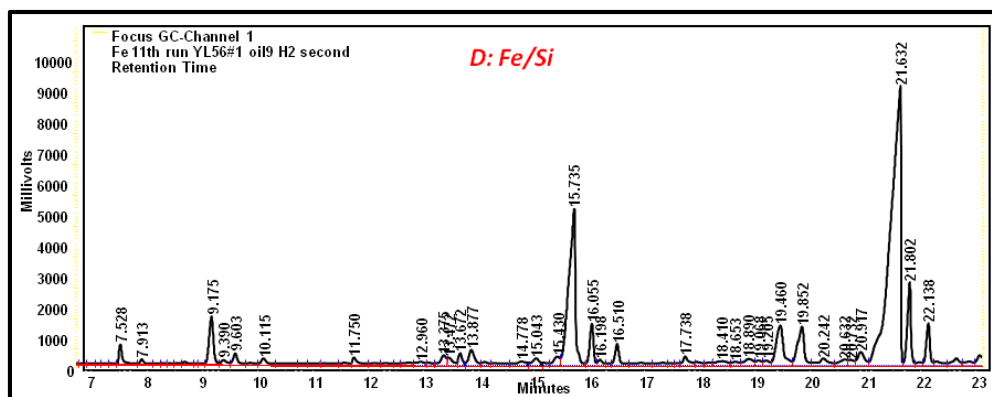


Figure 1.5 (continued). GC spectra of FTS product from C7 to C9: Co/Al/Pt(A); Ru/SiO₂(B); Fe/Si/K(C); Fe/Si(D)

The Co catalyzed FTS can be explained by the modified alkylidene mechanism. It is of interest to know what is the mechanism of the Ru and Fe catalyzed FT reactions. This research is aimed to answer the following questions: whether there is also inverse isotope effect and deuterium enrichment in Fe catalyzed FTS? If so, can this experimental phenomenon be explained by the modified alkylidene mechanism? What is the difference between Fe/Si/K catalyst and Fe/K catalyst? How the 2-alkenes were formed during the Fe catalyzed FTS? In order to answer these questions, two types of iron catalysts have been made in this study (1) Fe/Si/K (100 : 4.6 : 1.44 atomic ratio) and (2) Fe/Si (100 : 4.6 atomic ratio).

CHAPTER 2

REACTION METHODS

2.1 REAGENTS AND PREPARATION OF IRON CATALYSTS

Reagents

The $\text{Fe}(\text{NO})_3 \cdot 9\text{H}_2\text{O}$, NH_4OH , K_2CO_3 , white quartz sand and glassballs were purchased from Sigma-Aldrich company. The tetraethylorthosilicate was purchased from ACROS ORGANICS. The syngas and pure H_2 used in this research were purchased from Scott-Gross Company Inc. The syngas were $\text{CO} : \text{H}_2 : \text{N}_2$ (30% : 60% : 10%), $\text{CO} : \text{D}_2 : \text{N}_2$ (30% : 60% : 10%), $\text{CO} : \text{H}_2 : \text{D}_2 : \text{N}_2$ (30% : 30% : 30% : 10%). The pure hydrogen gas was used in the activation of iron catalyst.

Synthesis of Fe Catalysts

There are many advantages of iron catalyst, which have already been stated above. In a typical iron catalyst, silica, copper and potassium are added to improve the properties of the catalyst. Copper is added to help the reduction of iron [33-35], silica is a structural promoter added to stabilize the surface area [33, 35]. Silica may also have a chemical effect on the catalyst properties [37]. Potassium is considered to promote CO dissociation and enhance chain growth [33, 35, 36]. It increases both the FT activity and the olefin yield, but lowers the methane fraction [38, 39]. Potassium can also increase the catalytic activity for FTS and water-gas-shift reactions [34, 38].

Two types of iron catalysts were synthesized and used in this research. One is Fe/Si/K with an atomic ratio of 100 : 4.6 : 1.44, the other is Fe/Si with an atomic ratio 100 : 4.6. The synthesis of Fe/Si/K catalysts were followed the procedure from the literature [40] without modification.

Initially, 40 g of $\text{Fe}(\text{NO})_3 \cdot 9\text{H}_2\text{O}$ was dissolved with 40 mL of distilled water in a flask while stirring. Then, 1 g of tetraethylorthosilicate ($\text{SiC}_8\text{H}_{20}\text{O}_4$) was added into the $\text{Fe}(\text{NO})_3$ solution. A layer of oil was observed after the addition of tetraethylorthosilicate. The mixture was stirred vigorously for several hours till the tetraethylorthosilicate totally hydrolyzed, the solution became clear. The previous solution was added to another flask by pipette with the addition of NH_4OH at the same time while stirring. A slurry with a brown color was formed. The slurry was maintained at pH 9. The result slurry was then vacuum filtered. The filter cake was washed with 20 mL of distilled water three times. The filter cake was oven dried for 24 hours at 110 °C. The filter cake was then mashed into fine powder. A portion of 0.05 g of K_2CO_3 was dissolved in 5 mL of distilled water. The K_2CO_3 solution was then added into the previous powder with stirring. The mixture was oven dried for 24 hours at 110 °C. The crude catalyst was then calcinated at 350 °C for 4 hours to burn the organic matters.

The Fe/Si catalysts were synthesized with the similar method but without the addition of K_2CO_3 solution. The crude catalysts were sent to calcination for 4 hours directly after 24 hours oven dry at 110 °C. The Fe/Si (100 : 4.6) catalyst was obtained.

2.2 SET UP OF THE FIXED BED REACTOR

In industry different types of FTS reactor have been designed depending on the scale of the reaction. For example [41]: the entrained fluidized-bed with riser cooler, called the Synthol reactor is used at Sasol; the fixed fluidized-bed with internal coils reactor is used at Carthage Hydrocol plant at Texas; and for natural-gas-based Fischer-Tropsch distillate designs, Shell has selected the tubular fixed-bed for their new plant in Malaysia. In this research, a small scale fixed-bed reactor was used.

The set up of the fixed-bed reactor is shown in Figure 2.1. As shown in Figure 2.1, a portion of 1.5 g or 2.0 g of iron catalyst was mixed well with approximately 8 g of white quartz sand in a mortar. The catalyst mixture was placed in the middle of the reactor. Below and above the mixture, approximately 2.5 g of white quartz sand was added. The rest of the reactor was filled with 0.5 mm glassballs. The top and bottom parts were filled with glass wool. The whole reactor was wrapped with glass wool to avoid heat releasing. A thermocouple was injected into the mixture of catalyst and sand to monitor the reaction temperature. Then reactor was connected to the syngas feeds and the flow rate of the syngas is regulated by a mass flow controller. The liquid products with high carbon numbers (wax) were collected in the hot trap at 100 °C, the oil products were collected in the cold trap at 10 °C. The gas products were collected with air bags.

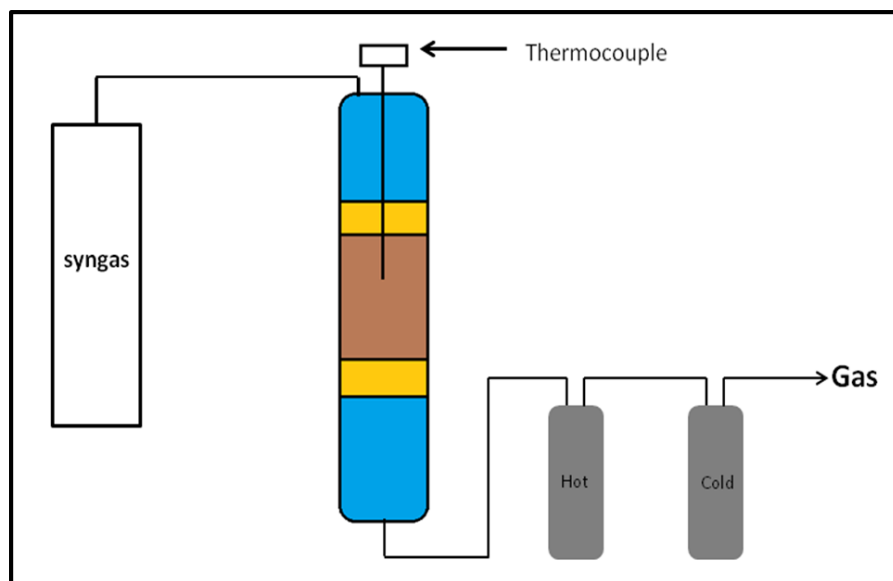


Figure 2.1 Set up of the Fixed Bed Reactor

2.3 FTS EXPERIMENTAL PROCEDURES

2.3.1 Activation of Iron Catalyst

Before the activation of iron catalyst, hydrogen gas tank was connected to the reactor and soap water was used to check the gas leaking at every screw connection part under the pressure range from 10 psi to 188 psi. After making sure there was no gas leaking, the pressure was decreased to 10 psi. Then the catalyst was activated.

Two activation methods have been employed based on in the literature [42].

Method I: Set the H₂ pressure to 10 psi. The temperature was increased very slowly (3 °C every minute) from 25 °C to 270 °C. The catalyst was activated for 24 hours. Method I was used in Run 1. Method II: Set up the H₂ pressure to 10 psi. The temperature was increased very slowly (3 °C every minute) to 230 °C. The catalyst was activated for 24 hours. Then, the temperature was decreased to 140°C very slowly. The gas tank was switched to syngas (H₂/D₂/CO), the pressure was increased to 188 psi and the

temperature was increased to 230 °C very slowly. The catalyst was activated for an additional 12 hours. Method II was used in Run 2, Run 3 and Run 4.

In method I, before the activation step, the pressure was increased to 188 psi. The gas flow rate was set up to 50% and the real gas flow rate was tested and expressed by milliliters per minute. The real flow rates are shown in Appendix Table A-1¹.

In method II, before the tank was switched to H₂/D₂/CO, the temperature was decreased to 140 °C. The gas flow rate was set up to 50% and the real gas flow rate was tested and expressed by milliliters per minute. The real flow rates are shown in Appendix Table A-1.

2.3.2 H₂/D₂ Switching Experiment Procedure

The reagents used in H₂/D₂ switching experiment were two different types of syngas H₂ : CO : N₂ (60% : 30% : 10%) and D₂ : CO : N₂ (60% : 30% : 10%). Initially, H₂/CO was used as syngas, the gas sample was collected every one or two hours, and the wax and oil samples were collected every 24 hours from hot trap and cold trap. After 120 hours, the syngas was switched from H₂/CO/N₂ to D₂/CO/N₂. The gas sample was collected every one or two hours; the wax and oil samples were collected every 24 hours. After 120 hours, the syngas was switched back to H₂/CO. The gas sample was collected periodically; the wax and oil samples were collected every 24 hours. After the collection of each gas sample, flow rate was tested in order to calculate the CO conversions.

¹ Table A-1 is only located in appendix.

2.3.3 H₂/D₂ Competition Experiment Procedure

The reagent used in H₂/D₂ competition experiment was a mixture of H₂ : D₂ : CO : N₂ (30% : 30% : 30% : 10%).

In Run 1, after activation of catalyst, the temperature was decreased to 140 °C. The H₂ gas was switched to H₂/D₂/CO/N₂. Then, the temperature was increased to 270 °C very slowly (3 °C every minute). After the temperature reached 270 °C, the gas pressure was increased to 188 psi. The gas sample was collected every 24 hours and the wax and oil samples were collected every 24 hours. After the collection of each gas sample, flow rate was tested in order to calculate the CO conversions.

In Runs 2-4, after activation, the temperature was increased to 270 °C very slowly. Then, the gas pressure was increased to 188 psi. The gas sample was collected every 24 hours and the wax and oil samples were collected every 24 hours. After the collection of each gas sample, flow rate was tested in order to calculate the CO conversions.

The H₂/D₂ experiment was run for 94 hours.

2.4 PRODUCT ANALYSIS

The wax and oil samples produced from H₂/D₂ switching experiment were analyzed by Focus GC with flame ionization detector. The wax and oil samples produced from H₂/D₂ competition experiment were sent to the Center of Applied Energy Research in University of Kentucky to be analyzed by HP 5890 GC/MS with a 60 m SPB -5 capillary column. The mole fraction of product with different carbon numbers was calculated based on the percent area of each corresponding peak. The chain growth probability (α)

was determined based on the product distribution of the wax and oil product. The relative amounts of isotopic isomers of an n-alkane were determined by GC/MS.

The gas samples were analyzed by Agilent 3000 Micro 4 channel gas chromatograph. The mole percent of each gas product and remaining reactants were obtained. From the Micro GC results, the relative amount of gas products and the excess CO can be obtained. Based on the real flow rate (mL/min), which was tested at 140 °C and 188 psi before H₂/D₂ competition experiment, the CO conversions can be calculated. For example, at 140 °C and 188 psi, the 50% of mass flow controller gives the real flow rate of 36 mL/min (Table A-1).

During FT reactions, the gas flow rate was measured in mL/min after the collection of each gas product. As mentioned before, the percentage of CO in the syngas is 30%, and the percentage of excess CO can be obtained from the Micro GC results. Therefore, the mole of CO (CO_{in}) which was introduced into the reactor and the mole of CO (CO_{out}) can be calculated by eq. 2.1 and 2.2.

$$\text{CO}_{\text{in}} (\text{mol}) = \text{real gas flow rate (mL/min)} * 30\% \quad (2.1)$$

$$\text{CO}_{\text{out}} (\text{mol}) = \text{measured gas flow rate (mL/min)} * (\text{CO\% in the gas sample}) \quad (2.2)$$

So, the CO conversion can be calculated by eq. 2.3.

$$\text{CO conversion (\%)} = \frac{\text{CO}_{\text{in}} (\text{mol}) - \text{CO}_{\text{out}} (\text{mol})}{\text{CO}_{\text{in}} (\text{mol})} \times 100\% \quad (2.3)$$

For example, if the real gas flow rate 140 °C and 188 psi is 36 ml/min, the measured gas flow rate is 30 mL/min and the CO% obtained from Micro GC is 10%. So, the CO conversion can be calculated: $\text{CO conversion (\%)} = \frac{36 \times 30\% - 30 \times 10\%}{36 \times 30\%} \times 100\% = 72.2\%$.

2.5 IDENTIFICATION OF BRANCHED HYDROCARBONS IN FTS

2.5.1 Hydrogenation of Heavy Chain FTS Product

Two grams of wax product was placed in a metal pump, 2 mL of diethyl ether was added to the pump and mixed well with the wax product. Then 0.05 g of Pt/C catalyst was added to the mixture. The pump was then connected to H₂ gas tank, the pressure was increased to 150 psi. The pump was shaken periodically for 4 hours. After the hydrogenation was completed, the product was filtered and then dissolved in CS₂. A GC spectrum of the hydrogenation product was obtained.

2.5.2 Identification of Branched Hydrocarbons

Through the complete hydrogenation of the wax product, all the olefins have been converted to corresponding paraffin. By comparing the product GC spectrum before and after hydrogenation, the branched hydrocarbons can be found. Because after hydrogenation, the peaks of olefins should be disappeared and merge to the peak of corresponding paraffin. Depending on the disappeared and remaining peaks, the branched hydrocarbons can be determined.

For example Figure 2.2 (A) shows the GC spectra of C₈ products from H₂/D₂

switching experiment catalyzed a Fe/Si/K catalyst with a CO conversion level of 56%.

Figure 2.2 (A) and Figure 2.2 (B) show the chromatogram of this C8 product before and after hydrogenation, respectively. Similar figures were obtained for the other carbon numbers as well as the other runs. By comparing Figure 2.2 (A) and Figure 2.2 (B), it can be found that the 1-olefin, trans-2-olefin and cis-2-olefin have been converted to n-paraffin. The branched olefins have been converted to corresponding branched paraffins. Based on this method, the branched hydrocarbons

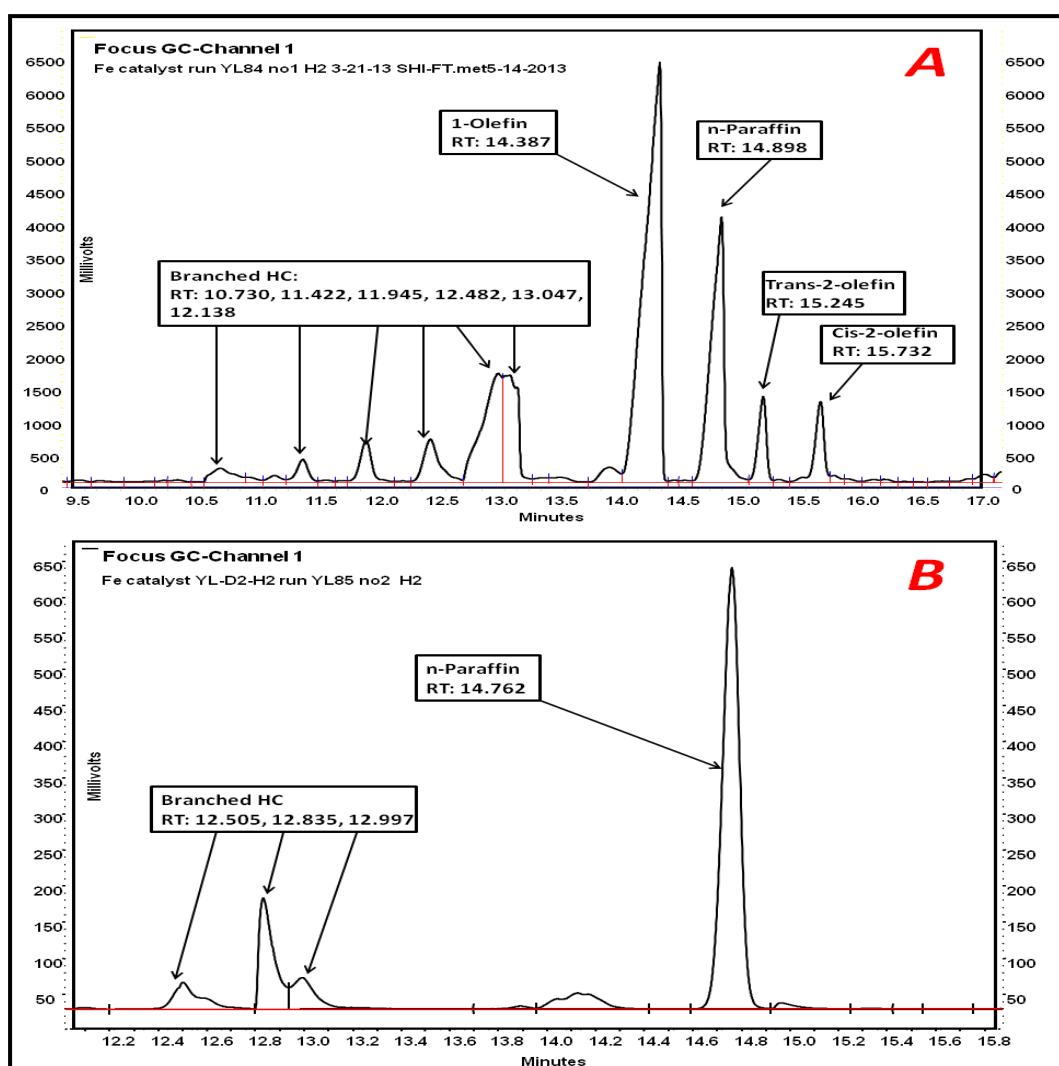


Figure 2.2 A GC spectrum of C8 product. (A): before hydrogenation; (B): after hydrogenation

CHAPTER 3

INVERSE ISOTOPE EFFECT IN IRON CATALYZED FISCHER-TROPSCH SYNTHESIS

3.1 INTRODUCTION

Fischer-Tropsch synthesis is a very useful and important reaction practically and technically. It has been studied by scientists for almost a century, even though a lot of study has been done, the mechanism of the FT reaction still remains uncertain [43-46].

One of the most useful experimental techniques that may be used in testing mechanisms of any reaction is the isotope study. The carbon and hydrogen isotope tracer studies have been widely used in the study of FTS mechanism. In 1981, Kellner and Bell reported that there was an inverse isotope effect during the formation of hydrocarbons from C₁ to C₅ in Ru catalyzed FTS [47]. Davis et al also reported that there was an inverse isotope effect during Co catalyzed FT reactions in 2009 [48]. By conducting H₂/D₂ switching experiment, Shi and Jin in 2011 studied that isotope effect in Co/SiO₂ catalyzed FTS and found that the CO conversion increased when the syngas H₂/CO was switched to D₂/CO and the ratio of $[\text{CO}_{\text{conv.}}]^{\text{H}} / [\text{CO}_{\text{conv.}}]^{\text{D}}$ was ranging from 0.66 to 0.86 [23]. By using H₂/D₂ competitive method, Shi and Jin found that there were deuterium enrichments in hydrocarbons from C₆ to C₂₄ and the H/D ratio decreased with the increasing carbon number [23].

In this study, in order to find out whether there exists the inverse isotope effect and deuterium enrichment in Fe catalyzed FTS or not, H₂/D₂ switching experiment and H₂/D₂

competition experiment have been conducted. The Fe/Si/K and Fe/Si catalysts have been used in this study.

3.2 RESULTS OF H₂/D₂ SWITCHING EXPERIMENT

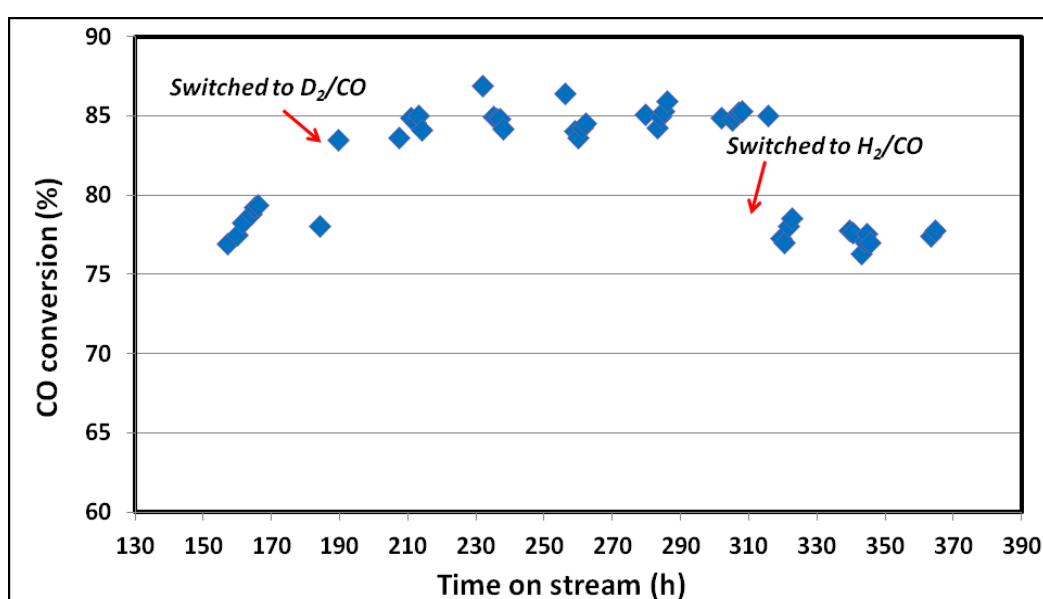
3.2.1 CO Conversions

The catalysts without potassium (Fe/Si) showed very low activities. The CO conversions were less than 10% and yield of liquid products were less than one gram every 24 hours. On the other hand, when the iron catalysts contained potassium (Fe/Si/K) were used, the CO conversions were relatively high which ranging from 59% to 76% among three runs and more than 4 g of liquid product was collected every 24 hours. Even though the amount of potassium added was relatively low, there was a large difference in CO conversion between Fe/Si/K and Fe/Si catalysts. It has been reported that potassium acted as a promoter for the iron catalyst [33, 34, 36]. Potassium can increase the catalytic activity for FTS and water-gas-shift (WGS) reactions [34, 39]. As a result, the CO conversion increased significantly when Fe/Si/K catalyst was used.

Results of the iron catalyzed H₂/D₂ switching experiments are shown in the Table 3.1. The results were from 4 iron catalyzed FTS runs. The second column shows the type of catalyst was used. The third column is the conditions in FTS runs. The average CO conversions and the standard deviations when H₂/CO and D₂/CO was used are shown in the fourth column. The CO conversion (%) ratios between H₂/CO and D₂/CO are shown. A detailed CO conversion (%) result is shown in Fig. 3.1.

Table 3.1 CO conversions during H₂/D₂ switching experiments

Run	Catalyst	Conditions		CO Conversion (%)			[CO _{conv.}] ^H /[CO _{conv.}] ^D
		T (°C)	P (psi)	H ₂ /CO	D ₂ /CO	H ₂ /CO	
1	Fe/Si/K	270	188	59.5 ± 1.9	70.8 ± 1.7	61.6 ± 1.7	0.86 ± 0.02
2	Fe/Si/K	270	188	11.8 ± 1.7	27.5 ± 2.4	17.0 ± 0.6	0.52 ± 0.13
3	Fe/Si/K	270	188	78.3 ± 0.9	84.8 ± 0.6	77.5 ± 0.6	0.92 ± 0.01
4	Fe/K	270	188	8.2 ± 0.9	18.8 ± 2.2	N/A	0.44

**Figure 3.1** CO conversion in Fe/Si/K catalyzed H₂/D₂ switching experiment of the 3rd run

In the first run, the catalyst used was Fe/Si/K. The CO conversion was 59.5% when H₂/CO was used as syngas, when the syngas was switched to D₂/CO, the CO conversion increase to 70.8%. Then, the CO conversion decreased to 61.6% when the syngas was switched back to H₂/CO. The CO conversion ratio between H₂/CO and D₂/CO was 0.86.

In the second run, the catalyst used was Fe/Si/K. The CO conversion was 11.8% when H₂/CO was used as syngas, when the syngas was switched to D₂/CO, the CO

conversion increase to 27.5%. Then, the CO conversion decreased to 17% when the syngas was switched back to H₂/CO. The CO conversion ratio between H₂/CO and D₂/CO was 0.52.

In the third run, the catalyst used was Fe/Si/K. The CO conversion was 78.3% when H₂/CO was used as syngas, when the syngas was switched to D₂/CO, the CO conversion increase to 84.8%. Then, the CO conversion decreased to 77.5% when the syngas was switched back to H₂/CO. The CO conversion ratio between H₂/CO and D₂/CO was 0.92.

In the fourth run, the catalyst used was Fe/Si. The CO conversion was 8.2% when H₂/CO was used as syngas and it was increased to 18.8% when the syngas was switched to D₂/CO. The CO conversion ratio between H₂/CO and D₂/CO was 0.44.

3.2.2 CO to Hydrocarbon Products Conversions in Different FTS Runs

Based on eq. 2.3, CO to hydrocarbon (HC), CO to C1+, CO to C2+, CO to C3+ and CO to C4+ conversions were calculated. The results are shown in Table 3.2. The run number is shown in the first column, the second and the third column shown the type of iron catalyst and the type of CO conversion, respectively.

Table 3.2 CO to hydrocarbon products conversions

Run	Catalyst	CO conversions	CO Conversion (%)			[CO _{conv.}] ^H /[CO _{conv.}] ^D
			H ₂ /CO	D ₂ /CO	H ₂ /CO	
1	Fe/Si/K	CO to HC	22.8 ± 1.9	41.3 ± 1.3	25.6 ± 1.1	0.59 ± 0.05
		CO to C1+	18.7 ± 1.9	37.4 ± 1.4	22.5 ± 1.1	0.55 ± 0.07
		CO to C2+	17.1 ± 1.9	36.1 ± 1.4	21.2 ± 1.1	0.53 ± 0.08
		CO to C3+	15.3 ± 2.0	34.4 ± 1.4	19.8 ± 1.1	0.51 ± 0.09
		CO to C4+	14.4 ± 2.1	33.5 ± 1.5	19.0 ± 1.1	0.50 ± 0.09
2	Fe/Si/K	CO to HC	10.2 ± 1.7	24.7 ± 2.2	13.2 ± 0.6	0.47 ± 0.08

Table 3.2 (continued)

Run	Catalyst	CO conversion	CO Conversion (%)			$[\text{CO}_{\text{conv.}}]^{\text{H}}/[\text{CO}_{\text{conv.}}]^{\text{D}}$
			H ₂ /CO	D ₂ /CO	H ₂ /CO	
2	Fe/Si/K	CO to C1+	9.0 ± 1.7	22.7 ± 2.1	11.7 ± 0.7	0.46 ± 0.08
		CO to C2+	8.5 ± 1.7	21.8 ± 1.9	11.1 ± 0.7	0.45 ± 0.08
		CO to C3+	7.9 ± 1.7	21.0 ± 1.9	10.4 ± 0.7	0.44 ± 0.08
		CO to C4+	7.2 ± 1.7	19.9 ± 1.9	9.6 ± 0.7	0.42 ± 0.08
3	Fe/Si/K	CO to HC	67.4 ± 0.9	75.4 ± 0.9	66.5 ± 0.9	0.89 ± 0.01
		CO to C1+	60.3 ± 1.0	67.7 ± 1.1	59.9 ± 1.1	0.89 ± 0.01
		CO to C2+	59.5 ± 1.0	66.8 ± 1.1	58.9 ± 1.1	0.89 ± 0.01
		CO to C3+	56.6 ± 1.0	63.9 ± 1.2	56.2 ± 1.2	0.89 ± 0.01
		CO to C4+	51.3 ± 0.9	57.6 ± 1.2	50.9 ± 1.3	0.89 ± 0.01
4	Fe/Si	CO to HC	6.2 ± 0.9	17.3 ± 1.4	N/A	0.36
		CO to C1+	4.1 ± 1.1	14. ± 1.5	N/A	0.29
		CO to C2+	3.6 ± 1.2	13.6 ± 1.5	N/A	0.26
		CO to C3+	3.1 ± 1.2	12.9 ± 1.5	N/A	0.24
		CO to C4+	2.8 ± 1.3	12.6 ± 1.6	N/A	0.22

As shown in Table 3.2, during all the H₂/D₂ switching runs, the CO conversions increase when the syngas was switched from H₂/CO to D₂/CO and it decreased when the syngas was switched back to H₂/CO. For example, in the first run, the CO to hydrocarbon (HC) conversion was 22.8% when H₂/CO was used as syngas, when the syngas was switched to D₂/CO, the CO conversion increase to 41.3%. Then, the CO conversion decreased to 25.6% when the syngas was switched back to H₂/CO.

The value of CO conversion ratios H₂/CO and D₂/CO are in the range of 0.42 to 0.89 during Fe/Si/K catalyzed FTS runs and in the range of 0.22 to 0.36 during the Fe/Si run.

3.2.3 The Inverse Isotope Effect during Methane Formation

Table 3.3 shows the methane formations when H₂/CO and D₂/CO was used during all of the FTS runs. As it can be seen from Table 3.3, the methane formation increased when the syngas was switched from H₂/CO to D₂/CO, and it decreased when the syngas

was switched back to H₂/CO. The ratios of methane formation of run 1 to 4 were smaller than one.

Table 3.3 Methane formations during iron catalyzed FTS

Run	Catalyst	CH ₄ formation (%)			[CH ₄] ^H /[CH ₄] ^D
		H ₂ /CO	D ₂ /CO	H ₂ /CO	
1	Fe/Si/K	3.70 ± 0.01	3.87 ± 0.10	3.08 ± 0.03	0.88 ± 0.11
2	Fe/Si/K	1.50 ± 0.19	2.34 ± 0.31	1.78 ± 0.14	0.70 ± 0.08
3	Fe/Si/K	7.02 ± 0.20	7.56 ± 0.27	6.57 ± 0.22	0.90 ± 0.04
4	Fe/Si	2.12 ± 0.25	3.07 ± 0.18	N/A	0.69

3.2.4 CO to Gas Phase Product Conversion and Methane – CO₂ Selectivity

Table 3.4 shows CO to light chain product (C1 to C4) conversion. The top is the reaction conditions, run number is shown in the first column, and the product distribution is shown from column two to eight. Results from H₂/CO and D₂/CO are obtained.

Table 3.4 Product distribution during iron catalyzed FTS

T = 270 °C, P = 188 psi, H ₂ /CO							
Run #	CO _{con} (%)	CO ₂ form. (%)	CH ₄ form. (%)	C2 form. (%)	C3 form. (%)	C4 form. (%)	C4+ form. (%)
1	60.41	36.44	3.67	1.40	1.65	0.89	16.37
2	14.59	3.66	1.65	0.29	0.63	0.39	8.94
3	77.77	10.98	6.74	0.88	2.83	5.29	51.05
4	8.63	2.41	2.12	0.51	0.53	0.27	2.79
T = 270 °C, P = 188 psi, D ₂ /CO							
Run #	CO _{con} (%)	CO ₂ form. (%)	CH ₄ form. (%)	C2 form. (%)	C3 form. (%)	C4 form. (%)	C4+ form. (%)
1	70.82	29.66	3.87	1.38	1.62	0.91	33.54
2	27.08	3.39	2.34	0.43	0.83	0.48	20.65
3	84.82	9.54	7.56	0.86	2.99	6.27	57.59
4	19.60	2.31	3.07	0.61	0.70	0.36	12.56

From Table 3.4, it can be found that during run 1, the CO₂ formation was 36.44% and 29.66% when H₂/CO and D₂/CO was used, which is the highest among all of the FTS runs; run 3 has the highest methane formations which were 6.74% and 7.56% when H₂/CO and D₂/CO was used; the C₂, C₃ and C₄ hydrocarbons formation were less than CO₂ and methane during all the FTS runs; most of CO has been converted to hydrocarbons which have carbon numbers higher than 4 except for run 1. Based on Table 3.4, a methane – CO₂ selectivity graph was obtained. Figure 3.2 shows the methane – CO₂ selectivity graph for different FT runs. Run 1 to 4 is shown in Figure 3.2 (A) to Figure 3.2 (D), respectively.

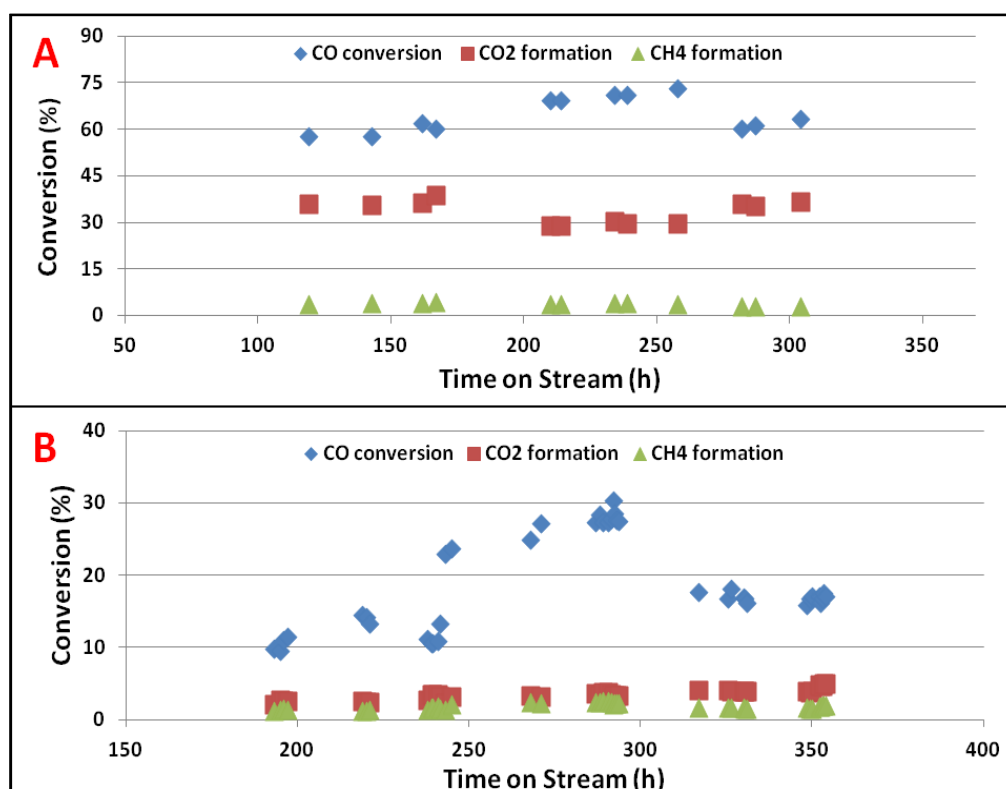


Figure 3.2 Methane – CO₂ selectivity for different runs: (A). Run 1; (B). Run 2; (C). Run 3; (D) Run 4.

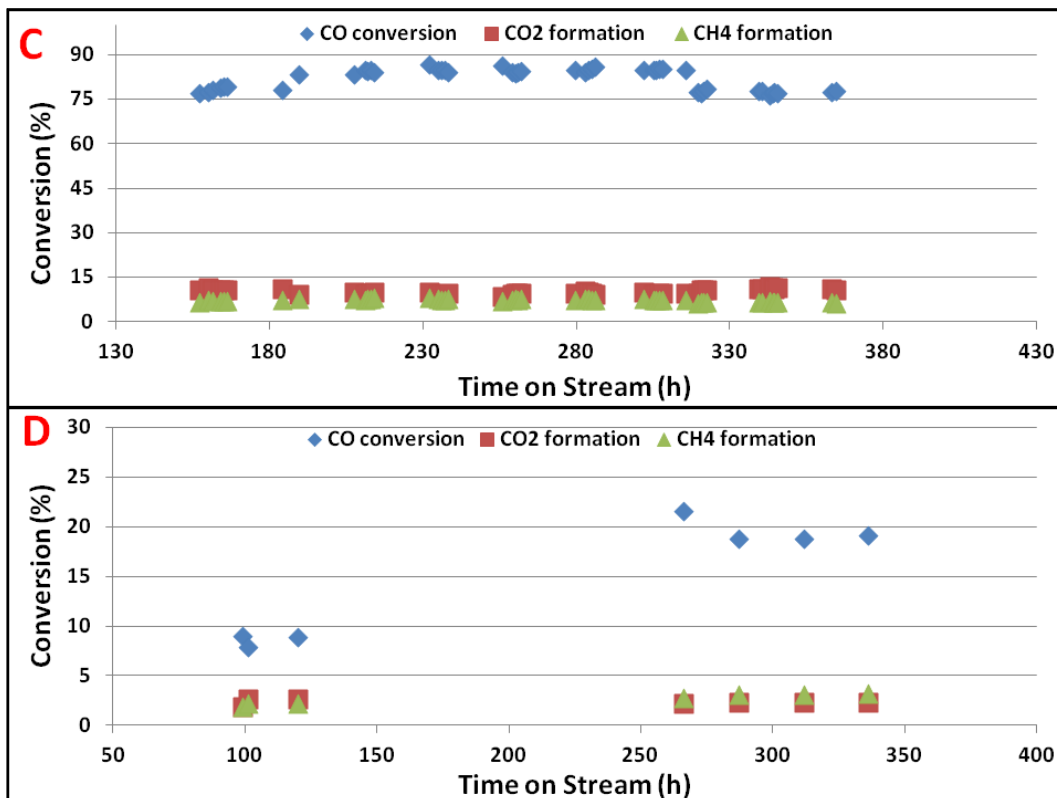


Table 3.5 shows CO to ethane, ethene, propane and propene formation. The reaction conditions are shown on top, run numbers and CO conversions are shown in column 1 to 5. Results from H₂/CO and D₂/CO are obtained. It can be seen from Table 3.5, the production of C₂ and C₃ products was relatively low among all the FTS runs. The ratio of [ethane]/[ethene] was lower than 1 during run 1 to run 3, the ratio of [propane]/[propene] was lower than 1 during run 1.

Table 3.5 Alkene and alkane selectivity of C₂ and C₃ products

T = 270 °C, P = 188 psi, H ₂ /CO				
Run #	Ethane form. (%)	Ethene form. (%)	Propane form. (%)	Propene form. (%)
1	0.57	0.83	0.33	1.32

Table 3.5 (continued)

T = 270 °C, P = 188 psi, H ₂ /CO				
Run #	Ethane form. (%)	Ethene form. (%)	Propane form. (%)	Propene form. (%)
2	0.09	0.20	0.63	0.01
3	0.42	0.46	2.80	0.03
4	0.48	0.03	0.32	0.21
T = 270 °C, P = 188 psi, D ₂ /CO				
Run #	Ethane form. (%)	Ethene form. (%)	Propane form. (%)	Propene form. (%)
1	0.45	0.93	0.33	1.29
2	0.12	0.31	0.82	0.01
3	0.35	0.51	2.96	0.03
4	0.56	0.05	0.40	0.29

3.3 DETERMINATION OF CHAIN GROWTH PROBABILITY (α) VALUE

The chain growth probability can be determined based on the ASF equation. The ASF equation can be expressed by eq. 3.1, where

$$r_n = r_1 \alpha^{n-1} \quad (3.1)$$

r_n is the production rate of a compound with carbon number n , r_1 is the formation rate of C1 species, α presents the chain growth probability.

The chain growth probability (α) can be determined experimentally based on the product distribution of the products. Figure 3.3 shows a sample of GC spectrum of products with carbon number 8 produced from H₂/D₂ switching experiment catalyzed by a Fe/Si/K catalyst with a CO conversion level of 59%. For straight chain hydrocarbon products in different carbon numbers, the 1-olefin has the shortest retention and followed by paraffin then trans-2-olefin, the cis-2-olefin product.

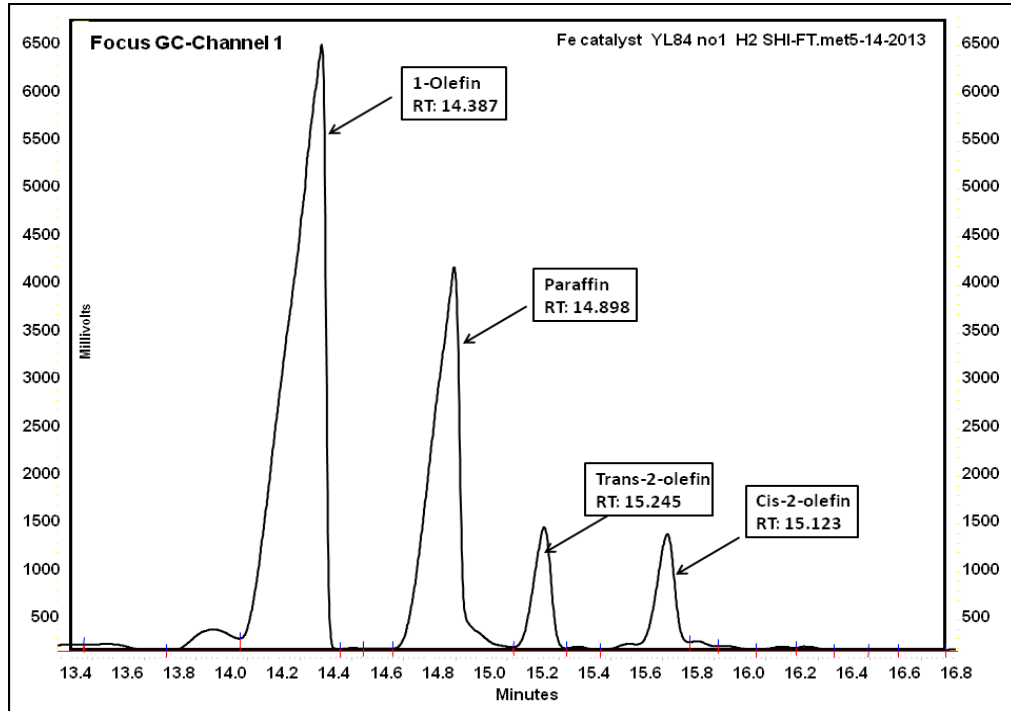


Figure 3.3 GC spectrum of C8 product

Based on the GC spectrum, the corresponding peak area of 1-olefin, paraffin, trans-2-olefin and cis-2-olefin product from C9 to C17 can be found. The area represents the weight of corresponding product. Then the weight percent of each product can be obtained by dividing the peak area of each product by the total peak area. Then, the number of moles of each product can be obtained by dividing the weight percent by the molar mass of the corresponding product. Then, the mole fraction of 1-olefin, paraffin, trans-2-olefin and cis-2-olefin in different carbon numbers can be determined. According to eq. 3.1, the mole of hydrocarbon with a carbon number n (C_n) can be calculated by eq. 3.2, where C_1 is the mole of methane.

$$C_n = C_1 \alpha^{n-1} \quad (3.2)$$

Both sides of eq. 3.2 divided by the total amounts of the product, eq. 3.3 and 3.4 can be obtained, where m_n is the mole fraction of hydrocarbon with carbon number n , and m_1 is the mole fraction of methane.

$$C_n/\text{total} = (C_1/\text{total})\alpha^{n-1} \quad (3.3)$$

$$m_n = m_1 \alpha^{n-1} \quad (3.4)$$

The m_n can be obtained by GC analysis. Eq. 3.4 can be converted to eq. 3.5 by taking natural log on both sides of eq. 3.4.

$$\ln(m_n) = \ln(m_1) + (n-1) \times \ln\alpha \quad (3.5)$$

In eq. 3.5, n is carbon number, m_n represents the mole fraction of product with carbon number n , m_1 is the mole fraction of methane, α is the chain growth probability. Finally, a $\ln(m_n)$ – carbon number straight line can be obtained, which is also known as the product distribution of FTS. Figure 3.4 shows a product distribution of FTS product from a Fe/Si/K catalyst with a CO conversion of 59%. The product distributions of other catalysts have also been obtained.

As shown in eq. 3.5, the slope of $\ln(m_n)$ – carbon number straight line, which is -0.2296 in the example is the natural log of the α value of this Fe/Si/K catalyst. So, α value of this catalyst equals $e^{-0.2296} = 0.79$.

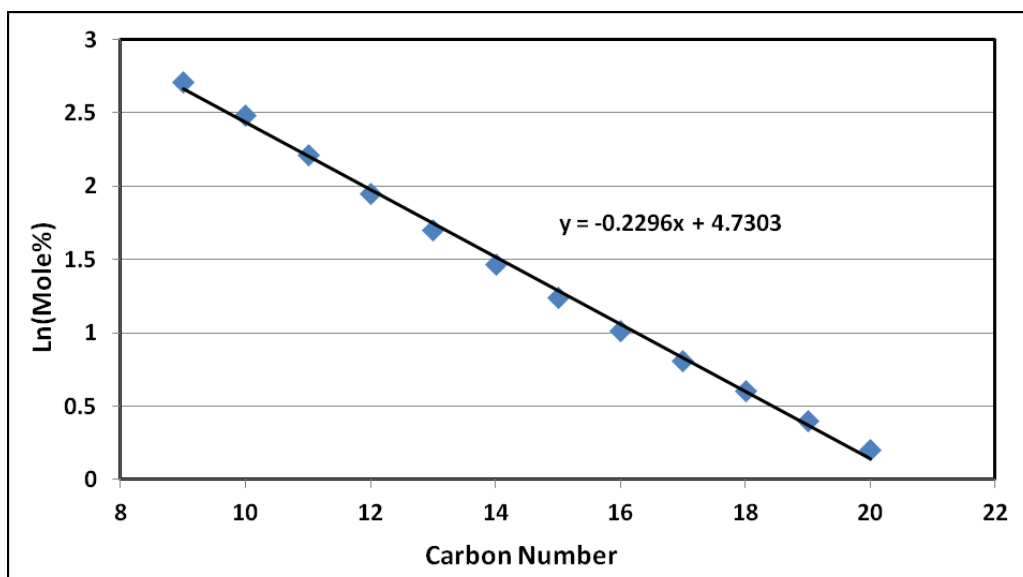


Figure 3.4 Production distribution of Fe/Si/K product

The chain growth probability (α) values of each FTS run are shown in Table 3.6. It summarizes the α value of each sample and the average α values of each iron catalyzed run.

Table 3.6 The α values of each FTS run

Catalyst	Fe/Si/K with CO conversion 60%					
Sample ID	1	2	3	4	5	Average
α value	0.80	0.80	0.83	0.78	0.78	0.80 ± 0.02
Catalyst	Fe/Si/K with CO conversion 15%					
Sample ID	1	2	3	4	5	Average
α value	0.78	0.80	0.77	0.81	0.82	0.80 ± 0.02
Catalyst	Fe/Si/K with CO conversion 77%					
Sample ID	1	2	3	4	5	Average
α value	0.80	0.80	0.79	0.79	0.81	0.80 ± 0.01
Catalyst	Fe/Si with CO conversion 8%					
Sample ID	1	2	3	4	5	Average
α value	0.71	0.76	N/A	N/A	N/A	0.74 ± 0.04

The α of the Fe/Si/K catalyst with a CO conversion 59% which was used in the first run is 0.80. The α of the Fe/Si/K catalyst with a CO conversion 15% which was used in the

second run is 0.80. The α of the Fe/Si/K catalyst with a CO conversion 77% which was used in the third run is 0.80. The α of the Fe/Si catalyst with a CO conversion 8% which was used in the fourth run is 0.74.

3.4 DISCUSSION

3.4.1 The Modified Alkylidene Mechanism

The results of iron catalyzed H₂/D₂ switching experiments in the Table 3.1 show that the CO conversions increased when the syngas was switched from H₂/CO to D₂/CO. The ratios of [CO_{conv.}]^H/[CO_{conv.}]^D ranging from 0.52 to 0.92 in the Fe/Si/K catalyzed H₂/D₂ switching experiments and the ratio of [CO_{conv.}]^H/[CO_{conv.}]^D was 0.44 in the Fe/Si catalyzed H₂/D₂ switching experiment. The results indicate that the reaction was faster when D₂/CO was used as syngas than H₂/CO was used, which clearly suggests that there is an inverse isotope effect during the iron catalyzed FTS.

From the previous study, the inverse isotope effects of Fischer-Tropsch Synthesis were observed in Co and Fe catalyzed reactions [23, 49]. Inverse isotope effects and deuterium enrichment in hydrocarbon produced by Co catalyzed FT reactions have been reported [23]. Based on the inverse isotope effect and deuterium enrichment in Co catalyzed FTS, a modified alkylidene mechanism of FTS has been published [23]. The modified alkylidene mechanism can explain the formation of straight hydrocarbon product and branched hydrocarbon product produced by cobalt catalyst; it can also explain the inverse isotope effect and deuterium enrichment in Co catalyzed.

The FTS can be considered as a polymerization reaction, in the modified alkylidene mechanism, the monomer of FTS is $M\equiv CH$. The Figure 3.5 shows the formation of C1 species and methane from the monomer. As shown in Figure 3.4, the reactant carbon monoxide can be absorbed to the surface of metal catalyst to form an intermediate which is a carbon – metal complex. This intermediate can be hydrogenated to form monomer $M=CH$, which can undergo further hydrogenation gives $M=CH_2$. With the additional hydrogenation of $M=CH_2$, an intermediate $M-CH_3$ can be formed and finally, methane is formed by the hydrogenation of $M-CH_3$.

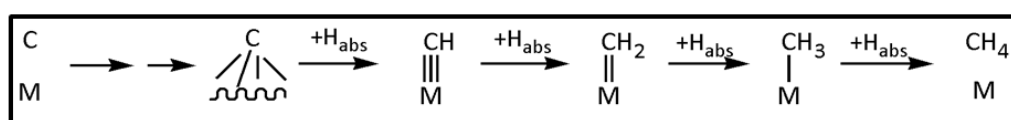


Figure 3.5 The formation of C1 species and methane

The formation of C2 species undergoes through two pathways which is shown in Figure 3.6. The following schemes show the formation of C2 species in FTS.

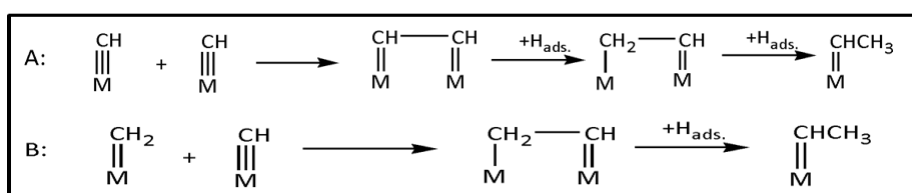


Figure 3.6 The formation of C-C bond and C2 species in FTS

In the pathway A, coupling of two $M\equiv CH$ monomers forms intermediate $M=CH-CH=M$, this intermediate can undergo hydrogenation gives ethylidene ($M=CH-CH_3$), which acted as the C2 initiator in FTS. In the pathway B, coupling of $M=CH_2$ and

$M\equiv CH$ generates the intermediate $M-CH_2-CH=M$ which can be hydrogenated to form ethylidene ($M=CH-CH_3$). The ethylidene can be terminated to ethene or ethane. It has been reported that the unsaturated ethene acted as an initiator in the growth of hydrocarbons in FTS [17, 50].

The unsaturated ethene can be re-absorbed to the surface of metal catalyst and can re-grow to longer chain hydrocarbons. Figure 3.7 shows the re-adsorption of ethene to form longer chain hydrocarbons. As it shows, ethene molecule is re-adsorbed to the metal catalyst to form ethylidene. The addition of FTS monomer to ethylidene group generates 1-propyliden, by the hydrogenation of 1-propyliden, propane can be formed; by the β elimination of 1-propyliden, propene can be formed.

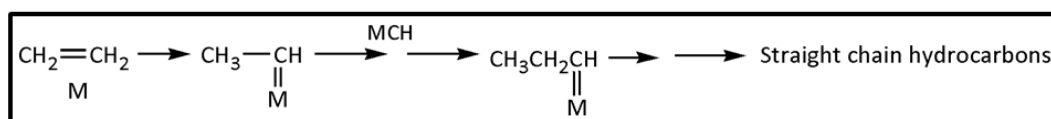


Figure 3.7 The chain propagation steps in FTS

The re-adsorption of propene and other heavier 1-alkenes can produce 1-alkylidenes and also 2-alkylidenes as shown in Figure 3.8. The re-growth 1-alkylidenes will produce straight chain hydrocarbons, while the re-growth of 2-alkylidenes will produce the branched hydrocarbons. In Figure 3.8A, the re-adsorbed propene will generate 2-methylpropane and 2-methylpropene; in Figure 3.8B the re-adsorbed 1-butene can produce 2-methylbutane as well as 2-methylbutene and 3-methyl branched hydrocarbons. In this case, the re-adsorbed 1-pentene can produce 2-methyl branched

hydrocarbons, 3-methyl branched hydrocarbons and 4-methyl branched hydrocarbons, and so on.

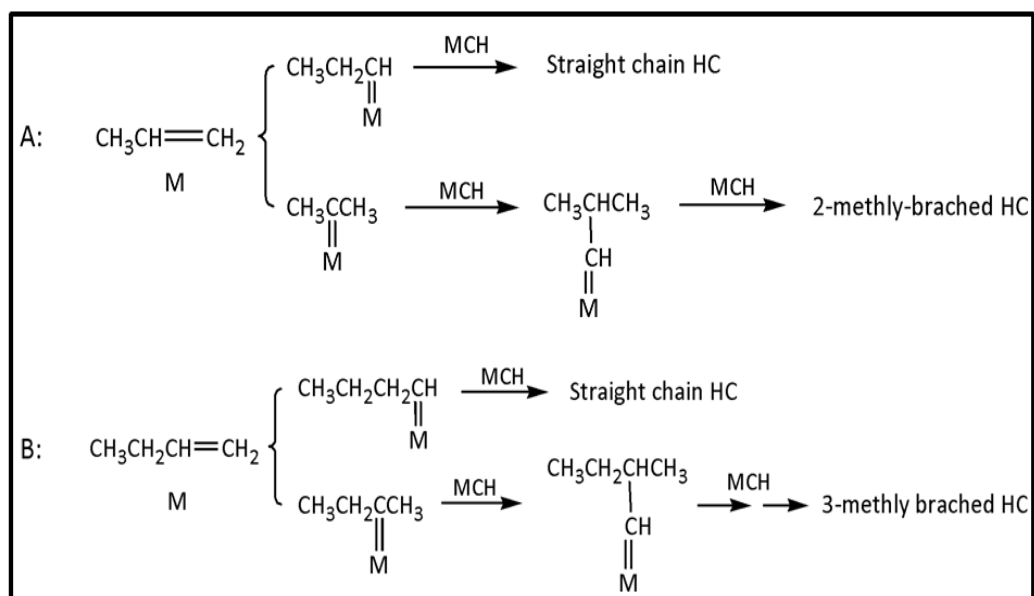


Figure 3.8 Formation of branched hydrocarbons in FTS

The Figure 3.9 shows the overall modified alkylidene mechanism for FTS. The monomer in this mechanism is $\text{M}\equiv\text{CH}$. As shown in Figure 3.9, the coupling of two monomers gives the ethylidene which acts as the C2 initiator of FTS. The termination of ethylidene will produce ethane and ethene. Unsaturated olefin such as ethene can be re-adsorbed to the surface of metal catalyst to reform 1-alkylidenes and 2-alkylidenes, the re-growth 1-alkylidenes will be terminated to straight chain hydrocarbons and the re-growth 2-alkylidenes will produce methyl branched hydrocarbons.

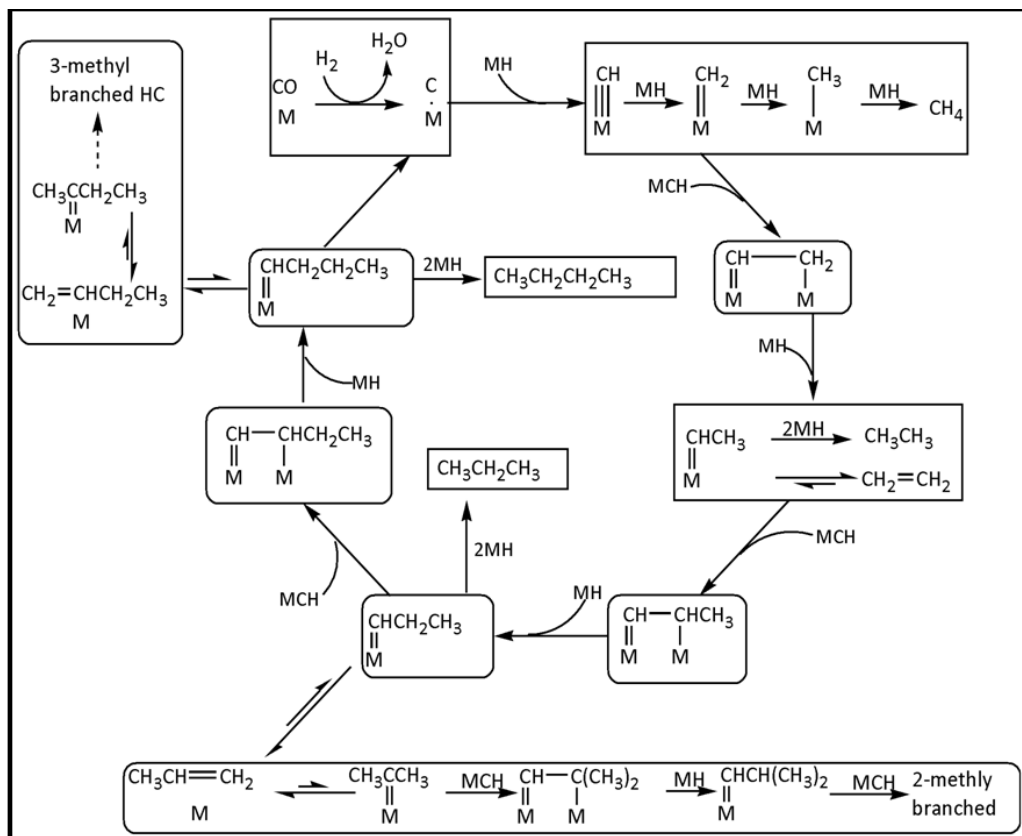


Figure 3.9 The modified alkylidene mechanism of FTS

3.4.2 Explanation of Inverse Isotope Effect Alkyl Mechanisms and Alkenyl Mechanism

The Alkyl mechanism was published in 1980, which is shown in Figure 3.10. The monomer of Alkyl mechanism is $M=CH_2$. As shown in Figure 3.10, there is a hybridization change in the carbon on the monomer from sp^2 to sp^3 during the carbon-carbon bond formation in Alkyl mechanism, which leads to K_H/K_D smaller than one. This mechanism can explain the inverse isotope in both iron and cobalt catalyzed FTS.

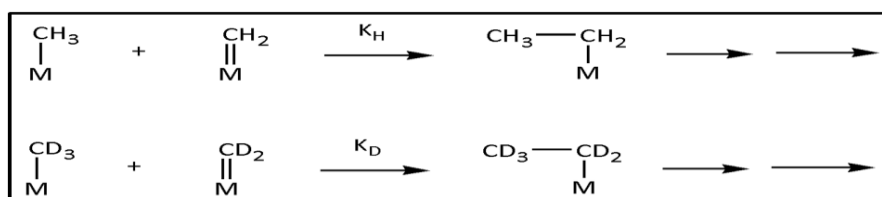


Figure 3.10 The carbon-carbon bond formation in Alkyl mechanism

Similar to Alkyl mechanism, the Alkenyl mechanism, as shown in Figure 3.11, during the carbon-carbon bond formation in Alkenyl mechanism, the unsaturated 1-olefin can be re-adsorbed to the surface of metal catalyst to form an intermediate ($\text{CH}_2=\text{CH-M}$), the coupling of this intermediate and a monomer generates $\text{CH}_2=\text{CH-CH}_2\text{-M}$ which undergoes isomerization to form $\text{CH}_3\text{-CH=CH-M}$. It can explain the inverse isotope effect in both iron and cobalt catalyzed FTS by the hybridization change of the carbon in the monomer ($\text{M}=\text{CH}_2$) from sp^2 to sp^3 .

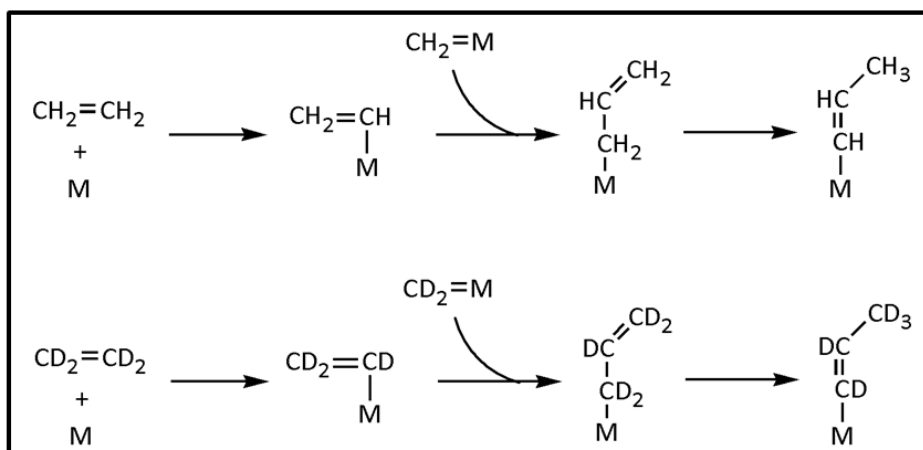


Figure 3.11 The C-C bond formation in Alkenyl mechanism

3.4.3 Explanation of Inverse Isotope Effect by the Modified Alkyliene Mechanism

It was believed that the origin of inverse isotope effect is the increase in bond order or the re-hybridization of carbon from sp to sp^2 or from sp^2 to sp^3 [34, 53].

Based on the modified alkylidene mechanism, during the formation of C1 species and methane, the sp carbon in monomer $\text{M}\equiv\text{CH}$ is hybridized into a sp^2 carbon and generates $\text{M}=\text{CH}$, the sp^2 carbon in $\text{M}=\text{CH}$ is hybridized into a sp^3 carbon and gives $\text{M}-\text{CH}_3$. Inverse isotope effect occurs in these two steps and then methane is formed with the

hydrogenation of M-CH₃ where there is no isotope effect. Figure 3.12 shows the formation of methane and deuterated methane when H₂/CO and D₂/CO are used. The reaction is faster when D₂/CO was used as syngas, so both K₁^H/K₁^D and K₂^H/K₂^D are smaller than one. This can explain the inverse isotope effect in the formation of methane shows in Table 3.3.

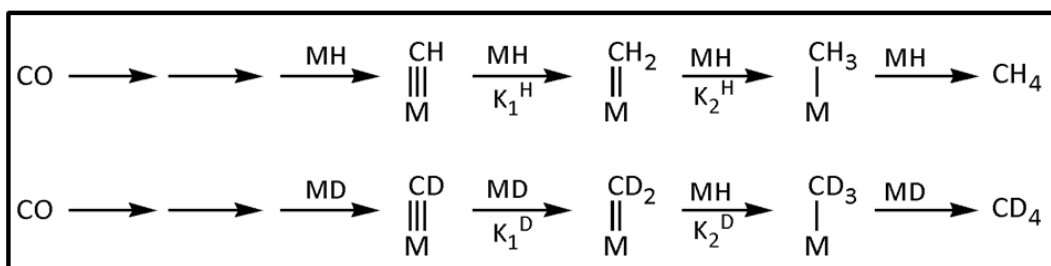


Figure 3.12 The formation of methane and deuterated methane

On the other hand, chain propagation step is shown in Figure 3.13. During the chain propagation step, carbon-carbon bond is formed with the hybridization change from sp² to sp³ on the growing chain and hybridization change from sp to sp² on monomer. These hybridization changes of carbon generate the inverse isotope effect in the chain propagation steps.

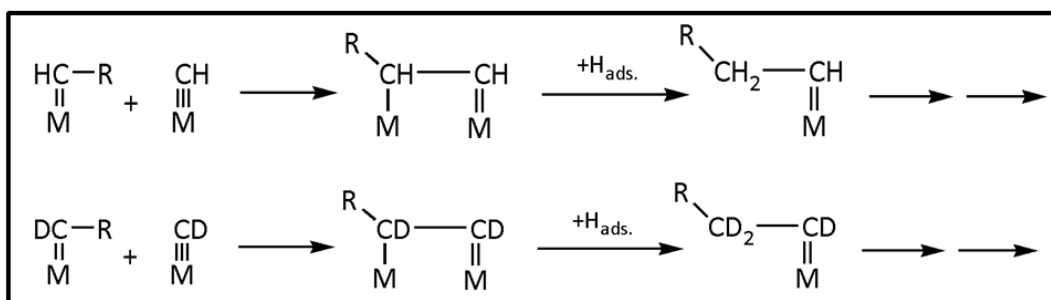


Figure 3.13 Carbon-carbon bond formations in FTS

Overall, during the chain propagation step in FTS, carbon-carbon bond was formed by the coupling of an alkylidene group and a monomer, which makes the carbon hybridization changed from sp^2 to sp^3 on the growing chain and hybridization changed from sp to sp^2 on monomer. So, the hybridization change presents not only on the formation of C1 species and chain propagation but both. Furthermore, the inverse isotope effect in FTS is the reason of deuterium enrichment which will be discussed in Chapter IV.

3.4.4 The Calculation of Inverse Isotope Effect in Iron Catalyzed FTS

According to the ASF equation, $r_n = r_1\alpha^{n-1}$, in which r_n is the formation rate of product with carbon number n , r_1 represents the formation rate of C1 species, α is the chain growth probability. So the ASF equation can be re-written as eq. 3.6

$$r_n = C_1\alpha^{n-1} \quad (3.6)$$

For the reaction that H_2/CO was used as syngas, $r_n^H = C_1^H(\alpha_H)^{n-1}$, when the syngas was switched to D_2/CO , $r_n^D = C_1^D(\alpha_D)^{n-1}$. In this way, the ratio of the product formation rate between H_2/CO and D_2/CO can be represented as eq. 3.7.

$$\frac{r_n^H}{r_n^D} = \frac{C_1^H}{C_1^D} \left(\frac{\alpha_H}{\alpha_D} \right)^{n-1} \quad (3.7)$$

If the formation of C1 species is not the rate determining and $C_1^H/C_1^D = 1$, so the eq. 3.7 can be re-written as eq. 3.8.

$$\frac{r_n^H}{r_n^D} = \left(\frac{\alpha_H}{\alpha_D}\right)^{n-1} \quad (3.8)$$

Unlike most organic reactions in which the isotope effect originates from one single step, the eq. 3.8 measures the overall isotope effect that originates from every propagation step during FTS. The eq. 3.8 means that the ratio of r_H/r_D is a function of carbon number n . However, the isotope effect should be a constant. Therefore, the isotope effect determined by eq. 3.8 is not the true isotope effect of FTS.

For a polymerization reaction produces hundreds of hydrocarbons such as FTS, the rate of formation of total hydrocarbons approximately equals to the rate of C_k hydrocarbon formation, where K is the carbon number of the hydrocarbon that has the average molecular weight in FTS [54]. The average molecular weight can be calculated based on the α value of a catalyst. Thus, the value of inverse isotope effect can be represented by α_H/α_D , which is shown in eq. 3.9, where k is the carbon number of the hydrocarbon that has the average molecular weight of the FT reaction.

$$\frac{\alpha_H}{\alpha_D} = \sqrt[k-1]{\frac{CO_{conv.}^H}{CO_{conv.}^D}} \quad (3.9)$$

If we assume iron catalyzed FTS can produce one mole of CH_4 and can produce hydrocarbons till C_{60} , according to ASF equation, the number of moles of hydrocarbons in every carbon number can be calculated based on $C_n = C_1\alpha^{n-1}$. Then the mole fraction of hydrocarbons with different carbon numbers can be calculated and the mass of different hydrocarbons can be obtained by multiplying the molar mass of hydrocarbon by the mole fraction. The sum of the total molar mass is the average molecular weight of this

iron catalyzed FTS. For Fe/Si/K catalysts, the α value is 0.80 for all these three catalysts, so the average molecular weight is 72 which means the corresponding K is 5.14. For Fe/Si catalyst, the α value is 0.74 and the average molecular weight is 56, the corresponding K is 3.99.

Based on the experimental value from Table 3.1 and Table 3.2, the α_H/α_D has been calculated for each H₂/D₂ switching experiment as shown in Table 3.7. For the Fe/Si/K catalyst used in the first run, the α_H/α_D values range from 0.88 to 0.96. For the Fe/Si/K catalyst used in the second run, the α_H/α_D values range from 0.83 to 0.90. For the Fe/Si/K catalyst used in the third run, the α_H/α_D values range from 0.97 to 0.98. For the Fe/Si catalyst, the α_H/α_D range from 0.71 to 0.81.

Table 3.7 Results of the inverse isotope effects (α_H/α_D) during iron catalyzed FTS

Run	Catalyst	Type of CO conversion	$[\text{CO}_{\text{conv.}}]^H/[\text{CO}_{\text{conv.}}]^D$	α_H/α_D
1	Fe/Si/K	CO to Total	0.86 ± 0.02	0.96 ± 0.01
		CO to HC	0.59 ± 0.05	0.88 ± 0.02
		CO to C1+	0.55 ± 0.07	0.89 ± 0.02
		CO to C2+	0.53 ± 0.08	0.90 ± 0.02
		CO to C3+	0.51 ± 0.09	0.91 ± 0.02
		CO to C4+	0.50 ± 0.09	0.92 ± 0.02
2	Fe/Si/K	CO to Total	0.52 ± 0.13	0.86 ± 0.04
		CO to HC	0.47 ± 0.08	0.83 ± 0.04
		CO to C1+	0.46 ± 0.08	0.86 ± 0.03
		CO to C2+	0.45 ± 0.08	0.88 ± 0.03
		CO to C3+	0.44 ± 0.08	0.89 ± 0.02
		CO to C4+	0.42 ± 0.08	0.90 ± 0.02
3	Fe/Si/K	CO to Total	0.92 ± 0.01	0.98 ± 0.01
		CO to HC	0.89 ± 0.01	0.97 ± 0.01
		CO to C1+	0.89 ± 0.01	0.98 ± 0.02
		CO to C2+	0.89 ± 0.01	0.98 ± 0.03
		CO to C3+	0.89 ± 0.01	0.98 ± 0.04

Table 3.7 (continued)

Run	Catalyst	Type of CO conversion	$[\text{CO}_{\text{conv.}}]^{\text{H}}/[\text{CO}_{\text{conv.}}]^{\text{D}}$	$\alpha_{\text{H}}/\alpha_{\text{D}}$
3	Fe/Si/K	CO to C4+	0.89 ± 0.01	0.98 ± 0.05
4	Fe/Si	CO to Total	0.44	0.76
		CO to HC	0.36	0.71
		CO to C1+	0.29	0.73
		CO to C2+	0.26	0.77
		CO to C3+	0.24	0.79
		CO to C4+	0.22	0.81

3.5 CONCLUSION

The results of Fe/Si/K and Fe/Si catalyzed H_2/D_2 experiments in Table 3.1, 3.2 and 3.3 indicate that there is inverse isotope effect in iron catalyzed FTS. The inverse isotope effect during iron catalyzed FTS can be explained by the alkyl mechanism, the alkenyl mechanism and the modified alkylidene mechanism. In these mechanisms, the inverse isotope effect is originated from each step of the propagations because of the hybridization of carbon in the growing chain changing from sp^2 to sp^3 .

The modified alkylidene mechanism can explain the inverse isotope effect during methane formation. This is due to the C-H bond order changes from sp to sp^2 in the monomer then the C-H(D) bond order changes from sp^2 to sp^3 in the intermediate $\text{M}=\text{CH}(\text{D})$.

The isotope effect of iron catalyzed FTS can be calculated by eq. 3.6. The inverse isotope effect in each step of the propagation $\alpha_{\text{H}}/\alpha_{\text{D}}$ is in a range of 0.88 – 0.96 for run 1; 0.83 – 0.90 for run 2, 0.97 – 0.98 for run 3 and 0.71 – 0.81 for run 4.

CHAPTER 4

DEUTERIUM ENRICHMENT IN IRON CATALYZED FISCHER-TROPSCH SYNTHESIS

4.1 INTRODUCTION

As mentioned before, isotope study is one of the most useful techniques that may be used in testing mechanisms of any reaction. For a long period of time the isotope tracer studies in FTS were focused on ^{14}C [17, 50, 55-58] and ^{13}C [17, 59] tracer studies because it was believed that deuterium would not be particularly informative due to possible H/D exchange reaction occurring on the surface of a metal catalyst [17].

Therefore, information regarding the behavior of H_2 on the FTS was limited in literatures before 1996 when Raje and Davis [60] published their review on isotope tracer studies in FT reactions. In this study, hydrogen and deuterium was used as tracers to study the mechanism of Fe catalyzed FTS.

As the results of inverse isotope effect, the deuterium was found enriched in hydrocarbons from C_6 to C_{24} and the magnitude of enrichments increased as the carbon number increases in Co catalyzed FTS [23]. The alky and alkenyl mechanisms for FTS can be used to explain the inverse isotope effect because it is known that the origin of inverse isotope effect is the increase in bond order at the transition state or the hybridization change of carbon from sp to sp^2 or from sp^2 to sp^3 [52, 53]. For both mechanisms, the surface species $\text{M}=\text{CH}_2$ is the monomer of the polymerization process. During the carbon-carbon bond formation in both mechanism, by coupling with the

growing chain $M-CH_2CH_2R$ (in alkyl mechanism) and $M-CH=CH-R$ (in alkenyl mechanism), the hybridization of the carbon in monomer $M=CH_2$ was changed from sp^2 to sp^3 , which can lead to an inverse isotope effect. Therefore, these mechanisms indicate that deuterium will be enriched in hydrocarbons during the H_2/D_2 competition experiment. However, the value of H/D ratio will be a constant because the inverse isotope effect is only a function of the monomer according to these two mechanisms.

The modified alkylidene mechanism published in 2011 [23] can explain the H/D ratio as a function of carbon number in Co catalyzed FTS. In this mechanism, the monomer is $M\equiv CH$, through the coupling of the monomer and the growing chain $M=CH-R$, the hybridization of the carbon in monomer was changed from sp to sp^2 and the carbon in the growing chain was rehybridized from sp^2 to sp^3 . This mechanism indicates that during the carbon-carbon bond formation, the inverse isotope effect not only originated from the monomer but also from the growing chain. Thus, the number of deuterium will be increased in higher carbon number compound.

In this study, H_2/D_2 competition experiment was also conducted in order to find out if there is deuterium enrichment during the iron catalyzed FTS or not and what is the difference between the results of Co and Fe catalyzed H_2/D_2 competitive experiment and also find out if the Fe catalyzed FTS follows the alkylidene pathway or not.

4.2 THE ANALYSIS OF ISOTOPIC ISOMERS BY GC-MS

Because the syngas used in H_2/D_2 competition experiment was a mixture of $H_2/D_2/CO/N_2$ (30% : 30% : 30% : 10%), the liquid and wax product contained both

deuterium and hydrogen atoms. For example, for C₁₂ hydrocarbons produced from H₂/D₂ competition experiment, the product may be a mixture of dodecane-d₀, dodecane-d₁ and all the way till dodecane-d₂₆ and deuterated dodecenes. In order to obtain the mol% of each isotopic isomer, the quantitative measurement for each isotopomer is a must. But it has been reported that hydrocarbons with one deuterium atom difference cannot be separated by GC-FID even though they do have the different retention time and only when the deuterium atom difference is or more than 4, the compounds can be separated completely and the quantitative measurements can be conducted by GC-FID [61]. In this case, GC-MS was used to determine the quantitative amounts of deuterated isomers. The GC-MS analysis is based on the total area of the molecular ions or the average scans of the molecular ions.

The Figure 4.1 displays a spectrum of mixture of isotopic isomers of n-dodecane and trans-2-dodecenes obtained from GC-MS. The peaks on the left are the n-dodecanes and the peaks on the right are the trans-2-dodecenes. Based on the different molecular weight of molecular ion, the peak of different isotopomer is shown in different color. As it can be seen in Figure 4.1, the peaks in black color correspond to the molecular ions have a molar weight of 181, which are dodecane-d₁₁ (on the left) and trans-2-dodecene-d₁₃ (on the right); the peaks in blue color correspond to the molecular ions have a molar weight of 185, which are dodecane-d₁₅ (on the left) and trans-2-dodecene-d₁₇ (on the right).

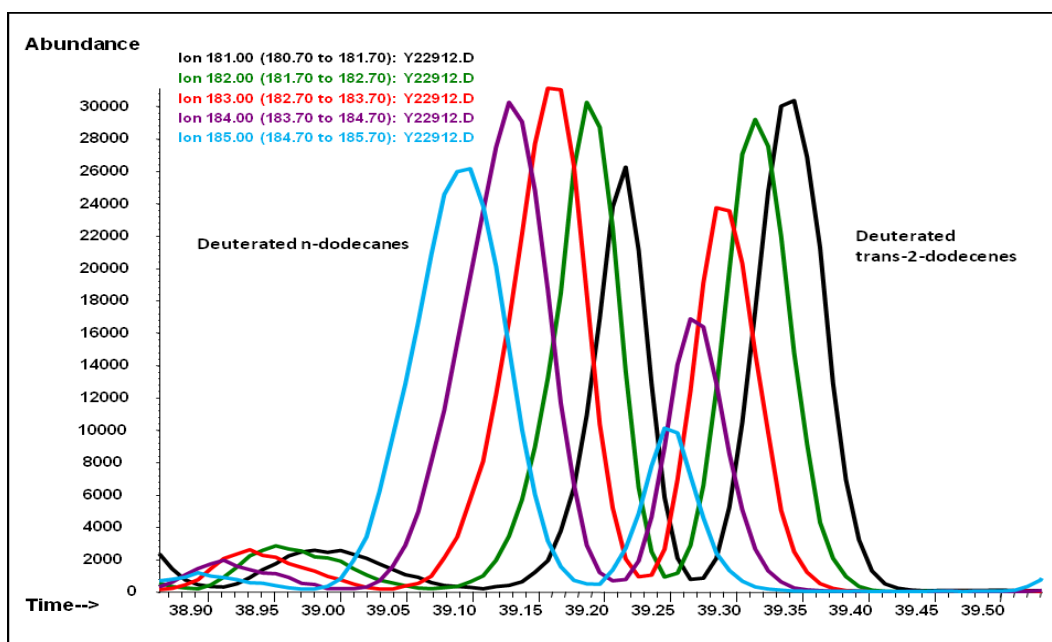


Figure 4.1 Mixture of isotopomers of n-dodecanes and trans-2-dodecenes

By using GC-MS, the total area of molecular ion of each isotopmer can be determined. However, there is ^{13}C and deuterium isotope in natural, so the corrections for M+1 and M+2 contributions have to be done. The M+1 and M+2 data of alkanes from C6 to C17 were taken from the literature [62]. After removal of M+1 and M+2 contributions, the relative amounts of isotopomers can be obtained. The H/D ratio can be calculated by eq. 4.1. In eq. 4.1, i is the number of hydrogen in an isotopic isomer of n-alkane with a carbon number n , the term iC_n^i is the mole% of an isotopic isomer with specific carbon number, the mol% can be obtained through the relative area obtained from GS-MS data. The term $(2n + 2 - i)C_n^i$ is the mole% of isotopic isomer of an alkane with a deuterium number $(2n+2-i)$ and carbon number n .

$$\frac{H}{D} = \frac{\sum_{i=0}^{2n+2} iC_n^i}{\sum_{i=0}^{2n+2} (2n+2-i)C_n^i} \quad (4.1)$$

Table 4.1 shows a GC-MS analysis of isotopomers of n-nonane produced from Fe/Si/K catalyst. Based on the mole percent of each isotopomer, the H/D ratio of n-nonane was calculated by eq. 4.1 to be 0.888. It is clearly indicating the presence of deuterium enrichment during the Fe catalyzed FTS.

Table 4.1 GC-MS analysis of isotopomers of n-nonane produced from Fe/Si/K catalyzed H₂/D₂ competition experiment

Number of D in Isotopomers	Molar Mass	Total Area of M+	After corrections for M+1 and M+2	Mol%
0	128	1	1	0.00
1	129	1	1	0.00
2	130	1	1	0.02
3	131	1	1	0.11
4	132	13174	13174	0.46
5	133	49634	48311	1.48
6	134	122729	117822	3.70
7	135	267036	254999	7.39
8	136	483596	457487	12.01
9	137	719210	672182	16.02
10	138	900459	831005	17.62
11	139	932860	846537	16.02
12	140	820197	731631	12.01
13	141	590108	513012	7.39
14	142	351104	296452	3.70
15	143	168677	136707	1.48
16	144	63859	48859	0.46
17	145	18953	13460	0.11
18	146	1562	1	0.02
19	147	59	1	0.00
20	148	0	0	0.00

4.3 THE RESULTS OF IRON CATALYZED H₂/D₂ COMPETITION EXPERIMENTS

4.3.1 The Results of Fe/Si/K Catalyzed H₂/D₂ Competition Experiments

The H₂/D₂ experiments were conducted under 270°C and 188 psi, the syngas used was H₂/D₂/CO/N₂ (30% : 30% : 30% : 10%). The isotopic isomer was identified by GC-MS. The mole% of each isotopic isomer in each n-alkane from C8 to C18 was obtained. Figure 4.2A and Figure 4.2B show the isotope isomer distribution of n-Octane and n-Nonadecane during H₂/D₂ competition experiment over Fe/Si/K at 270°C with a CO conversion level of 77%. The red line in both figures is the theoretical calculation of isotopic isomer distribution assuming there is no deuterium enrichment which means the H/D = 1. The blue line is the isotopic isomer distribution calculated based on experimental data. The isotopic isomer distributions of the rest carbons numbers are shown in the Appendix B (1-10).

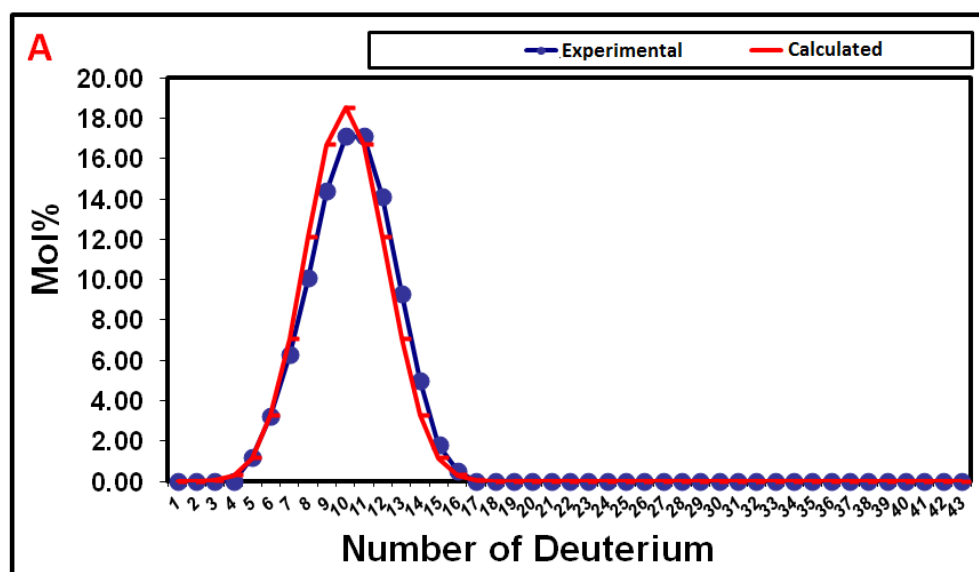


Figure 4.2 Isotopic isomer distributions in n-Octane (A) and n-Nonadecane (B) during Fe/Si/K catalyzed H₂/D₂ competition experiment

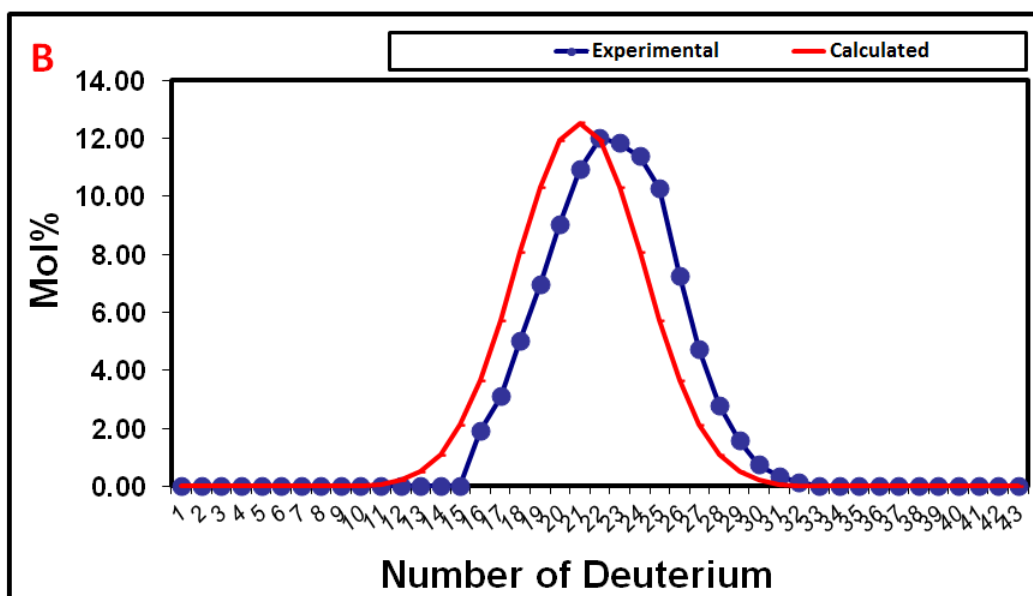


Figure 4.2 (continued) Isotopic isomer distributions in n-Octane (A) and n-Nonadecane (B) during Fe/Si/K catalyzed H₂/D₂ competition experiment

Based on the mol% of isotope isomer, the H/D ratio of each n-alkane over three Fe/Si/K runs was calculated, which is shown in Table 4.2. The CO conversion levels are shown on the top of the table. The H/D ratios with the standard deviation of each alkanes are listed in the table.

Table 4.2 Ratio of H/D during Fe/Si/K catalyzed runs

Run-1 Fe/Si/K with a CO conversion of 56%			
Carbon Number	H/D Ratio	Carbon Number	H/D Ratio
8	0.9407 ± 0.01	14	0.8786 ± 0.01
9	0.8938 ± 0.01	15	0.8872 ± 0.01
10	0.8931 ± 0.01	16	0.8916 ± 0.01
11	0.8893 ± 0.01	17	0.8963 ± 0.01
12	0.8877 ± 0.01	18	0.8913 ± 0.01
13	0.8877 ± 0.01	19	0.8854 ± 0.01
Run-2 Fe/Si/K with a CO conversion of 15%			
Carbon Number	H/D Ratio	Carbon Number	H/D Ratio
8	0.8919 ± 0.03	14	0.8481 ± 0.01
9	0.8470 ± 0.01	15	0.8457 ± 0.01
10	0.8495 ± 0.01	16	0.8512 ± 0.01

Table 4.2 (continued)

Run-2 Fe/Si/K with a CO conversion of 15%			
Carbon Number	H/D Ratio	Carbon Number	H/D Ratio
11	0.8438 ± 0.01	17	0.8564 ± 0.01
12	0.8379 ± 0.01	18	0.8542 ± 0.02
13	0.8412 ± 0.01	19	0.8684 ± 0.01
Run-3 Fe/Si/K with a CO conversion of 77%			
Carbon Number	H/D Ratio	Carbon Number	H/D Ratio
8	0.9327 ± 0.01	14	0.8769 ± 0.02
9	0.8956 ± 0.01	15	0.8636 ± 0.02
10	0.8792 ± 0.01	16	0.8892 ± 0.03
11	0.8805 ± 0.01	17	0.8734 ± 0.01
12	0.8814 ± 0.01	18	0.8874 ± 0.02
13	0.8800 ± 0.01	19	0.8784 ± 0.02

As indicated in Table 4.2, for all the Fe/Si/K catalyzed H₂/D₂ competition experiments, the H/D ratio is less than one. It can also be found that the H/D ratio decreased from C8 to C11 and became almost a constant from C11 to C19. Figure 4.3 displays the H/D ratios during Fe/Si/K catalyzed H₂/D₂ competition experiments.

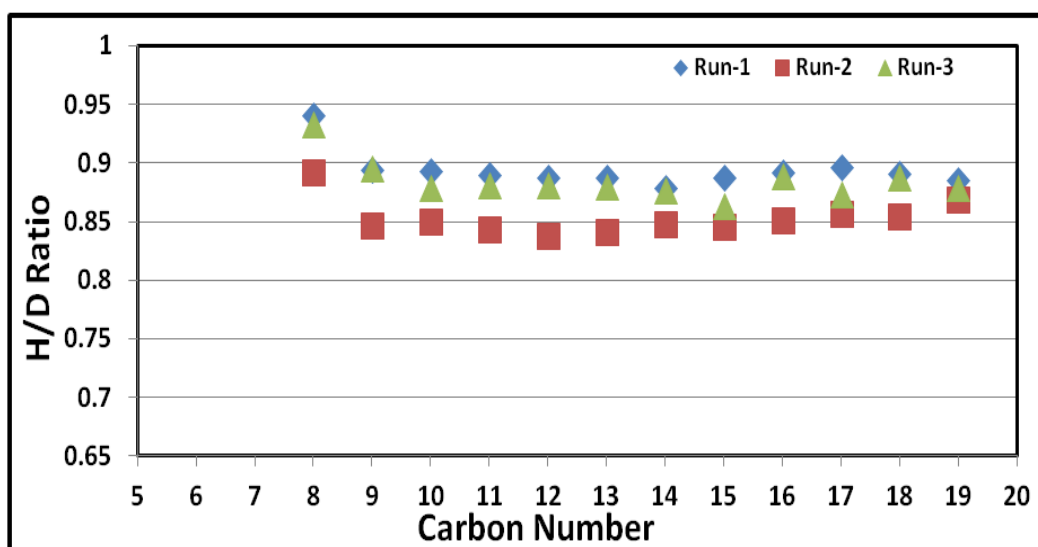


Figure 4.3 The H/D ratios during Fe/Si/K catalyzed H₂/D₂ competition experiments

4.3.2 The Results of Fe/Si Catalyzed H₂/D₂ Competition Experiments

The Fe/Si catalyzed H₂/D₂ was conducted follow the same procedure discussed previously. Based on the same analytical method, the mol% of isotopic isomer from C8 to C16 was calculated. Figure 4.4A and Figure 4.4B display the isotopic isomer distribution of n-Octane and n-Hexadecane. The distributions from C9 to C15 are listed in Appendix C (1-7).

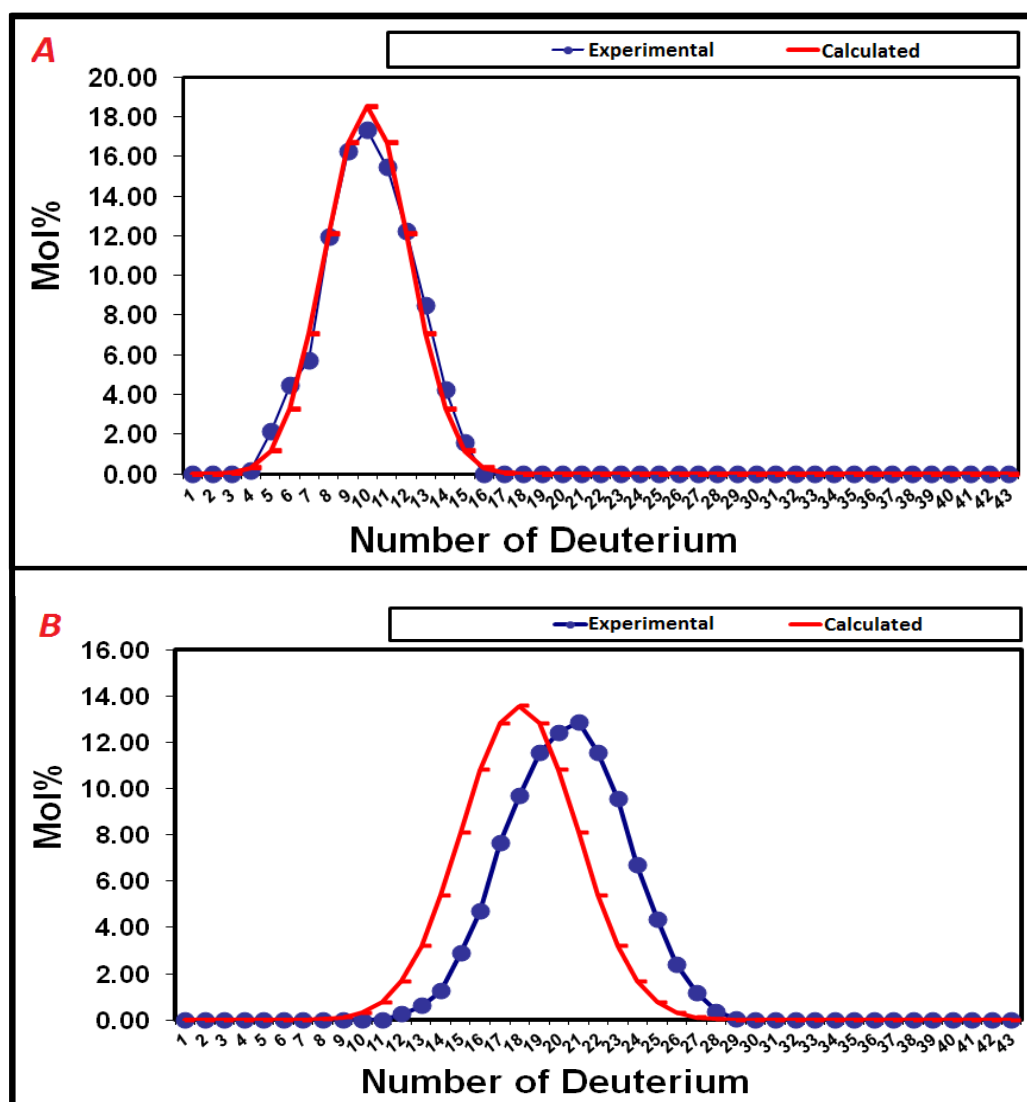


Figure 4.4 Isotopic isomer distributions in n-Octane (A) and n-Hexadecane (B) during Fe/Si catalyzed H₂/D₂ competition experiment

Also, the H/D ratio was calculated based on the mol% of each isotopic isomer from C8 to C16, which is listed in Table 4.3 and displayed in Figure 4.5.

Table 4.3 H/D ratio during Fe/Si catalyzed H₂/D₂ competition experiment

Fe/Si at 270 °C					
Carbon #	H/D Ratio	Carbon #	H/D Ratio	Carbon #	H/D Ratio
8	0.9872 ± 0.03	11	0.7585 ± 0.01	14	0.7499 ± 0.01
9	0.7793 ± 0.01	12	0.7575 ± 0.01	15	0.7504 ± 0.01
10	0.7698 ± 0.01	13	0.7559 ± 0.01	16	0.7573 ± 0.01

As it can be seen in Table 4.3 and Figure 4.5, the H/D ratio decreased from C8 to C14 and start increasing from C15 to C16.

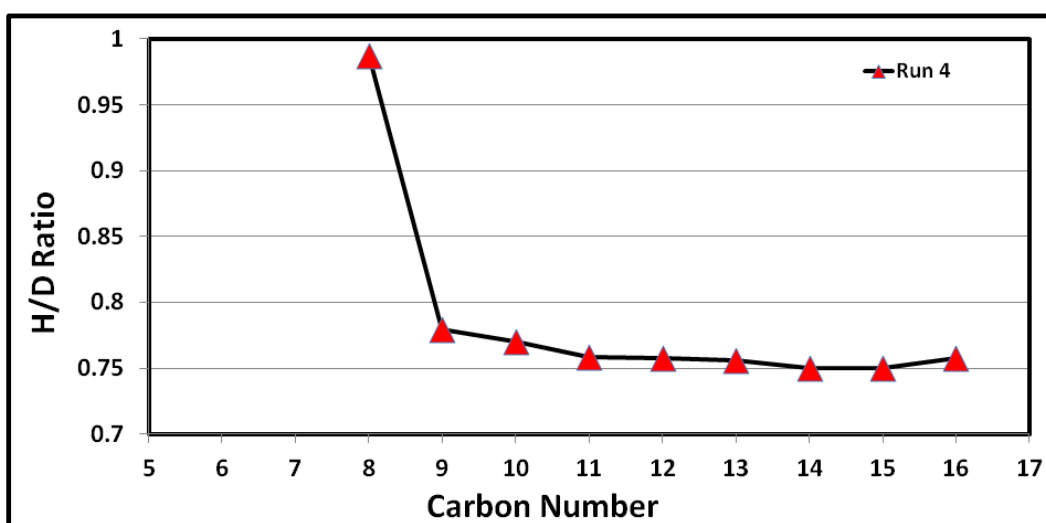


Figure 4.5 H/D ratio in Fe/Si catalyzed H₂/D₂ competition experiment

The results of Fe/Si/K and Fe/Si catalyzed FTS clearly indicate that there is deuterium enrichment during the iron catalyzed FTS.

4.4 DISCUSSION

4.4.1 The Difference of Iron and Cobalt Catalyzed H₂/D₂ Competition Experiment

Results

The results of H₂/D₂ switching experiments in the Table 3.1 and Table 3.2 show that there is inverse isotope effect in both Fe/Si/K and Fe/Si catalyzed FTS. These experimental facts have been explained by the modified alkylidene mechanism in Chapter III. The results of H₂/D₂ competition experiments in Table 4.1 and Table 4.2 showed that the H/D ratio in each n-alkane is smaller than one and as it can be seen from Figure 4.1 and Figure 4.2 that the experimental deuterium distributions were shifted to the right of the calculated distribution which assuming that the H/D ratio is equal to one. These results clearly indicate that there is a deuterium enrichment during the Fe catalyzed H₂/D₂ competition experiment. Because the H/D ratio in each n-alkane is smaller than one which means it reacted faster when D₂/CO was used as syngas than H₂/CO was used. The results consist with the results of inverse isotope effect obtained from H₂/D₂ switching experiments.

In 2011, Shi et al. conducted Co catalyzed FTS [23]. Inverse isotope effect and deuterium enrichment were found during their Co catalyzed FTS. Their results of H₂/D₂ competition experiments showed that H/D ratio decreased with the increasing carbon number during the Co catalyzed FTS [23]. This phenomenon can be explained by the modified alkylidene mechanism. As it has been reported that the origin of inverse isotope effect is the hybridization change of carbon from sp to sp² or from sp² to sp³ [52,

53], and in the modified alkylidene mechanism, during the formation of C1 species and chain propagation steps, there is a hybridization change of the carbon in the monomer MCH from sp to sp² and the carbon in the growing chain from sp² to sp³, respectively. This indicated that the inverse isotope effect was generated by both the monomer and the growing chain during the chain propagation. In the case of Co catalyzed FTS, more deuterium was added into longer chains, which led that H/D ratio decreased with increasing carbon number.

However, the results of Fe catalyzed H₂/D₂ competition experiments showed that H/D ratio decreased from C8 to C11 and remaining almost as constant from C11 to C19 during the Fe/Si/K catalyzed runs; the H/D ratio decreased from C8 to C14 and start increasing from C15 to C16 during the Fe/Si catalyzed run. Thus, the explanation of modified alkylidene mechanism is not enough, further explanation is needed for Fe catalyzed runs.

Because the syngas used in H₂/D₂ competition experiment was H₂/D₂/CO/N₂ (30% : 30% : 30% : 10%). The ratio of H₂ to D₂ was one initially which means the concentration of two monomers M≡CH and M≡CD on the surface of the Fe catalyst was the same. As indicated in the modified alkylidene mechanism, there is inverse isotope effect during the chain propagation steps which leads the monomer M≡CD reacts faster with the growing chain than the monomer M≡CH. Thus during the chain propagation, the local concentration of M≡CD becomes less and less which means the [M≡CH]/[M≡CD] will be greater than one. Since the concentration of M≡CH becomes higher than [M≡CD], the formation rate of M≡CH with the growing chain becomes higher than the formation rate

of $M\equiv CD$ with the growing chain. In this case, the H/D ratio became a constant or even started increasing with the increasing carbon number. Another possibility is this: since the reaction is going on, long and heavy chain hydrocarbons are formed. When the chain gets longer and longer, the inverse isotope effect could be less and less. This is another factor makes the H/D ratio became almost a constant or start increasing with the increasing carbon numbers. These two factors however are just hypothesis which we do not have experimental evidence to support yet. But they can to some extent explain the experimental results of the deuterium enrichment in the Fe catalyzed FTS.

Furthermore, it is reported that deuterated olefins can undergo H/D exchange with H_2 and hydrogen-containing olefins, but only a maximum of five H(D) atoms in 1-olefins and 2-olefins from C7 to C16 hydrocarbons were involved in the H/D exchange [63, 64, 65]. However, the maximum number of H(D) atoms can undergo exchange is five, for a long chain hydrocarbon has 30 to 40 hydrogen(deuterium) atom, five is not a significant amount and it has been reported that there was no H/D exchange between deuterated alkanes in Fe catalyzed FTS [63]. So, the effect of H/D exchange reaction would not be significant.

All these factors mentioned above may contribute to the experimental results.

4.4.2 Calculation of Theoretical H/D Ratio

The experimental H/D ratios have been obtained and displayed in Figure 4.3 and Figure 4.4. In the H_2/D_2 competition experiment, the fraction of deuterium in the growing chain with a carbon number n (f_n^D) can be calculated by eq. 4.2, C_1^H and C_1^D are

the fraction of H₂ and D₂, and the α_H/α_D is the isotope effect of the FT reaction. Since the fraction of H₂ and D₂ is the same for the H₂/D₂ competitive experiment, $C_1^H = C_1^D = 0.5$ in eq. 4.2. The first term in the parenthesis is related to the carbon-carbon bond formation (where the inverse isotope effect originates) and the second term in the parenthesis is related to the step of hydrogenation (no isotope effect presents). For the product with a carbon number n, the fraction of deuterium (f_n^D) can be calculated by eq. 4.3, where the term $C_1^D/(n+1)$ is related to the termination step with no isotope preference.

$$f_n^D(\text{chain}) = \frac{1}{2} \left\{ \frac{1}{C_1^H/C_1^D (\alpha_H/\alpha_D)^{n-1} + 1} + C_1^D \right\} \quad (4.2)$$

$$f_n^D(\text{product}) = \frac{n}{2n+2} \left\{ \frac{1}{C_1^H/C_1^D (\alpha_H/\alpha_D)^{n-1} + 1} + C_1^D \right\} + \frac{C_1^D}{n+1} \quad (4.3)$$

The H/D ratio in n-alkanes can be calculated by eq. 4.3. $H/D = (1 - f_n^D) / f_n^D$. For the Fe/Si catalyzed FTS with a α_H/α_D value 0.95 to 0.97, the theoretical H/D values for n-alkanes from C6 to C21 have been calculated depending on the assumption that the initial concentration of $M\equiv CH$ and $M\equiv CD$ is the same and during the chain propagation the ratio of $[M\equiv CH]/[M\equiv CD]$ becomes greater than one. The experimental H/D values are consistent with the theoretical values as shown in Figure 4.6.

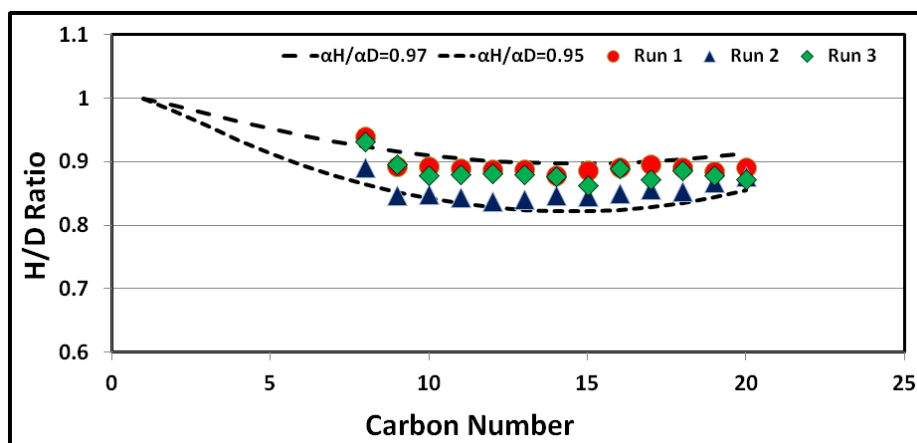


Figure 4.6 The experimental and theoretical H/D ratios in Fe/Si/K catalyzed H₂/D₂ competition experiments

For Fe/Si catalyzed FT reactions, because the number of gas sample was limited and the CO conversion has not reached a stable level before switching to D₂/CO in the H₂/D₂ switching experiment. The experimental isotope effect value α_H/α_D is larger than the true value. So we assume that the α_H/α_D values for Fe/Si catalyzed FTS is 0.91 to 0.93. The theoretical H/D ratios have also been calculated based on the same method, which is shown in Figure 4.7.

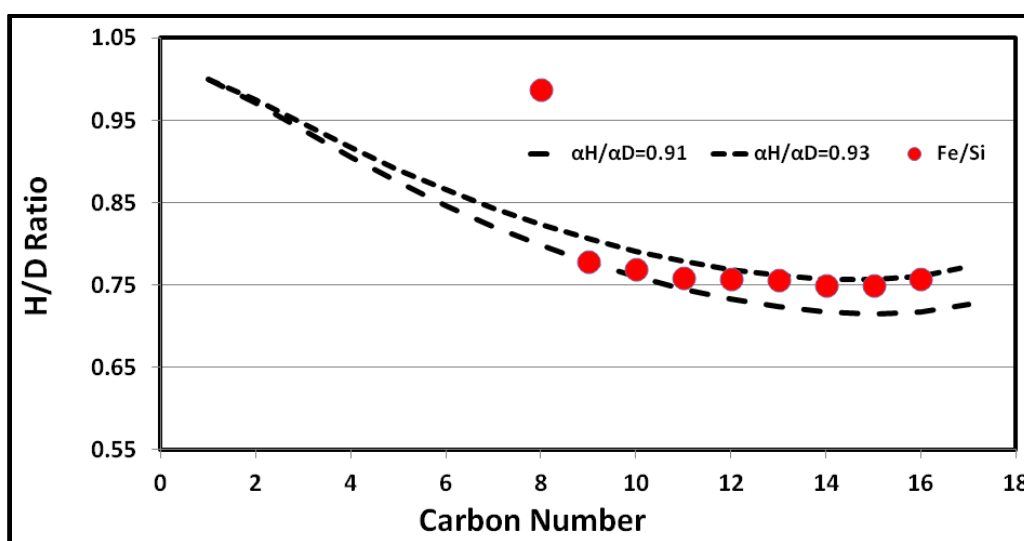


Figure 4.7 The experimental and theoretical H/D ratios in Fe/Si catalyzed H₂/D₂ competition experiments

As it can be seen in Figure 4.7, the experimental values consist with the theoretical H/D values.

4.5 CONCLUSION

By conducting the H₂/D₂ competition experiments, deuterium enrichment was found both in Fe/Si/K and Fe/Si catalyzed FTS. Different from the Co catalyzed FTS that the magnitude of deuterium enrichment increases with the increasing carbon number, the H/D ratio in Fe/Si/K catalyzed FTS decreased from C8 to C11 and remaining as almost a constant from C11 to C19; in the Fe/Si catalyzed FTS the H/D ratio decreased from C9 to C14 and started increasing from C15. The deuterium enrichment in iron catalyzed FTS can be explained by the modified alkylidene mechanism but some factors need to be taken into consideration.

CHAPTER 5

EXPLANATION OF FORMATION OF 2-OLEFINS AS SECONDARY PRODUCT DURING IRON

CATALYZED FTS

5.1 INTRODUCTION

It has been known that the Fischer-Tropsch Synthesis is a process that converts CO and H₂ to chemicals such as n-alkanes, 1-alkenes, 2-alkenes, oxygenates and also branched hydrocarbons. However, to explain how all of these compounds were formed during FT reactions is a challenge to all the mechanisms proposed.

Based on the isotope tracer study of Co catalyzed FTS, a modified alkylidene mechanism has been reported for FTS by Shi et al [23, 66]. The modified alkylidene mechanism has been discussed in chapter III. This mechanism can not only explain the inverse isotope effect and deuterium enrichment during the FTS, but also can explain the formation of n-alkanes, 1-alkenes and branched hydrocarbons [23, 27]. However, besides the n-alkanes, 1-alkenes and the branched hydrocarbons, other products can also be produced such as oxygenates and 2-alkenes. Through decades' studies, it is generally believed that the linear n-alkanes and 1-alkenes are the primary products of FTS [25, 26]. However, the most researchers agree that the 2-alkenes are the secondary products of FTS [25, 26, 67], while some groups consider that, like 1-alkenes and n-alkanes the 2-alkenes are the primary products formed through surface reaction of alkyl group on metal surface [28, 68].

The 1-octene-d₁₆ and 1-pentene-d₅ co-feed experiments during iron or cobalt catalyzed FTS [63, 69] showed that the deuterated octane can be converted to deuterated trans-2-octene, cis-2-octene and octane [63]. This experiment clearly showed that 1-olefin can be converted to 2-olefin and paraffin under FTS reaction conditions, however, it did not show that the internal olefins must be the secondary products of FTS.

During iron catalyzed FTS, significant amounts of trans-2-alkene and cis-2-alkene were produced. To understand how these internal alkenes were formed is important in understanding the mechanism of FTS.

In this study, by conducting H₂/D₂ switching experiment, we provided the evidence that 2-alkenes are the secondary products which were produced from 1-alkenes during Fe catalyzed FTS. The formation pathway of 2-alkenes was proposed based on the modified alkylidene mechanism.

5.2 THE NORMAL ISOTOPE EFFECT IN IRON CATALYZED FTS

5.2.1 The Product Profiles of Iron Catalyzed FTS

Based on the analysis of GC spectra of liquid and wax product from iron catalyzed H₂/D₂ switching experiments, the mole fraction of each kind of product has been obtained. The identification of branched hydrocarbons has already been discussed in Chapter II. Table 5.1 shows a detailed product profile of each Fe/Si/K catalyst. The mole percent of branched hydrocarbons, 1-olefin, paraffin, trans-2-olefin and cis-2-olefin with different carbon number are shown in the table.

Table 5.1 Detailed product profile of each Fe/Si/K catalyst

270 °C, Fe/Si/K with 60% CO conversion					
Carbon #	B%	1-O%	P%	2-T%	2-C%
7	33.2 ± 5.5	40.8 ± 4.6	19.0 ± 0.3	3.4 ± 0.3	3.5 ± 0.2
8	33.5 ± 3.0	39.0 ± 1.9	19.6 ± 0.3	3.9 ± 0.3	4.0 ± 0.5
9	29.8 ± 1.4	39.0 ± 0.9	21.2 ± 0.1	4.9 ± 0.4	5.0 ± 0.2
10	30.0 ± 0.3	36.4 ± 0.2	21.9 ± 0.4	5.9 ± 0.2	5.8 ± 0.1
11	29.3 ± 1.1	33.6 ± 0.8	23.4 ± 0.6	7.2 ± 0.2	6.5 ± 0.2
12	27.7 ± 2.7	31.0 ± 1.6	25.8 ± 1.3	8.4 ± 0.1	7.1 ± 0.1
13	26.9 ± 2.4	27.7 ± 1.5	27.9 ± 0.8	9.5 ± 0.5	8.0 ± 0.4
14	24.9 ± 2.8	24.6 ± 2.7	31.0 ± 0.1	11.0 ± 0.2	8.6 ± 0.2
15	22.7 ± 4.2	22.3 ± 3.2	33.2 ± 0.5	12.3 ± 0.9	9.5 ± 0.3
16	22.5 ± 4.3	18.7 ± 1.5	34.9 ± 1.1	14.2 ± 2.2	9.7 ± 0.6
17	21.7 ± 5.1	16.0 ± 0.5	36.4 ± 0.6	16.3 ± 4.1	9.6 ± 0.1
270 °C, Fe/Si/K with 15% CO conversion					
Carbon #	B%	1-O%	P%	2-T%	2-C%
7	25.0 ± 5.9	41.6 ± 1.4	21.3 ± 0.8	6.5 ± 1.9	5.7 ± 1.8
8	29.3 ± 4.8	38.7 ± 0.1	20.4 ± 1.1	6.1 ± 1.6	5.5 ± 1.7
9	28.2 ± 1.8	38.0 ± 1.4	21.0 ± 0.7	6.8 ± 1.4	6.0 ± 1.1
10	29.8 ± 2.0	35.5 ± 2.1	20.7 ± 1.4	7.4 ± 1.5	6.6 ± 1.2
11	30.4 ± 3.0	32.6 ± 1.8	21.8 ± 1.8	8.4 ± 1.5	6.9 ± 1.5
12	28.7 ± 2.9	30.3 ± 1.7	24.4 ± 1.6	9.2 ± 1.7	7.4 ± 1.3
13	28.3 ± 1.5	28.0 ± 3.2	25.5 ± 2.5	10.3 ± 1.0	7.9 ± 1.2
14	27.3 ± 0.9	26.4 ± 2.1	26.5 ± 1.3	11.5 ± 0.8	8.3 ± 1.0
15	27.9 ± 2.4	23.7 ± 1.1	27.7 ± 1.7	12.2 ± 0.5	8.5 ± 1.3
16	29.1 ± 3.3	20.0 ± 0.5	28.9 ± 2.2	13.2 ± 0.3	8.8 ± 1.2
17	29.2 ± 3.2	17.2 ± 0.2	29.8 ± 2.8	14.9 ± 0.5	8.9 ± 1.1
270 °C, Fe/Si/K with 78% CO conversion					
Carbon #	B%	1-O%	P%	2-T%	2-C%
7	37.5 ± 0.6	28.9 ± 0.6	21.3 ± 0.7	6.1 ± 0.4	6.3 ± 0.4
8	34.7 ± 0.3	27.5 ± 0.5	22.9 ± 0.4	7.6 ± 0.3	7.4 ± 0.1
9	29.5 ± 0.1	26.2 ± 0.8	26.9 ± 0.4	9.3 ± 0.3	8.2 ± 0.1
10	30.6 ± 1.1	22.7 ± 0.6	27.7 ± 1.1	10.6 ± 0.4	8.6 ± 0.3
11	29.6 ± 1.1	19.5 ± 0.6	29.7 ± 1.3	12.0 ± 0.2	9.3 ± 0.3
12	27.4 ± 1.3	17.0 ± 0.8	32.9 ± 1.7	13.2 ± 0.2	9.5 ± 0.1
13	26.3 ± 1.8	14.7 ± 0.8	35.3 ± 2.5	14.1 ± 0.1	9.8 ± 0.2
14	24.3 ± 2.5	14.1 ± 1.1	36.9 ± 3.5	14.9 ± 0.1	9.9 ± 0.1
15	22.4 ± 2.7	13.2 ± 0.8	39.3 ± 3.6	15.5 ± 0.1	9.7 ± 0.1
16	21.5 ± 2.9	10.0 ± 0.6	43.5 ± 3.7	16.2 ± 0.1	9.0 ± 0.2
17	22.4 ± 4.2	9.3 ± 0.8	43.1 ± 5.2	16.8 ± 0.1	8.4 ± 0.3

As shown in Table 5.1, significant amount of 2-olefins were produced by Fe/Si/K catalyst in each run and the mole percent increased with increasing carbon numbers.

5.2.2 The $[1\text{-Olefi}]_H/[1\text{-Olefi}]_D$ and $[2\text{-Olefin}]_H/[2\text{-Olefin}]_D$ Ratios in Fe Catalyzed FTS

The liquid and wax samples produced from both H₂/CO and D₂/CO runs were analyzed by GC-FID. The 1-olefin and 2-olefin fractions when H₂/CO and D₂/CO were used as syngas were obtained. Table 5.2 shows the 1-olefin and 2-olefin fractions during the H₂/D₂ switching experiment of the first run. The catalyst and reaction temperature is shown on the top of the table. The mole percent of 1-olefin fraction when H₂/CO was used, 1-olefin fraction when D₂/CO was used, 2-olefin fraction when H₂/CO was used, 2-olefin fraction when D₂/CO was used are shown in the table.

Table 5.2 The 1-olefin and 2-olefin fractions during H₂/D₂ switching experiment

270 °C, Fe/Si/K with a 60% CO conversion				
Carbon #	1-O% (H)	1-O% (D)	2-O% (H)	2-O% (D)
7	0.61 ± 0.01	0.69 ± 0.01	0.10 ± 0.01	0.073 ± 0.01
8	0.60 ± 0.01	0.66 ± 0.01	0.12 ± 0.01	0.088 ± 0.01
9	0.56 ± 0.01	0.63 ± 0.01	0.14 ± 0.01	0.11 ± 0.01
10	0.53 ± 0.01	0.61 ± 0.01	0.16 ± 0.01	0.14 ± 0.01
11	0.49 ± 0.01	0.59 ± 0.01	0.19 ± 0.01	0.15 ± 0.01
12	0.44 ± 0.01	0.53 ± 0.01	0.21 ± 0.01	0.18 ± 0.01
13	0.39 ± 0.01	0.50 ± 0.01	0.24 ± 0.01	0.19 ± 0.01
14	0.36 ± 0.01	0.46 ± 0.01	0.26 ± 0.01	0.22 ± 0.01

By comparing the 1-olefin and 2-olefin produced when H₂/CO and D₂/CO were used as syngas feeds during H₂/D₂ switching experiment, the ratios of 1-alkene (H/D) and 2-alkene (H/D) were obtained, which is shown in Figure 5.1. The ratios of 1-alkene (H/D)

and 2-alkene (H/D) are shown in the figure. Figure 5.1 clearly indicates that the ratio of 1-alkene (H/D) from C7 to C14 is less than one, ranging from 0.79 to 0.85. But the ratio of 2-alkene (H/D) is greater than, ranging from 1.16 to 1.40. The result indicates that there is a primary isotope effect during the formation of 2-alkenes.

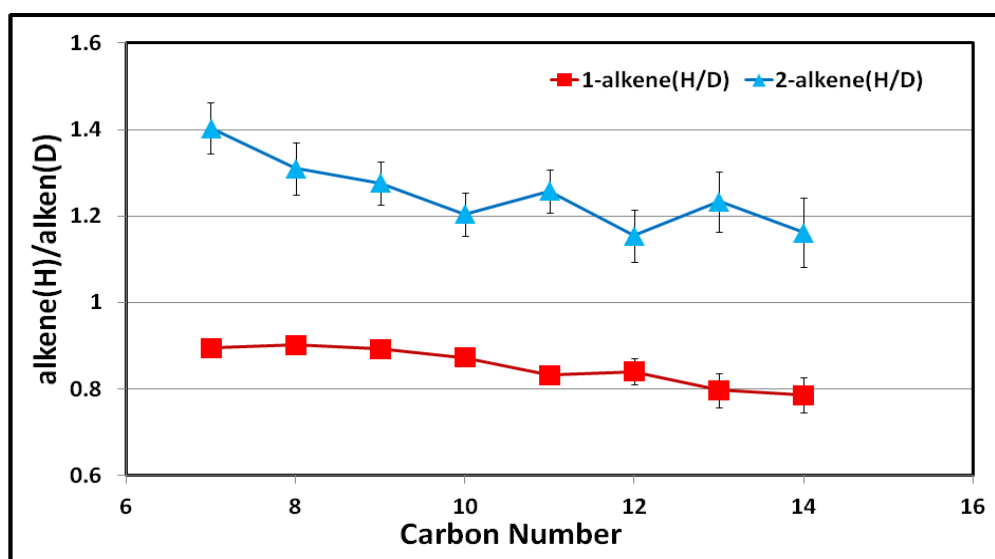


Figure 5.1 The ratio of 1-alkene (H/D) and ratio of 2-alkene (H/D) in the first run

Similar results were found in the second and third run, the ratio of 1-alkene (H/D) and 2-alkene (H/D) in the second and third run are shown in Figure 5.2 and Figure 5.3. As shown in Figure 5.2, the ratio of 1-alkene (H/D) from C7 to C10 is less than one, ranging from 0.85 to 0.88. However, the ratio of 2-alkene (H/D) is greater than one and ranging from 1.10 to 1.39.

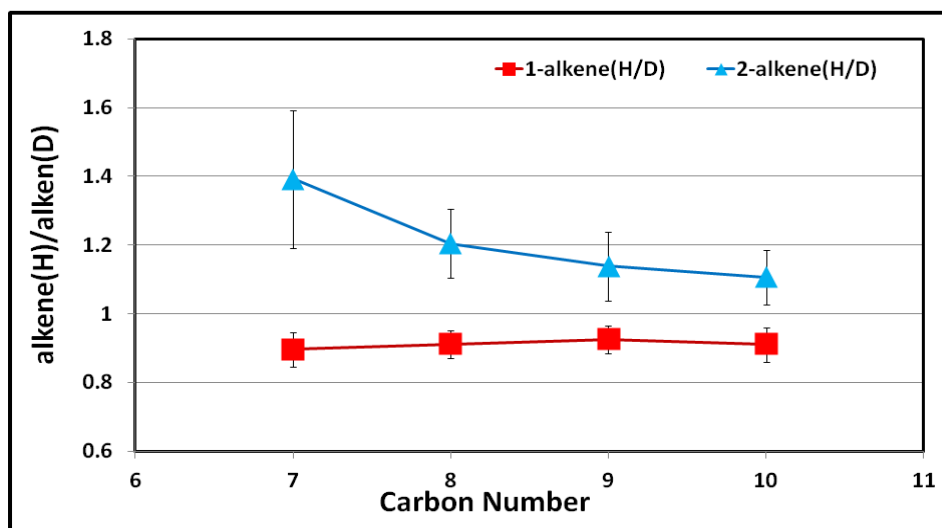


Figure 5.2 The ratio of 1-alkene (H/D) and ratio of 2-alkene (H/D) in the second run

Figure 5.3 shows that the ratio of 1-alkene (H/D) from C7 to C11 is less than one and ranging from 0.80 to 0.82. But the ratio of 2-alkene (H/D) is greater than one, ranging from 1.01 to 1.20.

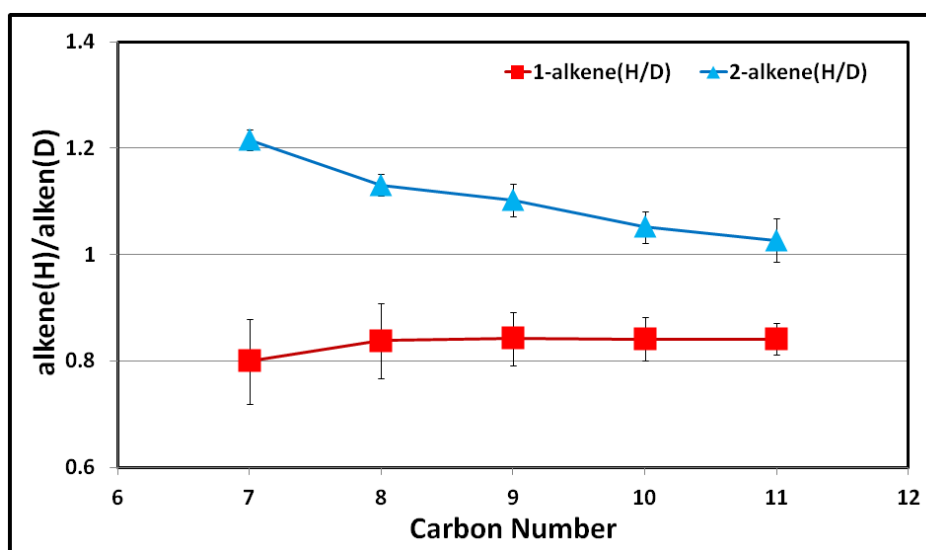


Figure 5.3 The ratio of 1-alkene (H/D) and ratio of 2-alkene (H/D) in the third run

As it shows, the results from Fe/Si/K catalyzed H₂/D₂ experiments from Run 1 to Run 3 indicate that there is a primary isotope effect during the formation of 2-alkenes.

5.3 THE PROPOSED 2-OLEFIN FORMATION PATHWAY

5.3.1 The Hypothetical Formation Pathway of 2-Alkenes

Based on the results shown in Table 5.1, it was found that during the iron catalyzed FTS, significant amount of 2-alkenes were produced. According to the modified alkylidene mechanism, the formations of 1-alkenes, n-alkanes and branched hydrocarbons can be explained. However, the formation pathway of 2-alkenes is still unknown. Whether the 2-alkenes are the primary product or secondary product is still a topic of debating.

However, there are only two possibilities, either the 1-alkenes and 2-alkenes are produced from the same pathway or through different pathways. Figure 5.4 shows a hypothetical formation pathway of 1-alkenes and 2-alkenes by assuming both of them are produced through β -elimination from the growing chain when H_2/CO and D_2/CO are used as syngas. As shown in Figure 5.4, during the chain propagation steps, FTS monomer MCH is added to the growing chain $RCH_2CH=M$ to form $RCH_2CH(M)CH_2=M$, through the hydrogenation of $RCH_2CH(M)CH_2=M$, intermediate $RCH_2CH(M)CH_3$ or $RCD_2CD(M)CD_3$ is formed. This intermediate undergoes β -elimination to form both 1-alkenes and 2-alkenes.

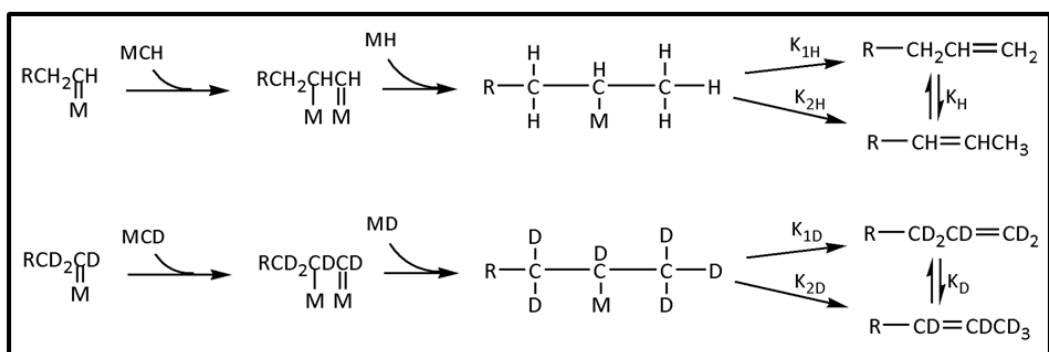


Figure 5.4 The hypothetical formation pathway of 1-alkenes and 2-alkenes in FTS

In this mechanism, 1-alkenes and 2-alkenes are produced through the same pathway. If both 1-alkenes and 2-alkenes were formed through the same pathway shown in Figure 5.4, the chemical behavior during the formation of both 1-alkenes and 2-alkenes should be the same, in other word, they should have same isotope effect, either both of them are inverse isotope effect or primary isotope effect. Then we have $K_{1H}/K_{1D} = K_{2H}/K_{2D}$, which means $[1\text{-alkene}]_H/[1\text{-alkene}]_D = [2\text{-alkene}]_H/[2\text{-alkene}]_D$. However, The results of iron catalyzed H_2/D_2 switching experiments in the Figure 5.1 to Figure 5.3 indicate that the ratios of 1-alkane fraction between hydrogen and deuterium product ($[1\text{-alkane}]_H/[1\text{-alkane}]_D$) are less than one, but the ratios of 2-alkane fraction between hydrogen and deuterium product ($[2\text{-alkane}]_H/[2\text{-alkane}]_D$) are greater than one. These experimental results indicate that there is a primary isotope effect during the formation of 2-alkenes.

It clearly indicated that this hypothesis is not true, in other words, the formation of 1-alkanes are through a totally different pathway from the formation of 2-alkenes in iron catalyzed FTS.

5.3.2 The Explanation for 2-Alkenes Formation by Modified Alkylidene Mechanism

It has been proved that 1-alkenes and 2-alkenes were produced from different pathways above, if we believe that the 1-alkenes are the primary product of FTS, the 2-alkenes cannot be the primary product. Therefore, the 2-alkenes should be the secondary product. Figure 5.5 shows a brief production pathway of iron catalyzed FTS when H₂/CO and D₂/CO are used as syngas. As shown in Figure 5.5, the 1-olefin and paraffin are the primary product and 1-olefin can convert to 2-olefin through isomerization and it can also convert to paraffin through hydrogenation.

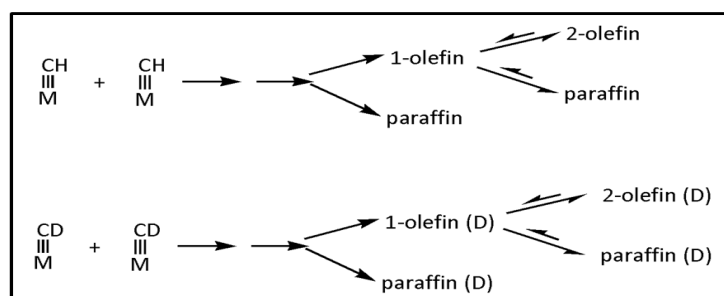


Figure 5.5 A brief production pathway of iron catalyzed FTS

Assuming the ratio of $[1\text{-olefin } \%]_{\text{H}}/[1\text{-olefin } \%]_{\text{D}} = [\text{paraffin } \%]_{\text{H}}/[\text{paraffin } \%]_{\text{D}} = 1$

when they are produced originally, a possible formation pathway of 2-alkenes during the iron catalyzed FTS has been proposed based on the modified alkylidene mechanism.

Figure 5.6 shows the proposed formation pathway of 2-alkenes during iron catalyzed FTS based on the modified alkylidene mechanism.

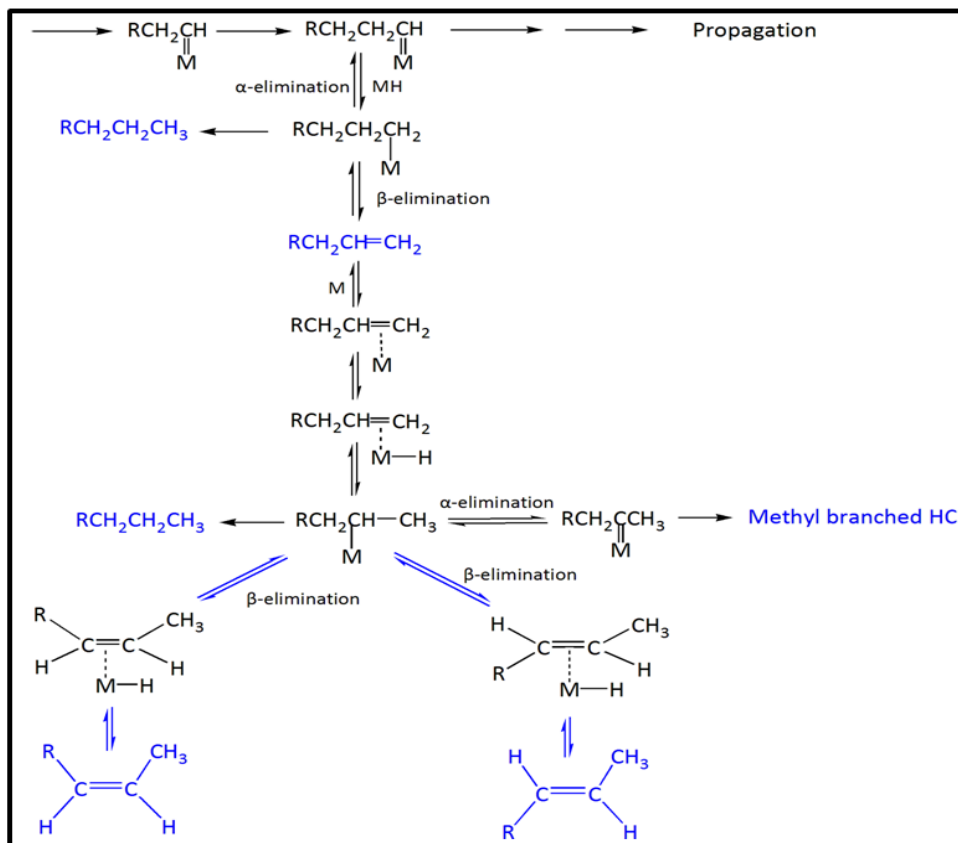


Figure 5.6 The proposed mechanism for the formation of 2-alkenes

As shown in Figure 5.6, during the chain propagation steps, the hydrogenation of the growing chain $\text{RCH}_2\text{CH}_2\text{CH}=\text{M}$ generates the intermediate $\text{RCH}_2\text{CH}_2\text{CH}_2-\text{M}$. Through the hydrogenation of this intermediate, n-alkanes are formed. On the other hand, 1-alkenes can be produced by the β -elimination of $\text{RCH}_2\text{CH}_2\text{CH}_2-\text{M}$. The 1-alkenes can be reabsorbed on the surface of metal catalyst to form an intermediate $\text{RCH}_2\text{CH}(\text{M})\text{CH}_3$. This intermediate can undergo α -elimination to form corresponding 2-alkylidene, which can re-grow to produce methyl branched hydrocarbons. However, this intermediate would more likely to undergo either the hydrogenation to form the corresponding n-alkanes or β -elimination to form trans-2-alkenes and cis-2-alkenes.

During the formation of 2-alkenes, C-H and C-D bonds cleavages are involved. The primary isotope effect involves C-H (C-D) bond breakage, and the reaction rate over hydrogen is faster than the reaction over deuterium. Because the bond-dissociation energy (BDE) for C-H bond is 104 Kcal/mol, the BDE for C-D bond is 106 Kcal/mol. In this case, the 1-alkenes are more likely to be converted to 2-alkenes when H₂/CO is used than that D₂/CO is used, which leads to a primary isotope effect. So [2-alkane]_H/[2-alkane]_D is greater than one. Once there is more 1-alkenes have been converted to 2-alkenes, there is less 1-alkenes remaining when H₂/CO is used as syngas. Thus, [1-alkane]_H/[1-alkane]_D is less than one, which consists with the experimental results.

In 2001, Shi et al. conducted an experiment that 1-octene-d₁₆ was added to the FTS reactor over 5 hours, at the end of addition of 1-octene-d₁₆, the product traps were emptied and emptied again after 19 hours [61].

Based on the GC/MS analysis of liquid and wax product, they found that 1-octene-d₁₆ has been isomerized to deuterium-containing cis-plus trans-2-octene and hydrogenated to deuterium-containing n-octane. A metal-hydrogen atom addition-elimination mechanism was proposed which is shown in Figure 5.7. As shown in Figure 5.7, the half-hydrogenated intermediate RCD₂CD(M)-CD₂H can be converted to corresponding 2-olefin and can also be hydrogenated to n-paraffin. This result consists with the previous explanation of 2-olefin formation pathway.



Figure 5.7 The metal-hydrogen atom addition-elimination mechanism

5.3.3 The Explanation of [paraffin]_H/[paraffin]_D Ratio in Iron Catalyzed FTS

The 2-alkenes formation pathway (Figure 5.6) has been proposed based on the modified alkylidene mechanism. As shown in Figure 5.6, paraffin can also be produced by the half-hydrogenated intermediate $RCH_2CH(M)CH_3$ exclusively from the hydrogenation of the growing chain (hydrogenation of $RCH_2CH_2CH_2-M$). If the paraffin produced from the hydrogenation of $RCH_2CH(M)CH_3$ is represented by dp (secondary product); paraffin produced from the hydrogenation of growing chain is represented by P (primary product). Then we have the total paraffin fraction $[P_{Total}] = [dp] + [P]$. The total ratio of $[P_{Total}]_H/[P_{Total}]_D$ was obtained and shown in Table 5.3. Total fraction of paraffin when H_2/CO was used as syngas and the total paraffin fraction when D_2/CO was used were measured experimentally, and the ratio of $[P_{Total}]_H/[P_{Total}]_D$ can be calculated.

Table 5.3 The ratio of $[paraffin]_H/[paraffin]_D$ during the iron catalyzed FTS

270 °C, Fe/Si/K with a CO conversion of 77%			
Carbon #	$[P_{Total}]_H$	$[P_{Total}]_D$	$[P_{Total}]_H/[P_{Total}]_D$
7	0.362 ± 0.01	0.288 ± 0.01	1.26 ± 0.01
8	0.363 ± 0.01	0.308 ± 0.01	1.18 ± 0.01
9	0.375 ± 0.01	0.327 ± 0.01	1.15 ± 0.01
10	0.390 ± 0.01	0.341 ± 0.01	1.14 ± 0.01
11	0.409 ± 0.01	0.363 ± 0.01	1.13 ± 0.01
12	0.432 ± 0.02	0.385 ± 0.01	1.12 ± 0.02
13	0.445 ± 0.01	0.420 ± 0.01	1.06 ± 0.01
14	0.485 ± 0.01	0.450 ± 0.01	1.08 ± 0.01
15	0.517 ± 0.02	0.454 ± 0.01	1.14 ± 0.02
16	0.491 ± 0.03	0.488 ± 0.08	1.01 ± 0.06

As it can be seen in Table 5.3, the ratio of $[P_{Total}]_H/[P_{Total}]_D$ from C7 to C16 is greater than one, ranging from 1.01 to 1.26. Similar results were found during the other two

Fe/Si/K catalyzed H₂/D₂ switching experiments, the values of $[P_{\text{Total}}]_{\text{H}}/[P_{\text{Total}}]_{\text{D}}$ from C7 to C16 are ranging from 1.18 to 1.26 and 1.04 to 1.25 for the Fe/Si/K catalyst with a CO conversion of 60% and for the Fe/Si/K catalyst with a CO conversion of 15%, respectively.

This results indicated that when paraffin was produced as a secondary product, it is more favorably to be converted from 1-olefin when when H₂/CO was used as syngas . Therefore, the $[dP]_{\text{H}}/[dP]_{\text{D}}$ is greater than one, which leads the $[P_{\text{Total}}]_{\text{H}}/[P_{\text{Total}}]_{\text{D}}$ to be greater than one

5.4 CONCLUSION

The product analysis of H₂/D₂ switching experiments indicated that 1-alkenes and 2-alkenes were formed through different pathways. While n-alkanes and 1-alkenes are the primary product of FTS, the 2-alkenes are the secondary product and the formation of which shows a primary isotope effect.

The n-alkanes can also be produced from the re-adsorption of 1-alkenes. The M-H dominated the formation of n-alkanes and 2-alkenes from the re-adsorption of 1-alkenes, which leads the total paraffin ratio $[P_{\text{Total}}]_{\text{H}}/[P_{\text{Total}}]_{\text{D}}$ greater than one.

The formation of 2-alkenes can be explained by the modified alkylidene mechanism. This mechanism can also explain the primary isotope effect observed during the formation of 2-alkenes.

CHAPTER 6

SUMMARY AND FUTURE WORK

6.1 SUMMARY

By conducting H₂/D₂ switching experiments we found that the rate of hydrocarbon production when D₂/CO was used as syngas was higher than that of H₂/CO was used, an indication of inverse isotope effect during iron catalyzed FTS. This experimental fact can be explained by the modified alkylidene mechanism, in which the monomer of FTS is M≡CH and the growing chain is 1-alkylidene RCH₂CH=M. In this mechanism, the inverse isotope effect is originated from each step of propagation due to the hybridization of carbon changed from sp² to sp³.

The inverse isotope effect has been calculated using eq. 3.9, where k is the carbon number of the hydrocarbon that has the average molecular weight of the FT reaction. According to eq. 3.9, the inverse isotope effect in each step of propagation has been calculated to be 0.88 to 0.96, 0.83 to 0.90 and 0.97 to 0.98 in run 1 to run 3, respectively, and 0.71 to 0.81 during run 4.

Based on the alkylidene mechanism, the 1-alkenes were produced from β-elimination of the intermediate RCH₂CH₂M which produced from the hydrogenation of the growing chain RCH₂CH=M. Both 1-alkenes and n-alkanes are the primary products of iron catalyzed FTS, however, n-alkanes can also be produced from the hydrogenation of 1-alkenes as secondary product. When H₂/CO was used as syngas, the amount of

n-alkanes produced as secondary product is more than when D₂/CO was used.

The results of H₂/D₂ switching experiments showed that the ratios of of [1-alkenes]_H/[1-alkenes]_D were smaller than 1 while the ratios of of [2-alkenes]_H/[2-alkenes]_D were greater than 1, ranging from 1.1 to 1.4, indicating that there is primary isotope effect during the formation of 2-alkanes, therefore, the 1-alkenes and 2-alkenes were produced from different pathways. A mechanism of 2-alkene formation has been proposed based on the modified alkylidene mechanism. According to the mechanism we proposed, the 2-alkenes were produced from the isomerization of 1-alkenes, therefore they are the secondary products of FTS.

The deuterium enrichment was found during the iron catalyzed FTS based on the results of H₂/D₂ competitive experiments. The H/D ratios were obtained and the theoretical H/D ratios have been calculated based on the inverse isotope effect obtained from the H₂/D₂ switching experiments. The experimental H/D ratios are in the range of theoretical values. These facts can also be explained by modified alkylidene mechanism by considering the local concentration of the monomer M≡CH (M≡CD) and the decreasing of inverse isotope effect with increasing carbon numbers.

6.2 FUTURE WORK

Study the mechanism of FTS catalyzed by Ru catalyst. To find out whether there is inverse isotope effect and deuterium enrichment in the Ru catalyzed FT reaction or not. How the magnitude of deuterium enrichment functions with carbon number in Ru catalyzed FTS.

Study the 2-alkenes formation during the Ru catalyzed FTS. Find out whether the formation of 2-alkenes over Ru catalyzed FTS can be explained by the mechanism proposed or not.

LIST OF REFERENCES

1. Fischer, F.; Tropsch, H., *Chem. Ber.* (1926), 59,830-836.
2. Leckel, Dieter. "Diesel production from Fischer– Tropsch: The past, the present, and new concepts." *Energy & Fuels* 23.5 (2009): 2342-2358.
3. "Technologies & processes" Sasol
4. Hu, Jin, Fei Yu, and Yongwu Lu. "Application of Fischer–Tropsch Synthesis in Biomass to Liquid Conversion." *Catalysts* 2.2 (2012): 303-326.
5. Lollar, B. Sherwood, et al. "Abiogenic formation of alkanes in the Earth's crust as a minor source for global hydrocarbon reservoirs." *Nature* 416.6880 (2002): 522-524.
6. Taran, Y. A., et al. "Carbon and hydrogen isotopic compositions of products of open-system catalytic hydrogenation of CO₂: Implications for abiogenic hydrocarbons in Earth's crust." *Geochimica et Cosmochimica Acta* 74.21 (2010): 6112-6125.
7. CHRISTOFFERSEN, ROY, and PETER R. BUSECK. "Epsilon carbide: a low-temperature component of interplanetary dust particles." *Science* 222.4630 (1983): 1327-1329.
8. Bradley, J. P., D. E. Brownlee, and P. Fraundorf. "Carbon compounds in interplanetary dust: evidence for formation by heterogeneous catalysis." *Science* 223.4631 (1984): 56-58.
9. Kress, Monika E., and Alexander GGM Tielens. "The role of Fischer-Tropsch catalysis in solar nebula chemistry." *Meteoritics & Planetary Science* 36.1 (2001): 75-91.
10. Llorca, Jordi. "Are organic molecules produced by nebular Fischer-Tropsch processes preserved in comets?" *Advances in Space Research* 30.6 (2002): 1469-1472.

11. Konn, Cécile, et al. "Hydrocarbons and oxidized organic compounds in hydrothermal fluids from Rainbow and Lost City ultramafic-hosted vents." *Chemical Geology* 258.3 (2009): 299-314.
12. Lollar, B. Sherwood, et al. "Isotopic signatures of CH₄ and higher hydrocarbon gases from Precambrian Shield sites: A model for abiogenic polymerization of hydrocarbons." *Geochimica et Cosmochimica Acta* 72.19 (2008): 4778-4795.
13. Flory, Paul J. "Molecular Size Distribution in Linear Condensation Polymers1." *Journal of the American Chemical Society* 58.10 (1936): 1877-1885.
14. Henrici-Olivé, G., and S. Olive. "The Fischer-Tropsch Synthesis: Molecular Weight Distribution of Primary Products and Reaction Mechanism." *Angewandte Chemie International Edition in English* 15.3 (1976): 136-141.
15. Herington, E. F. G. "Fischer-Tropsch synthesis considered as a polymerization reaction." *Chem. Ind.(London)* (1946).
16. Brady III, Robert C., and R1 Pettit. "Mechanism of the Fischer-Tropsch reaction. The chain propagation step." *Journal of the American Chemical Society* 103.5 (1981): 1287-1289.
17. Turner, Michael L., et al. "The Alkenyl Mechanism for Fischer-Tropsch Surface Methylene Polymerisation; the Reactions of Vinylic Probes with CO/H₂ over Rhodium Catalyst." *Chemistry-a European Journal* 1.8 (1995): 549-556.
18. Storch, Henry H., Robert A. Anderson, and Norma Golumbic. *The Fischer-Tropsch and related syntheses*. Vol. 6. New York: Wiley, 1951.
19. Teng, Bo-Tao, et al. "Oxygenate kinetics in Fischer-Tropsch synthesis over an

- industrial Fe–Mn catalyst." *Fuel* 84.7 (2005): 791-800.
20. Akin, A. Nilgün, and Z. İlsen Önsan. "Kinetics of CO hydrogenation over coprecipitated cobalt–alumina." *Journal of Chemical Technology and Biotechnology* 70.3 (1997): 304-310.
 21. Wang, Yuguo, and Burtron H. Davis. "Fischer–Tropsch synthesis. Conversion of alcohols over iron oxide and iron carbide catalysts." *Applied Catalysis A: General* 180.1 (1999): 277-285.
 22. Deng, Baolin, Timothy J. Campbell, and David R. Burris. "Hydrocarbon formation in metallic iron/water systems." *Environmental science & technology* 31.4 (1997): 1185-1190.
 23. Shi, Buchang, and Chunfen Jin. "Inverse kinetic isotope effects and deuterium enrichment as a function of carbon number during formation of C–C bonds in cobalt catalyzed Fischer–Tropsch synthesis." *Applied Catalysis A: General* 393.1 (2011): 178-183.
 24. Friedel, Robert A., and A. G. Sharkey Jr. "similar compositions of alkanes from coal, petroleum, natural gas, and fischer-tropsch product." *Coal Science* 3 (1966): 32-42.
 25. Maitlis, Peter M., and Valerio Zanotti. "The role of electrophilic species in the Fischer–Tropsch reaction." *Chemical Communications* 13 (2009): 1619-1634.
 26. Bukur, Dragomir B., et al. "Effect of process conditions on olefin selectivity during conventional and supercritical Fischer-Tropsch synthesis." *Industrial & engineering chemistry research* 36.7 (1997): 2580-2587.
 27. Shi, Buchang, et al. "Explanations of the Formation of Branched Hydrocarbons

- During Fischer–Tropsch Synthesis by Alkylidene Mechanism." *Topics in Catalysis* 57.6-9 (2014): 451-459.
28. Madon, Rostam J., Sebastian C. Reyes, and Enrique Iglesia. "Primary and secondary reaction pathways in ruthenium-catalyzed hydrocarbon synthesis." *The Journal of Physical Chemistry* 95.20 (1991): 7795-7804.
29. Rao, V. U. S., et al. "Iron-based catalysts for slurry-phase Fischer-Tropsch process: Technology review." *Fuel processing technology* 30.1 (1992): 83-107.
30. Anderson, Robert Bernard, Herbert Kölbel, and Milos Ralek. *The Fischer-Tropsch Synthesis*. Vol. 16. New York: Academic Press, 1984.
31. Dry, M. E. "The Fischer-Tropsch Synthesis." *Catalysis science and technology* 1 (1981): 159-160.
32. Givens, Edwin N., and Burtron H. Davis. "Synthetic lubricants: Advances in Japan up to 1945 based on Fischer-Tropsch derived liquids." *Fischer-Tropsch Synthesis, Catalysts and Catalysis* 163 (2006): 29.
33. Lee, Joong Kee, and Dalkeun Park. "Hydrogen production from fluidized bed steam reforming of hydrocarbons." *Korean Journal of Chemical Engineering* 15.6 (1998): 658-662.
34. Ko, Ki-Dong, et al. "Kinetics of steam reforming over a Ni/alumina catalyst." *Korean Journal of Chemical Engineering* 12.4 (1995): 478-480.
35. Rostrup-Nielsen, Jens R. "New aspects of syngas production and use." *Catalysis today* 63.2 (2000): 159-164.
36. Christensen, Kjerst Omdahl, et al. "Effect of supports and Ni crystal size on carbon

- formation and sintering during steam methane reforming." *Applied Catalysis A: General* 314.1 (2006): 9-22.
37. Borowiecki, Tadeusz, Andrzej Gołbiowski, and Beata Stasińska. "Effects of small MoO₃ additions on the properties of nickel catalysts for the steam reforming of hydrocarbons." *Applied Catalysis A: General* 153.1 (1997): 141-156.
 38. Matsumura, Yasuyuki, and Toshie Nakamori. "Steam reforming of methane over nickel catalysts at low reaction temperature." *Applied Catalysis A: General* 258.1 (2004): 107-114.
 39. Takahashi, Ryoji, et al. "Addition of zirconia in Ni/SiO₂ catalyst for improvement of steam resistance." *Applied Catalysis A: General* 273.1 (2004): 211-215.
 40. Luo, Mingsheng, Hussein Hamdeh, and Burtron H. Davis. "Fischer-Tropsch Synthesis: Catalyst activation of low alpha iron catalyst." *Catalysis Today* 140.3 (2009): 127-134.
 41. Fox, Joseph M. "Fischer-Tropsch reactor selection." *Catalysis Letters* 7.1 (1990): 281-292.
 42. Bukur, Dragomir B., et al. "Activation studies with a promoted precipitated iron Fischer-Tropsch catalyst." *Industrial & engineering chemistry research* 28.8 (1989): 1130-1140.
 43. Liu, Zhi-Pan, and P. Hu. "A new insight into Fischer-Tropsch synthesis." *Journal of the American Chemical Society* 124.39 (2002): 11568-11569.
 44. Davis, Burtron H. "Fischer-Tropsch synthesis: current mechanism and futuristic needs." *Fuel processing technology* 71.1 (2001): 157-166.

45. Schulz, Hans. "Short history and present trends of Fischer–Tropsch synthesis." *Applied Catalysis A: General* 186.1 (1999): 3-12.
46. Ojeda, Manuel, et al. "CO activation pathways and the mechanism of Fischer–Tropsch synthesis." *Journal of Catalysis* 272.2 (2010): 287-297.
47. Kellner, C. Stephen, and Alexis T. Bell. "Evidence for H₂D₂ isotope effects on fischer-tropsch synthesis over supported ruthenium catalysts." *Journal of Catalysis* 67.1 (1981): 175-185.
48. Davis, B. H., M. K. Gnanamani, and W. Ma. "A paper presented in the 21st North American Catalysis Society Meeting." *San Francisco, CA* (2009). Ojeda, Manuel, et al. "Kinetically Relevant Steps and H₂/D₂ Isotope Effects in Fischer–Tropsch Synthesis on Fe and Co Catalysts." *The Journal of Physical Chemistry C* 114.46 (2010): 19761-19770.
49. Ojeda, Manuel, et al. "Kinetically Relevant Steps and H₂/D₂ Isotope Effects in Fischer–Tropsch Synthesis on Fe and Co Catalysts." *The Journal of Physical Chemistry C* 114.46 (2010): 19761-19770.
50. Tau, Li Min, Hossein A. Dabbagh, and Burtron H. Davis. "Fischer-Tropsch synthesis: comparison of carbon-14 distributions when labeled alcohol is added to the synthesis gas." *Energy & fuels* 5.1 (1991): 174-179.
51. James, Olusola O., et al. "Reflections on the chemistry of the Fischer–Tropsch synthesis." *Rsc Advances* 2.19 (2012): 7347-7366.
52. Anslyn, Eric V., and Dennis A. Dougherty. *Modern physical organic chemistry*. University Science Books, 2006.

53. Lowry, Thomas H., and Kathleen Schueller Richardson. "Mechanism and theory in organic chemistry." (1987): 748
54. The α value of an FT reaction using CO/H₂ as the synthesis gas is used to determine the average molecular weight of the reaction since the small change in α when switched to CO/D₂ will not significantly change the value of n , which equals to (average-molecular-weight)/14.
55. Hall, W. Keith, R. J. Kokes, and P. H. Emmett. "Mechanism studies of the Fischer-Tropsch synthesis. The addition of radioactive methanol, carbon dioxide and gaseous formaldehyde." *Journal of the American Chemical Society* 79.12 (1957): 2983-2989.
56. Tau, Li-Min, et al. "Fischer-Tropsch synthesis with an iron catalyst: Incorporation of ethene into higher carbon number alkanes." *Catalysis Letters* 7.1-4 (1990): 141-149.
57. Shi, Buchang, et al. "Fischer-Tropsch synthesis: ¹⁴C labeled 1-alkene conversion using supercritical conditions with Co/Al₂O₃." *Fuel* 84.9 (2005): 1093-1098.
58. Shi, Buchang, and Burtron H. Davis. "Fischer-Tropsch synthesis: evidence for chain initiation by ethene and ethanol for an iron catalyst." *Topics in catalysis* 26.1-4 (2003): 157-161.
59. Krishna, Kamala R., and Alexis T. Bell. "The role of C₂ intermediates in Fischer-Tropsch synthesis over ruthenium." *Catalysis letters* 14.3-4 (1992): 305-313.
60. A. Raje, BH Davis; "Fischer-Tropsch synthesis. Mechanism studies using isotopes." JJ Spring (Ed.), *Catalysis*, vol. 12 The Royal Society of Chemistry, Cambridge (1996), pp. 52-131.

61. Shi, Buchang, et al. "Deuterium Tracer Studies and Gas Chromatography–Mass Spectrometry Analysis of Deuterated Products during Fischer–Tropsch Synthesis." *Topics in Catalysis* 57.6-9 (2014): 460-469.
62. R.M. Silverstein, G.C. Bassler, T.C. Morrill, *Spectrometric identification of organic compounds, 4th edition*. John Wiley & Sons, (1981) 46-89.
63. Shi, Buchang, et al. "Mechanism of the isomerization of 1-alkene during iron-catalyzed Fischer–Tropsch synthesis." *Journal of Catalysis* 199.2 (2001): 202-208.
64. Zheng, Shenke, et al. "Deuterium tracer study of pressure effect on product distribution in the cobalt-catalyzed Fischer–Tropsch synthesis." *Applied Catalysis A: General* 330 (2007): 63-68.
65. Liu, Yanli, et al. "Deuterium tracer study of Fischer–Tropsch synthesis: A method to eliminate accumulation problems." *Journal of Molecular Catalysis A: Chemical* 276.1 (2007): 110-115.
66. Shi, Buchang, and Chunfen Jin. "Deuterium tracer studies on cobalt catalyzed Fischer–Tropsch synthesis: Addition of alcohols." *Applied Catalysis A: General* 398.1 (2011): 54-58.
67. M. E. Dry, in "Catalysis-Science and Technology", Springer-Verlag, New York, 1 (1981) 160.
68. Madon, Rostam J., and Enrique Iglesia. "The Importance of Olefin Readsorption and H₂/CO Reactant Ratio for Hydrocarbon Chain Growth on Ruthenium Catalysts." *Journal of catalysis* 139.2 (1993): 576

69. Gnanamani, Muthu Kumaran, et al. "Deutero-1-pentene tracer studies for iron and cobalt Fischer–Tropsch synthesis." *Applied Catalysis A: General* 393.1 (2011): 130-137.

APPENDIX A:

TABLE

Table A-1 Measured Real Flow Rate of Different Runs

Run 1, P = 270 °C, T = 188 psi		Run 2, P = 140 °C, T = 188 psi	
Flow rate setup	50%	Flow rate setup	50%
Flow rate measured (mL/min)	44.19	Flow rate measured (mL/min)	58.43
	44.07		58.21
	45.61		57.56
	45.61		57.99
	45.35		58.21
	45.22		58.21
	45.57		58.43
	45.01		58.43
	44.81		57.56
44.22	57.56		
Average (mL/min)	44.97	Average (mL/min)	58.06
STDEV	0.61	STDEV	0.37
Run 3, P = 140 °C, T = 188 psi		Run 4, P = 140 °C, T = 188 psi	
Flow rate setup	50%	Flow rate setup	50%
Flow rate measured (mL/min)	36.11	Flow rate measured (mL/min)	46.99
	36.19		46.57
	36.11		45.22
	36.03		45.61
	36.03		45.22
	36.11		44.57
	36.11		45.09
	36.11		45.22
	36.03		44.70
36.03	44.70		
Average (mL/min)	36.09	Average (mL/min)	45.39
STDEV	0.10	STDEV	0.80

The temperatures and pressures in each row were the temperatures and pressures that the real flow rates were measured. They were not the actual reaction conditions. The real flow rate was different under each run, that is due to the reactor's seal ability has been changed in different runs.

APPENDIX B:

FIGURES

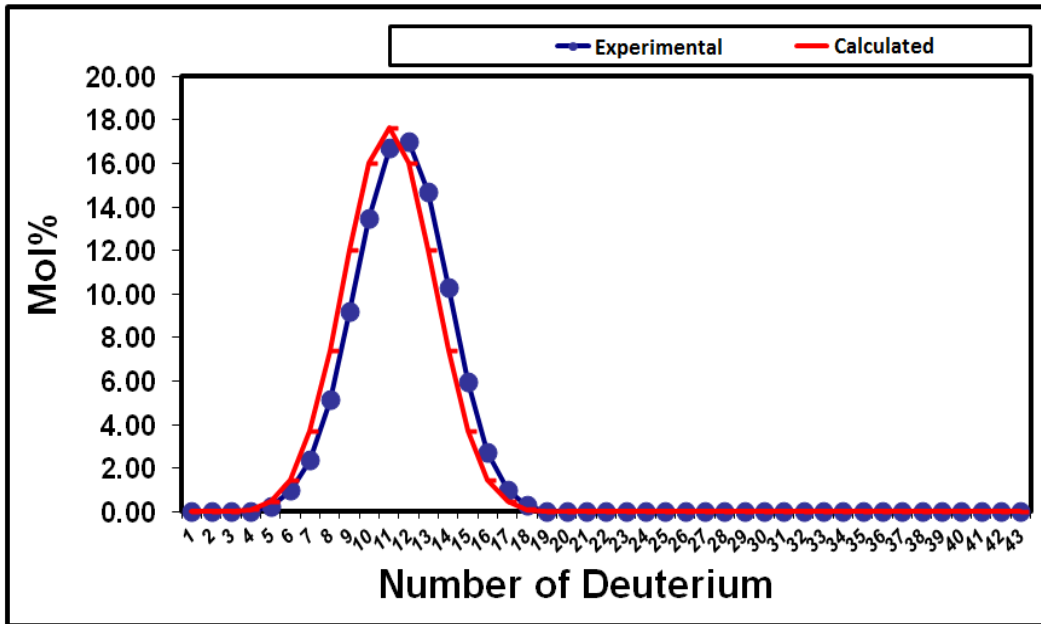


Figure B-1 Isotopic isomer distributions in n-Nonane

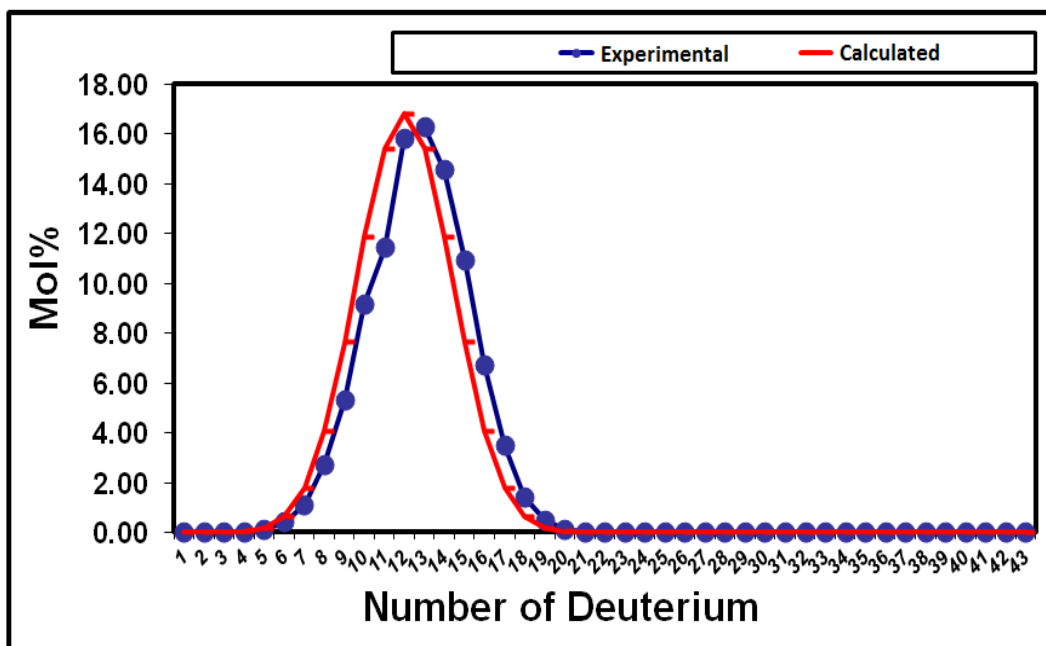


Figure B-2 Isotopic isomer distributions in n-Decane

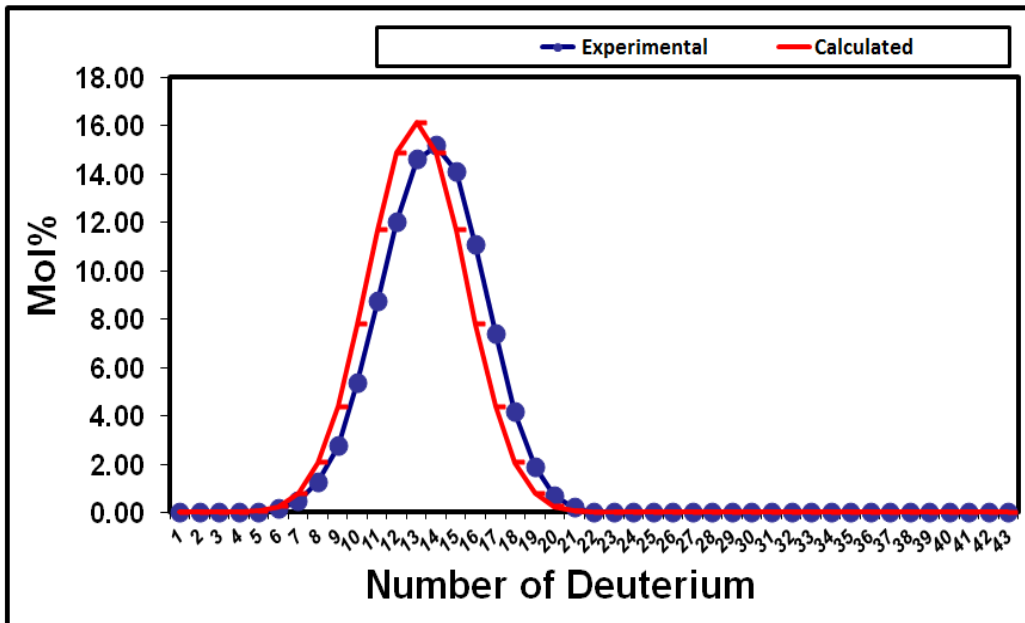


Figure B-3 Isotopic isomer distributions in n-Undecane

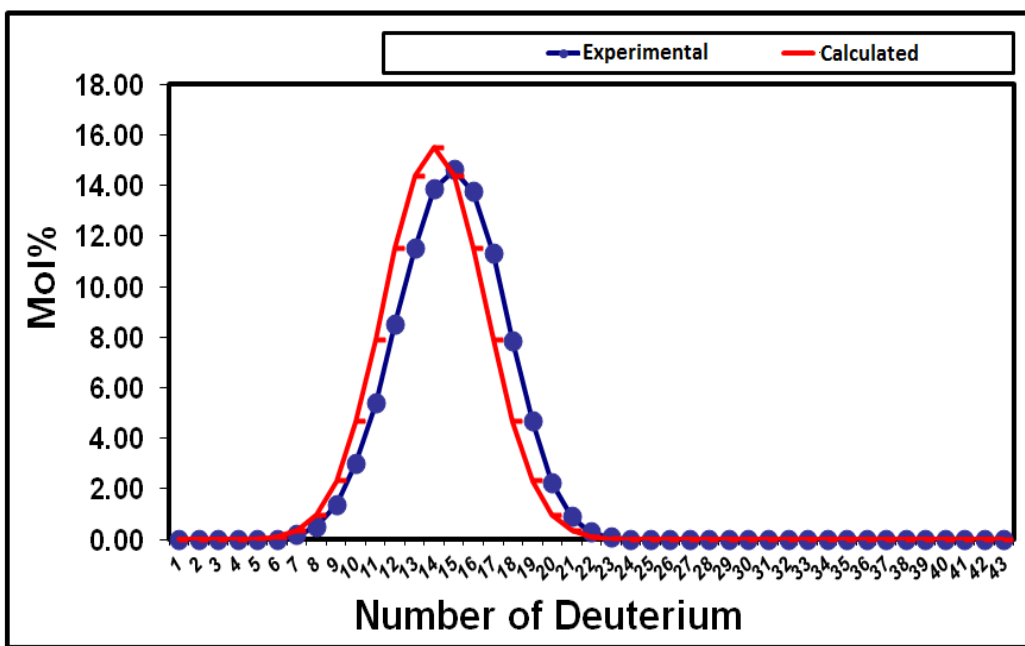


Figure B-4 Isotopic isomer distributions in n-Dodecane

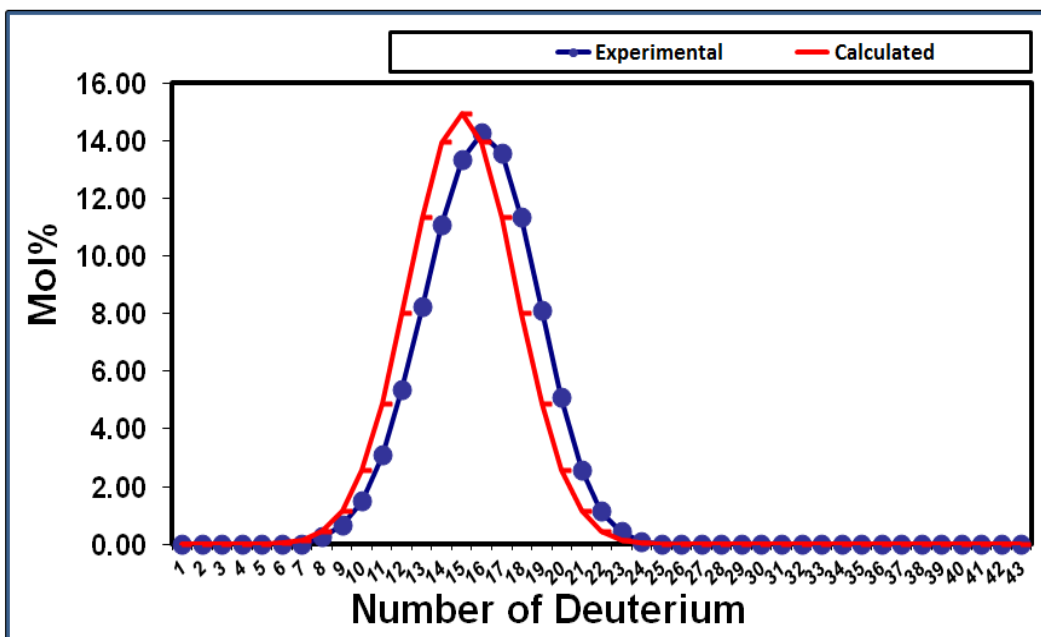


Figure B-5 Isotopic isomer distributions in n-Tridecane

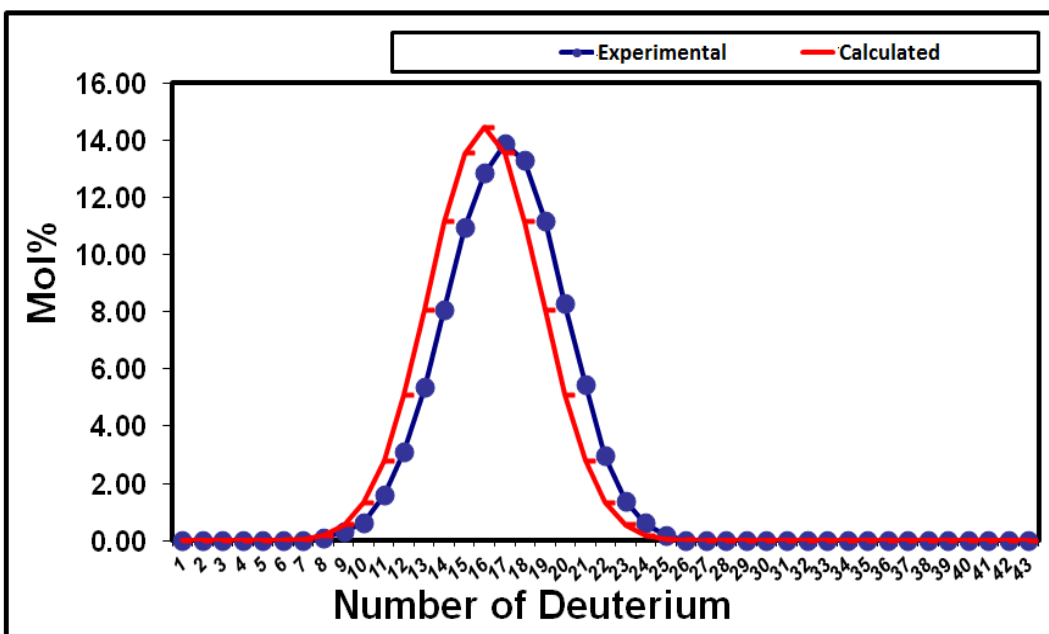


Figure B-6 Isotopic isomer distributions in n-Tetradecane

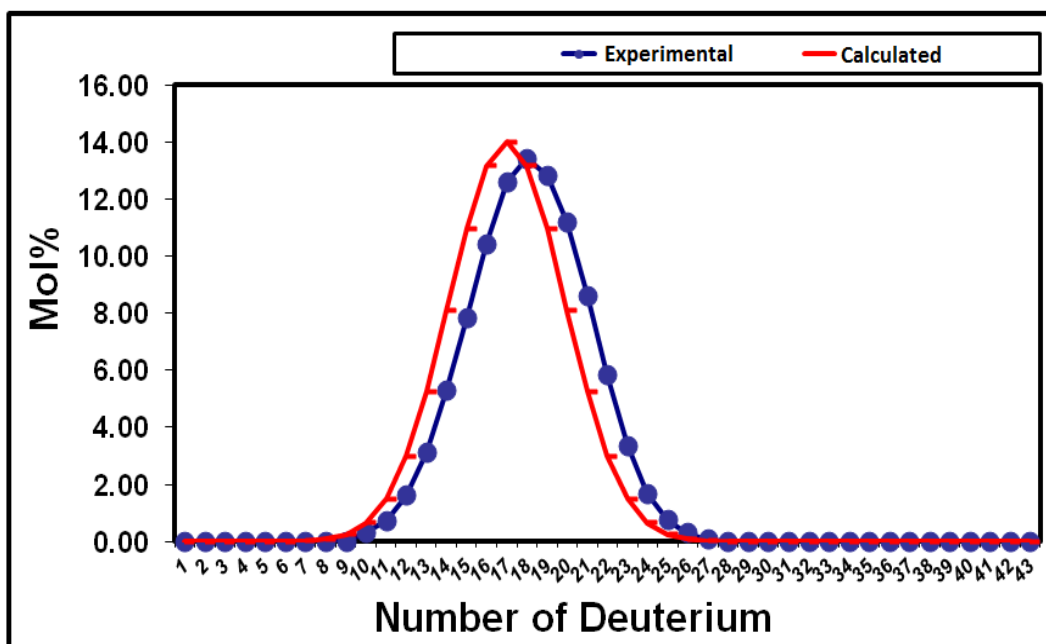


Figure B-7 Isotopic isomer distributions in n-Pentadecane

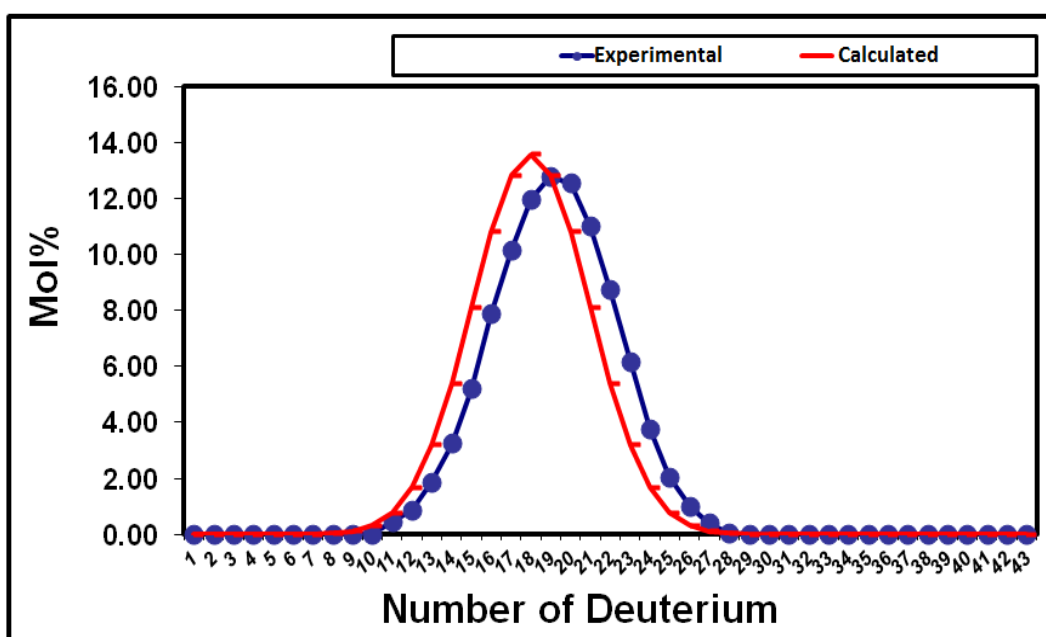


Figure B-8 Isotopic isomer distributions in n-Hexadecane

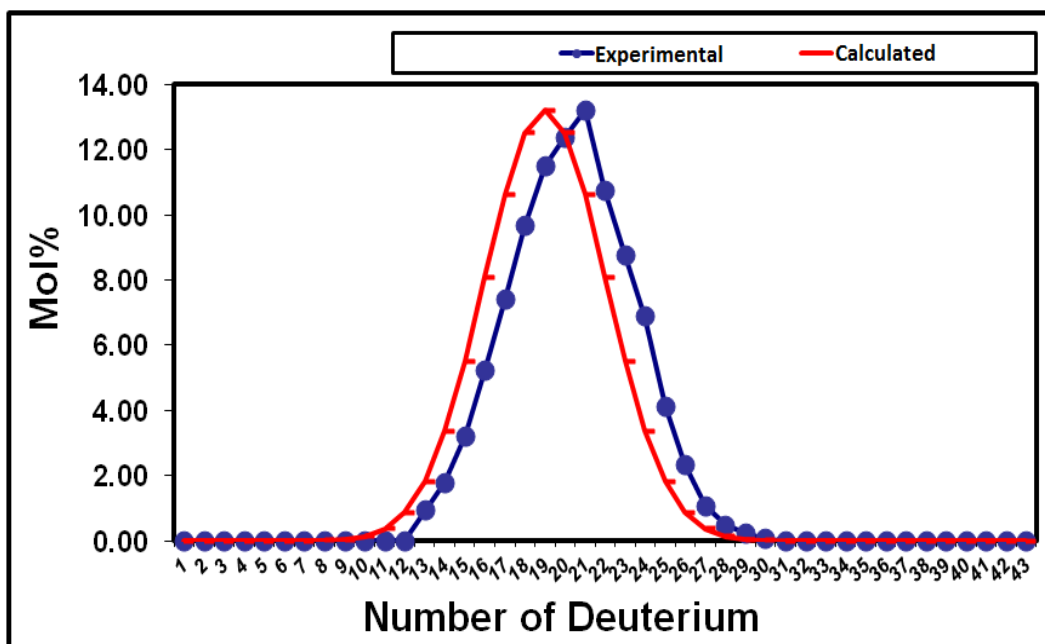


Figure B-9 Isotopic isomer distributions in n-Heptadecane

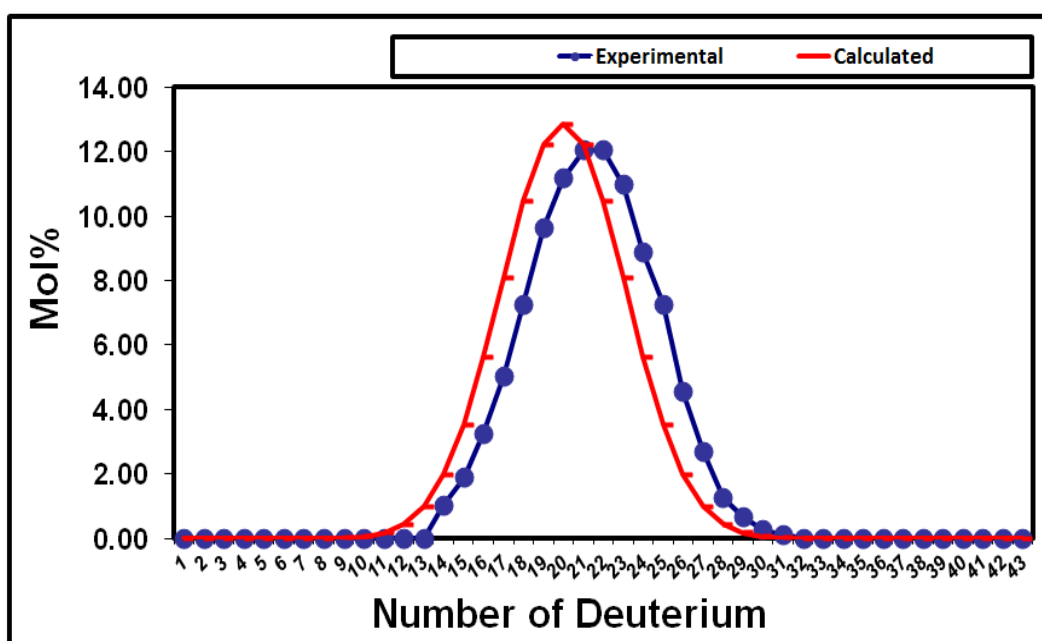


Figure B-10 Isotopic isomer distributions in n-Octadecane

APPENDIX C:

FIGURES

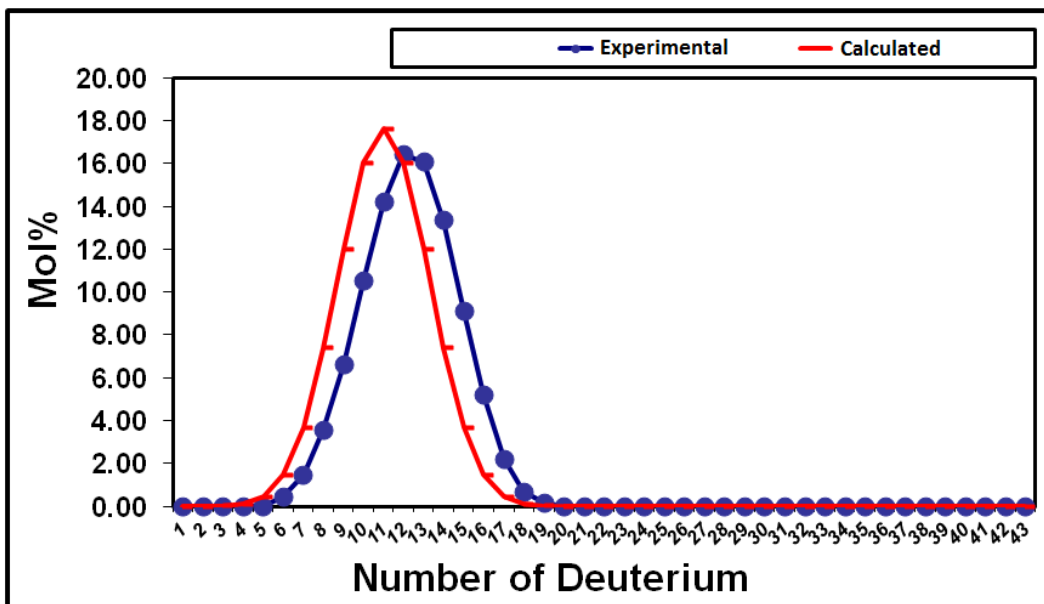


Figure C-1 Isotopic isomer distributions in n-Nonane

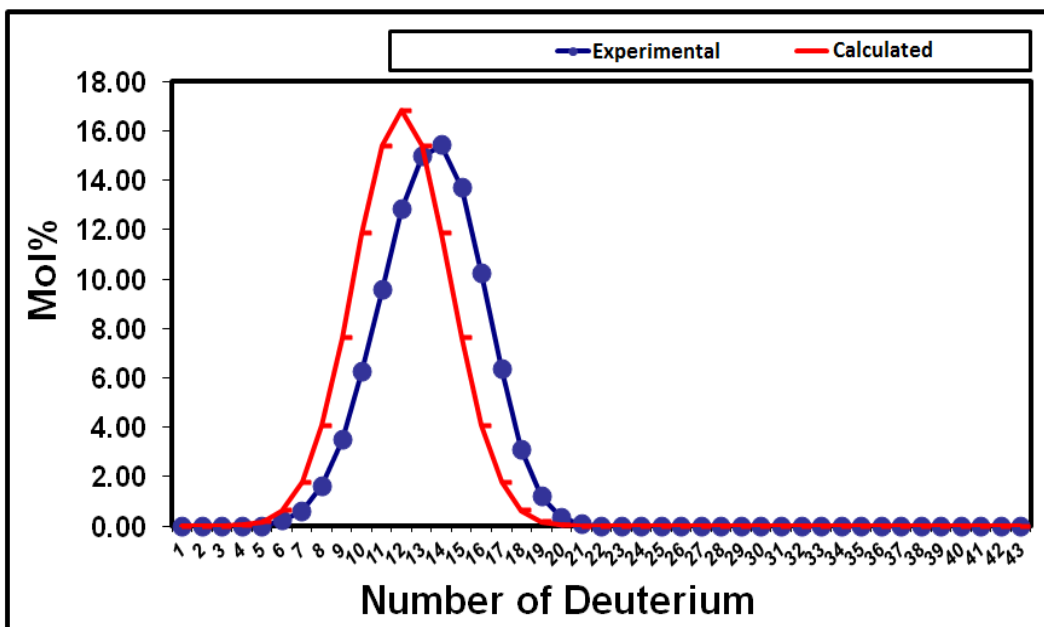


Figure C-2 Isotopic isomer distributions in n-Decane

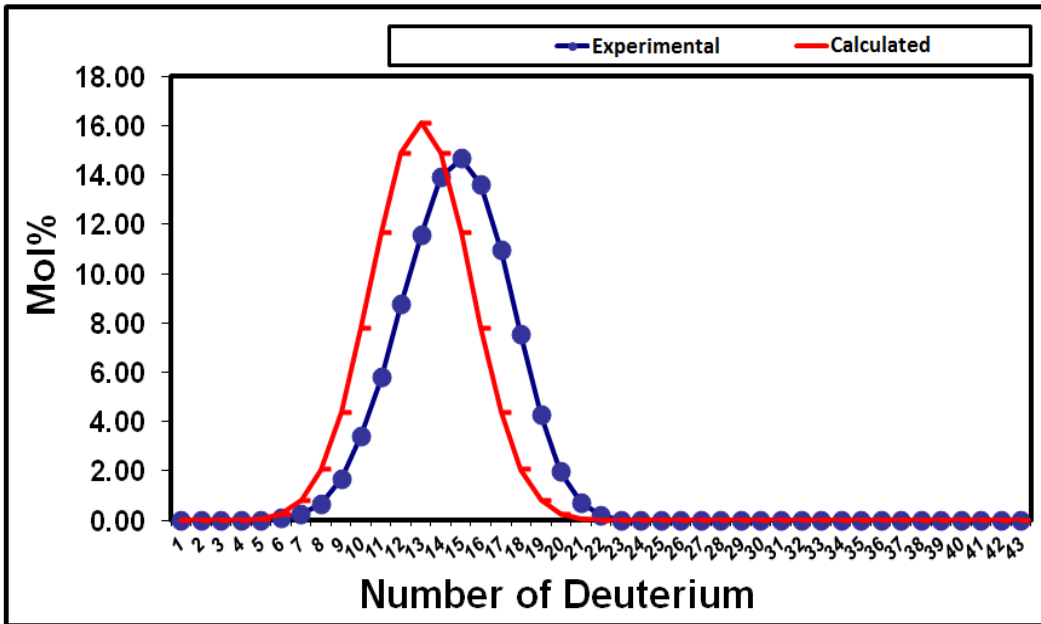


Figure C-3 Isotopic isomer distributions in n- Undecane

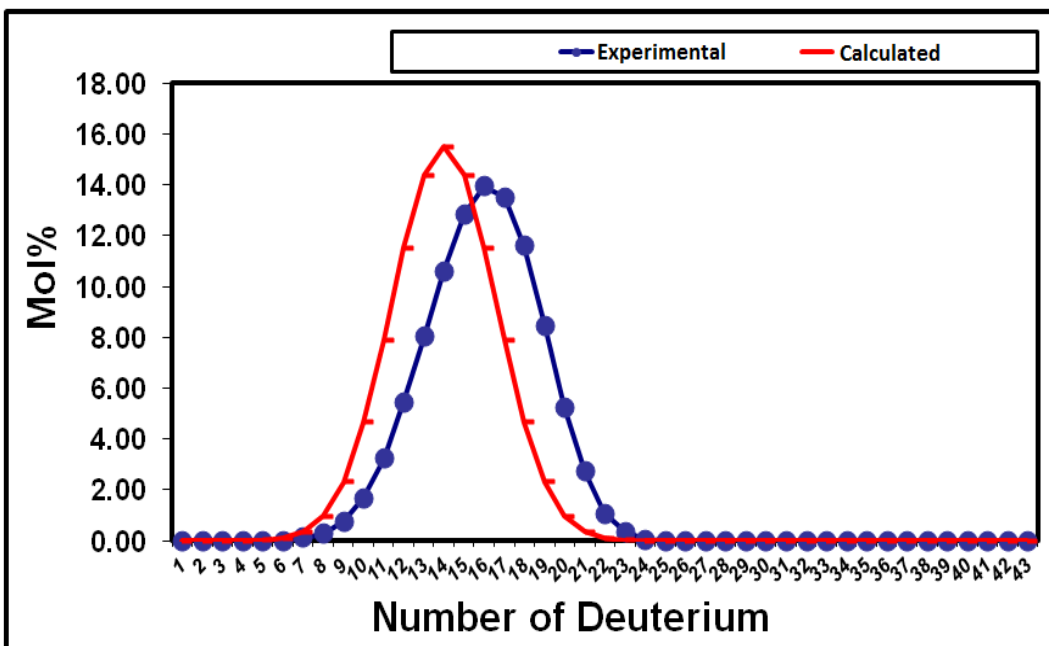


Figure C-4 Isotopic isomer distributions in n- Dodecane

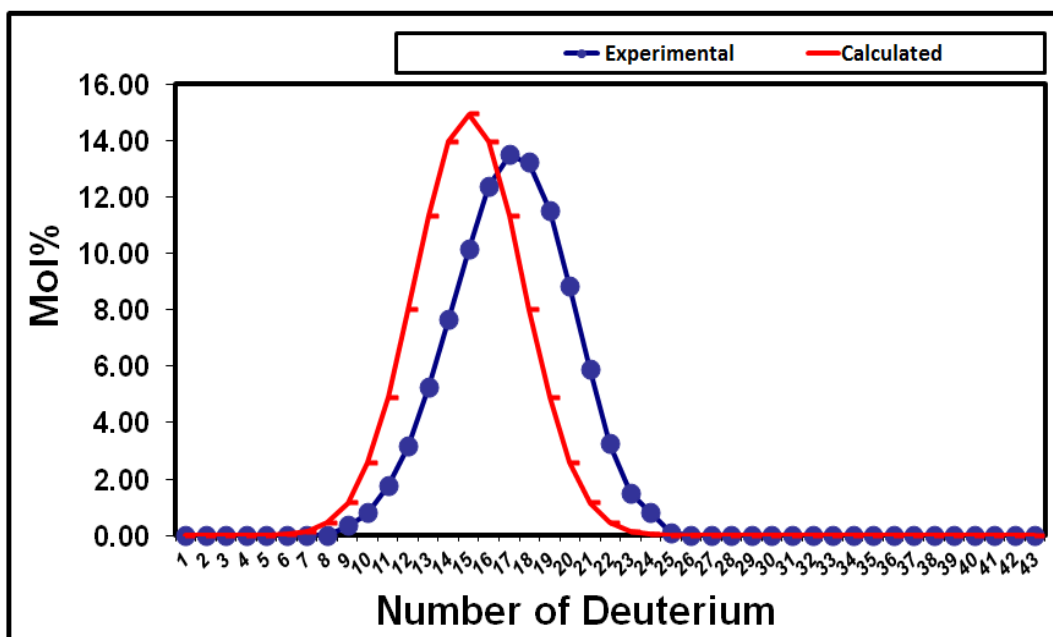


Figure C-5 Isotopic isomer distributions in n- Tridecane

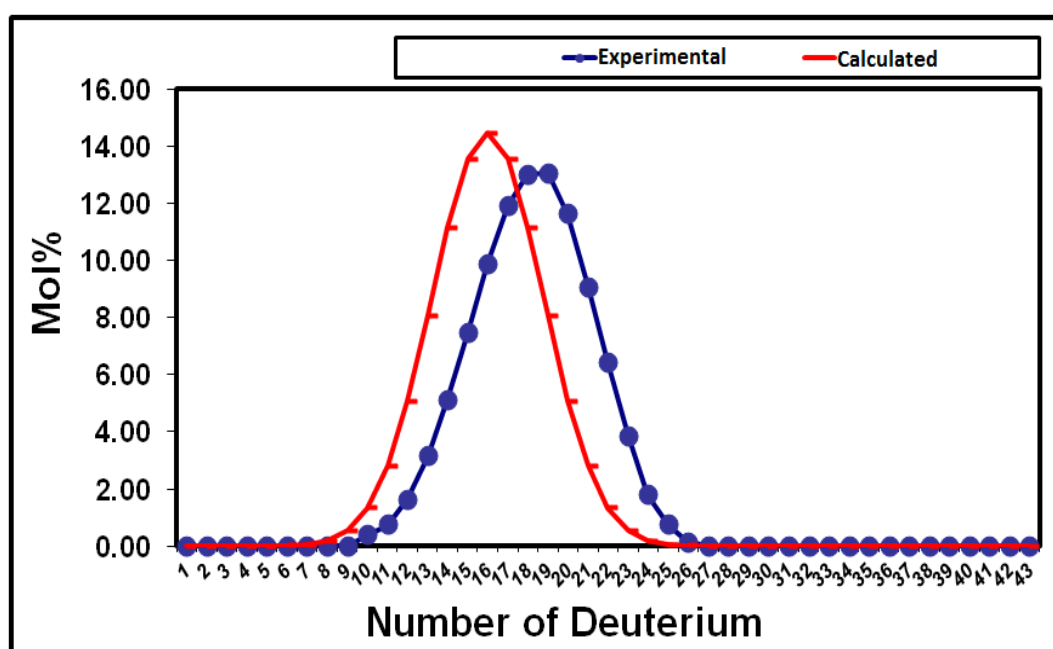


Figure C-6 Isotopic isomer distributions in n- Tetradecane

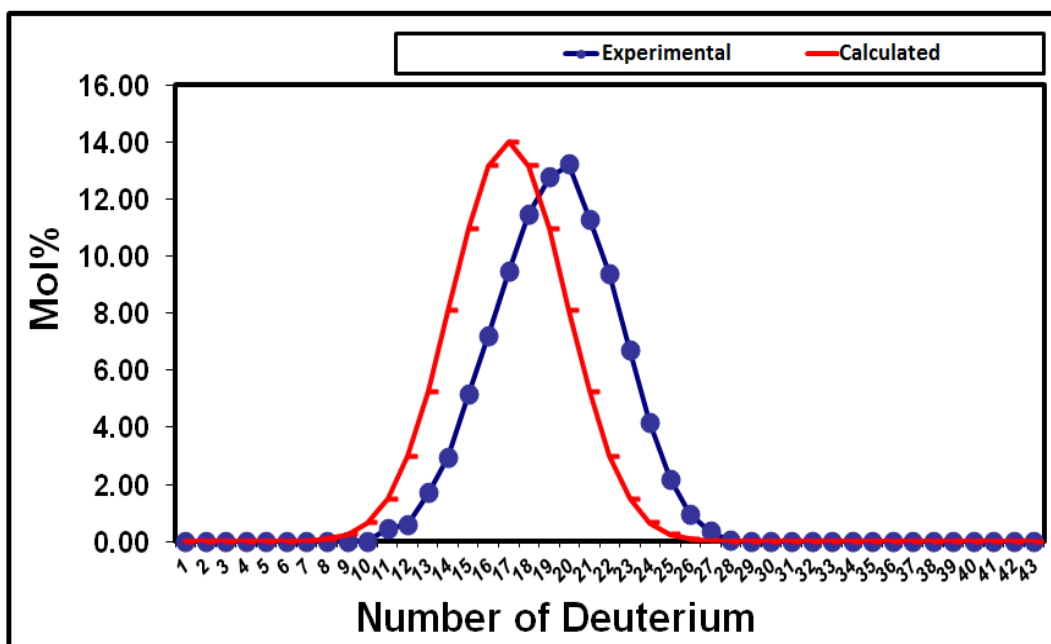


Figure C-7 Isotopic isomer distributions in n- Pentadecane